DISSERTATIONS IN
FORESTRY AND
NATURAL SCIENCES

Jarkko Leskinen

Ultrasound Stimulation of Bone and Cartilage — Interactions in Common In Vitro and Tissue Engineering Configurations

Publications of the University of Eastern Finland
Dissertations in Forestry and Natural Sciences

UNIVERSITY OF
EASTERN FINLAND

JARKKO LESKINEN

Ultrasound Stimulation of Bone and Cartilage — Interactions in Common In Vitro *and Tissue Engineering Configurations*

Publications of the University of Eastern Finland
Dissertations in Forestry and Natural Sciences
No 172

Academic Dissertation
To be presented by permission of the Faculty of Science and Forestry for public examination in Auditorium SN200 in Snellmania Building at the University of Eastern Finland, Kuopio, on January, 31, 2015, at 12 o'clock noon.

Department of Applied Physics

Kopio Niini Oy
Kuopio, 2015

Editors: Prof. Pertti Pasanen,
Prof. Pekka Kilpeläinen, Prof. Kai Peiponen, Prof. Matti Vornanen

Distribution:
Eastern Finland University Library / Sales of publications
P.O. Box 107, FI-80101 Joensuu, Finland
tel. +358-50-3058396
http://www.uef.fi/kirjasto

ISBN: 978-952-61-1682-2 (printed)
ISBN: 978-952-61-1683-9 (PDF)
ISSNL: 1798-5668
ISSN: 1798-5668
ISSN: 1798-5676 (PDF)

Author's address: University of Eastern Finland
Department of Applied Physics
P.O. Box 1627
70211 KUOPIO, FINLAND
email: jarkko.leskinen@uef.fi

Supervisors: Professor Kullervo Hynynen, Ph.D.
University of Toronto
Department of Medical Physics and
Sunnybrook Health Sciences Centre
2075 Bayview Avenue
TORONTO, ON M4N 3M5, CANADA
email: khynynen@sri.utoronto.ca

Research Director Mikko Lammi, Ph.D.
University of Eastern Finland
Department of Applied Physics
P.O. Box 1627
70211 KUOPIO, FINLAND
email: mikko.lammi@uef.fi

Reviewers: Professor Diane Dalecki, Ph.D.
University of Rochester
Department of Biomedical Engineering
P.O. Box 270168
ROCHESTER, NY, 14627-0168, USA
email: dalecki@bme.rochester.edu

Professor Cheri X. Deng, Ph.D.
University of Michigan
Department of Biomedical Engineering
2111 Carl A. Gerstacker Building
2200 Bonisteel Boulevard
ANN ARBOR, MI, 48109-2099, USA
email: cxdeng@umich.edu

Opponent: Professor Chrit Moonen, Ph.D.
Image Sciences Institute
University Medical Center Utrecht
P.O. Box 85500
3508 GA UTRECHT, THE NETHERLANDS
email: C.Moonen@umcutrecht.nl

ABSTRACT

Therapeutic ultrasound is clinically used to accelerate bone fracture healing. It alleviates osteoarthritic pain and improves joint functionality in the form of physiotherapy. The combination of stem cell engineering and therapeutic ultrasound has potential to differentiate and stimulate cells in scaffolds. However, the exact ultrasound mechanism causing these effects is unclear. *In vitro* studies form the biological and physical bases for this technique, and also provide the environment wherein the engineered cell structures are exposed. Ultrasound stimulation may not be repeatable in common *in vitro* setups that are usually optimized for culturing and biochemical assays. This results in variation in the exposure, and may affect the properties of the engineered material. In this thesis, cartilage and bone cells were sonicated in *in vitro* systems. Ultrasound-induced temperature elevation was measured and the stimulating effect of ultrasound was compared with temperature elevation alone. In addition, non-invasive acoustic and optical measurement methods were used to show the complex nature of *in vitro* sonications. Results indicated that ultrasound stimulation, not temperature rise alone, induces proteoglycan synthesis in primary bovine chondrocytes. Ultrasound activated Wnt/β-catenin signaling in human osteoblastic MG-63 cells through both the thermal and non-thermal routes. Thermocouple and infrared camera measurements showed that many configurations are likely to have ultrasound-induced temperature elevations. Ultrasound standing waves were generated in typical exposure conditions and were sensitive to setup details. Optical measurements indicated that guided Lamb waves are generated on the commercial cell wells. Our results indicate that ultrasound exposures in common *in vitro* configurations are complex and highly variable.

Universal Decimal Classification: 534-8, 534.29, 534.321.9

National Library of Medicine Classification: QT 34, QT 36, WB 515, WE 200, WE 300

Medical Subject Headings: Ultrasonics; Ultrasonic Therapy; Sonication; Bone and Bones; Fractures, Bone; Osteoblasts; Cartilage; Chondrocytes; Osteoarthritis; Temperature; Proteoglycans/biosynthesis; Wnt Signaling Pathway; Microarray Analysis; Optical Imaging; Thermography; Stem Cells; Tissue Engineering; In Vitro Techniques

Yleinen Suomalainen Asiasanasto: Ultraääni; Ultraäänihoito; Luu; Luunmurtumat; Rusto; Nivelrikko; Lämpötila; Kuvantaminen; Lämpökuvaus; Kantasolut; Kudosteknologia; In vitro -menetelmä

Preface

This work was done at the University of Eastern Finland (formerly the University of Kuopio) in the Department of Applied Physics during the years 2005 to 2014. I would like to acknowledge the following persons and institutions that have made it possible to accomplish this work, a work which turned out to be much more time-consuming and laborious than I could ever imagine.

I am sincerely grateful to my principal supervisor, Professor Kullervo Hynynen, Ph.D. It has been a privilege to work under his guidance and be able to witness a small part of his (immeasurable) knowledge in the field of ultrasound. I am utmost grateful to my supervisor Research Director Mikko Lammi, Ph.D. He has patiently guided and helped me throughout the thesis. I acknowledge the Department of Applied Physics for the possibility to complete the thesis.

I thank the official reviewers, Professor Diane Dalecki, Ph.D. and Professor Cheri X. Deng, Ph.D. for their willingness to pre-examine this work. I acknowledge Professor Chrit Moonen, for his work as an official thesis opponent. I am deeply grateful for the vital contribution that these experts have given for the thesis and dissertation.

I acknowledge my co-authors and research partners, Docent, senior lecturer Anitta Mahonen, Ph.D.; Anu Olkku, Ph.D.; Hannu Karjalainen, Ph.D.; and Milla Kopakkala-Tani, M.Sc., M.D. You have been a vital part of this work. Anu, Milla, and Hannu: I will never forget the time we spent working together.

I also thank my other co-authors, Professor Juha Töyräs, Ph.D.; Professor Jukka Jurvelin, Ph.D.; and Tero Karjalainen, M.Sc. I acknowledge Meaghan O'Reilly, Ph.D. for the extensive English review and detailed comments to my articles and thesis. I acknowledge editor Michelle Hynynen and Anna Kristoffersen, Ph.D. for the English review and comments to my

thesis. I am grateful to instrument designer Jukka Laakkonen and technician Juhani Hakala for guiding the very basics of, for example, the lathe and milling machines. I acknowledge laboratory technicians Elma Sorsa and Eija Korhonen for their help. I also thank the personnel of the Department of Applied Physics.

I am in debt to Tero Karjalainen, my colleague in the Biomedical Ultrasound Group and manager in department. He has been an indispensable person to creating a framework for this work and a great source of motivation. I acknowledge other group members, Janne Heikkilä, Ph.D.; Aki Pulkkinen, Ph.D.; and Jussi Aarnio, M.Sc.

I am in deep debt to my loving parents, Tarja and Esko, for their sincere support throughout my life. I thank my older sister Katja for backing up her little brother. My deepest gratitude goes to my dear wife Saara for her endless support and encouragement. In so many occasions she has helped me to "see the wood for the trees." This work is dedicated to her and to our two superb sons, Olavi and Otto ("The Quicksilvers").

Finally, I acknowledge the funding from the Academy of Finland, the Heikki and Hilma Honkanen Foundation, the Finnish Cultural Foundation North Savo Trust, and the TBGS Graduate School.

Kuopio, January 7, 2015

Jarkko Leskinen

LIST OF ABBREVIATIONS

CW	continuous wave
dc	duty cycle
I_{SAPA}	intensity, spatial-average pulse-average
I_{SATA}	intensity, spatial-average temporal-average
I_{SATP}	intensity, spatial-average temporal-peak
I_{SPTP}	intensity, spatial-peak temporal-peak
I_{TA}	intensity, temporal-average
LIPUS	low-intensity pulsed ultrasound
PRF	pulse repetition frequency
P_{TA}	acoustic power averaged over pulse period
PZT	plumbum(lead)-zirconate-titanate
RF	radio frequency

LIST OF SYMBOLS

a	radius
C_P	specific heat capacity
c, c_β	longitudinal phase speed of sound and phase speed including medium nonlinearity, respectively
c_P	Lamb wave speed of sound
c_R	Rayleigh speed of sound
c_s	shear phase speed of sound
d, h	plate full-thickness and half-thickness, respectively
F	radiation force
f	frequency
f_M	Minneart frequency
I	intensity
K, G	bulk and shear modulus, respectively
k	wavenumber
P_0	ambient pressure
p	acoustic pressure amplitude
Q	geometric factor
R, T	reflection and transmission coefficient, respectively
R_0	mean bubble radius

T	temperature
t	time
u	particle displacement amplitude
v	flow velocity
W	ultrasound beam total power
Z	acoustic impedance
z	axial distance
z_{LAM}	distance to last axial maximum
z_R	Rayleigh distance
α	absorption
β	nonlinearity parameter
γ	polytropic coefficient
λ	wavelength
$\theta_{i,r,t}$	indices of incident, reflection, and refraction, respectively
ν	kinematic viscosity
ρ	density
ω	angular frequency

LIST OF ORIGINAL PUBLICATIONS

The thesis is based on the original following articles, referred to by the bold Roman numerals **I** to **V**.

I M. Kopakkala-Tani*, J. J. Leskinen*, H. M. Karjalainen, T. Karjalainen, K. Hynynen, J. Töyräs, J. S. Jurvelin, and M. J. Lammi, "Ultrasound stimulates proteoglycan synthesis in bovine primary chondrocytes," *Biorheology* **43**(3–4), 271–282 (2006).

II J. J. Leskinen, H. M. Karjalainen, A. Olkku, K. Hynynen, A. Mahonen, and M. J. Lammi, "Genome-wide microarray analysis of MG-63 osteoblastic cells exposed to ultrasound," *Biorheology* **45**(3–4), 345–354 (2008).

III A. Olkku*, J. J. Leskinen*, M. J. Lammi, K. Hynynen, and A. Mahonen, "Ultrasound-induced activation of Wnt signaling in human MG-63 osteoblastic cells," *Bone* **47**(2), 320–330 (2010).

IV J. J. Leskinen, A. Olkku, A. Mahonen, and K. Hynynen, "Nonuniform temperature rise in *in vitro* osteoblast ultrasound exposures with associated bioeffect," *IEEE Trans Biomed Eng* **61**(3), 920–927 (2014).

V J. J. Leskinen and K. Hynynen, "Study of factors affecting the magnitude and nature of ultrasound exposure with *in vitro* set-ups," *Ultrasound Med Biol* **38**(5), 777–794 (2012).

*equal contribution

AUTHOR'S CONTRIBUTION

The publications are a result of collaboration of all persons mentioned in the original studies. The author has participated in the study design of each publication. In each publication, the author has constructed, calibrated, and operated the sonication systems. The author has analyzed the data and reduced it to publishable format. The author has been the main writer in all publications, in publications **I**, **II**, and **III** together with M. K-T., H. M. K., and A. O., respectively. The work has been supervised by the supervisor Prof. Lammi and the principal supervisor Prof. Hynynen.

Contents

1 Introduction

In therapeutic ultrasound applications, high frequency sound waves alleviate pain, stimulate tissue repair, modify cells and cell constructs, or destroy malignant, diseased tissue. Ultrasound administration is routinely made from the outside of the body, non-invasively. Ultrasound can be targeted with high precision even into deep tissues and is non-ionizing, allowing repeated treatments through normal healthy tissue.

Several therapeutic ultrasound techniques can be regarded as tools for regenerative medicine [209] and tissue engineering [177]. For example in sonoporation, the interaction of ultrasound and gas bubbles causes the cell permeability to temporarily increase, enabling transportation of materials, for example, DNA, into the cells [19,22,83,137,159,295]. Similarly among patients with leg ulcers, ultrasound treatments have been shown to accelerate the impaired wound healing [29,69,70].

Specific interest has been focused on traumatized or diseased bone and cartilage tissues and their biophysical manipulation using therapeutic ultrasound. In principle, this method is used in somewhat comparable manner to mechanical micromanipulation [104] and other non-invasive methods like external electric or electromagnetic fields [20,27]. It is often referred to as low-intensity ultrasound or low-intensity pulsed ultrasound (LIPUS) when ultrasound is applied in repeated short bursts. It shares many conventions and settings with ultrasound physiotherapy, which is routinely used on soft tissues and cartilage ailments. However, generally in low-intensity applications the treatment is administered in regular short intervals (daily) for long times (up to several months) using average acoustic intensities from tens to few hundreds of mW/cm^2 which is less than 1–2 W/cm^2 that is typically used with physiotherapy [82,248]. Importantly, the mechanism behind the favorable tissue effect is thought not to be the ultrasound-

induced temperature elevation, but primarily some other (mechanical) ultrasound effect [46,59,65,71,259]. This is often called a non-thermal effect. Technically it is distinct from shock-wave lithotripsy therapy, which utilizes extremely high acoustic pressure pulses of only a few microseconds in length (review of this topic [336]).

To further develop this technique and to overcome the limited tissue healing capabilities of bone and cartilage, ultrasound stimulation methods to enhance stem cell–based tissue engineering [226,261] have been developed. At its best, ultrasound could differentiate, stimulate, and maturate bone and especially cartilage structures *in vitro* and *in vivo*.

Ultrasound sonication has been shown to accelerate bone fracture healing in animal models and in clinical studies. At the moment, a LIPUS device for the treatment of human fresh bone fractures and bone non-unions lacking the normal bone healing capacity is commercially available (Exogen®, Smith & Nephew, TN/Bioventus LLC, NC, USA). Animal models have suggested that ultrasound intervention could be used, for example, in osteoporotic bones and fractures [30,38,191]. In cartilage, traditional higher-intensity ultrasound stimulation has been reported to alleviate osteoarthritic pain and improve joint functionality [274]. In animals, ultrasound has been reported to repair injured or arthritic cartilage using acoustic intensities comparable to those produced by the clinical bone-healing device [49,109,134]. Studies have further indicated that the combination of stem cell tissue engineering and low-intensity ultrasound has the potential to differentiate and stimulate cell constructs [42,53,74]. Unfortunately, despite extensive research and numerous biological findings, the exact physical ultrasound mechanism causing these favorable effects is not known [46,158,207].

A large number of *in vitro* studies have formed the biological and also physical bases for the stimulation (see Chapter 3.6). These studies provide guidance especially for ultrasound tissue engineering that uses similar *in vitro* setups to grow and expose the cells or cell constructs. The common culturing conditions

and configurations that are optimized for cell welfare and biochemical assay accuracy allow ultrasound implementation, but in many cases in a simplified fashion that creates acoustically complex exposure conditions that may not be repeatable without demanding calibration measurements. The lack of adequate calibration measurements may result in variations during and between the ultrasound exposures that will affect the biological material properties and quality.

In many studies, the cells are placed close to the transducer face in the acoustic near field (for example [57,239,252]). This short distance simplifies the experimental setup in that it allows the use of acoustic gel to couple the transducer to the cell chamber instead of using liquid coupling. However, this simple setup creates an acoustically complex situation: a spatially varying ultrasound exposure. The acoustic field is further complicated by the transmission through the cell chamber. The cell chamber or tube is usually made of a plastic material. Cells in monolayer or three-dimensional matrix are in direct contact to this plastic. Before ultrasound can propagate to the cells, sound waves must travel through the plastic bottom of the chamber. During the transmission, the reflection and absorption of the wave at the plastic-liquid interfaces and in the plastic material, respectively, attenuate the wave. After passing though the cells, the sound travels inside the chamber in the culture medium column, which is in most cases only a few millimeters high. Nearly perfect sound reflection occurs at the medium-air interface, resulting in reverberations and standing waves between the air, cell chamber bottom, and transducer face.

The sound absorption in plastics combined with the multiple reflections makes the *in vitro* systems very vulnerable to temperature elevations. Unfortunately, temperature measurements are not routinely conducted or reported in studies. As the sound transmits to the cell culture chamber, wave mode conversion may occur. Therefore, the ultrasound exposure of the cells may be influenced not only by longitudinal waves, which are usually considered, but also by shear waves, and surface waves.

All these factors complicate the calibration and repeatability of the exposures. The co-existence of multiple wave modes also hinders the specification and optimization of effective ultrasound exposures. However, detailed studies exploring these phenomena in common *in vitro* configurations have not been reported.

The aims of this thesis were (1) to establish and expand the effectiveness of ultrasound exposures for tissue engineering by conducting cartilage and bone cell *in vitro* sonications; (2) to systematically measure the ultrasound-induced temperature elevations, show the susceptibility of *in vitro* configurations to ultrasound-induced heating, and compare the stimulating effect of ultrasound and temperature elevation on bone cells; and (3) to show, using non-invasive measurements, the complex nature of *in vitro* ultrasound exposures relevant to tissue regeneration and engineering.

First, the bovine cartilage cells were exposed to ultrasound or temperature elevation alone (publication **I**). After one to five days of daily exposures, the proteoglycan synthesis levels were measured and the two exposure methods were compared. In the second study, human osteoblastic MG-63 cells were exposed to ultrasound using a setup with minimal temperature elevation and standing wave formation (publication **II**). Through a genome-wide microarray analysis, the genes responsive to ultrasound stimulation were sorted. Based on the micro-array observation, in the third study activation of Wnt cell signaling in MG-63 cells after ultrasound exposure was studied (publication **III**). The exposure setup was modified from the previous one based on the observations from the sonoporation study [160] and a review of the literature. The sonications were done using two setups, either including or excluding a thermal component arising from the ultrasound. In the fourth study, the temperature elevation distribution after ultrasound exposure was studied using temperature-dependent Wnt signaling, fine-wire thermocouple measurements, and non-invasive infrared imaging (publication **IV**). Finally, to characterize the *in vitro* acoustic exposure conditions, sound transmission, standing

wave formation, radiation force effect, and wave mode conversion were studied using pulse-echo ultrasound, non-invasive laser Doppler vibrometery and acousto-optical Schlieren measurements (publication **V**).

2 Ultrasound Wave Propagation and Interaction with Tissue and Tissue Culture Plates

2.1 ACOUSTIC FIELD

In most therapeutic ultrasound applications, the temporal duration of the ultrasound wave is long, and the wave is delivered either as a continuous wave (CW) or as wave bursts comprising ten or more acoustic cycles. Thus, the delivered ultrasound may be approximated as narrow-band, nearly monochromatic longitudinal waves.

The acoustic pressure field from a planar ultrasound source in a homogenous medium is commonly divided into two distinct regions. The first is the field close to the transducer. This acoustic near-field, or Fresnel zone, is governed by diffraction. For a transducer operating at a fixed frequency, the near-field has pronounced pressure variation both in the direction of sound propagation and perpendicular to it (Fig. 2.1). The span of the near-field depends on the speed of sound in the medium c, the acoustic frequency f, and the radius of the transducer a. For a circular plane piston transducer, the near-field can be estimated to extend to distance $z_{LAM} = a^2/(c/f) = a^2/\lambda$, where z_{LAM} is the distance from the source to the last axial maximum and λ = acoustic wavelength [60]. A more conservative estimate for the near-field distance is the Rayleigh distance $z_R = \pi z_{LAM}$. For the plane non-focused transducer, the distance z_{LAM} is the natural

focal distance from the source. The half beamwidth is minimized [244,365] at this distance.

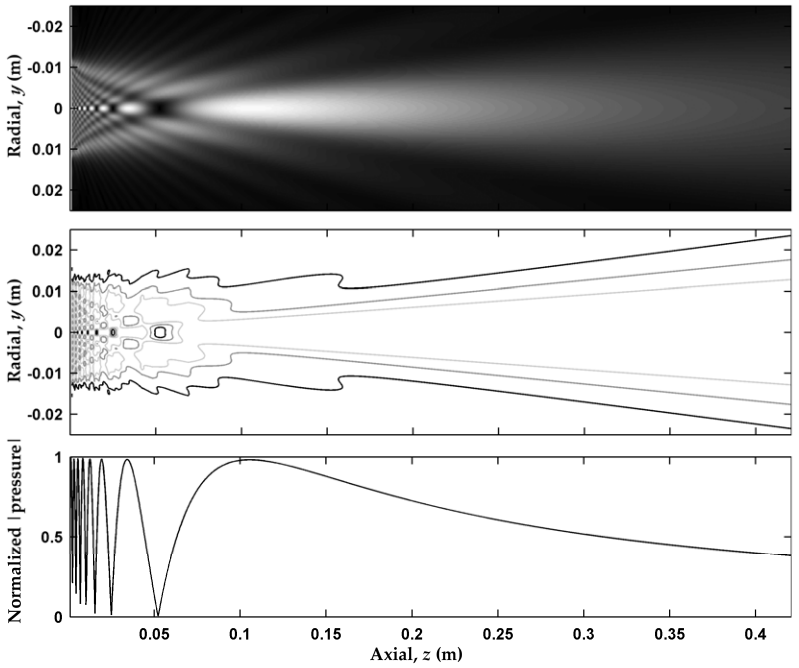

Figure 2.1. *(Top). Normalized acoustic pressure amplitude distribution for a planar circular transducer. Normalization is relative to the point* (z_{LAM}, *0). (Center). Contour plot showing the -3, -6 and -12 dB pressure contours. Contours are normalized at each axial distance. (Bottom). Normalized axial pressure distribution when y = 0. (c = 1485 m/s, f = 1 MHz, a = 12.5 mm,* z_{LAM} *= 105 mm, radial and axial axes are not in scale).*

The last axial maximum can be enhanced by moving it closer to the transducer, using an acoustic lens or a spherically curved transducer. The acoustic focus will be located close to the geometric focus of the curved transducer. By decreasing the radius of curvature, the diameter and the length of the focus can be decreased resulting in an increase in pressure amplitude at the focus for a given source pressure. Focusing can also be accomplished using acoustic reflectors, or electrical focusing of phased arrays [142].

The second sound field region after the near-field is the acoustic far-field (Fraunhofer zone). In this region, the wave

fronts resemble expanding spherical waves and the spatial amplitude decreases accordingly in the axial direction (Fig. 2.1).

2.2 SOUND PROPAGATION IN A MEDIUM

During propagation in a medium, the ultrasound wave is subjected to non-linearity and attenuation. At high acoustic pressures, the sound wave propagation is distorted. During the positive acoustic pressure phase of the wave, the propagating wave and the particle velocity are in the same direction, resulting in a higher speed of sound. Where there is negative pressure, the particle velocity opposes that of the propagating wave, resulting in a lower speed of sound. Thus the compressional part of wave catches up to the rarefactional part. This is known as the convective nonlinearity. If the material stiffness is higher (lower) at the compressional (rarefactional) locations, this results in a higher (lower) speed of sound and a larger distribution of speeds within the pressure wave. This effect is known as the material nonlinearity. The non-linear phase of the speed of sound, c_β, for the propagating pulse can now be defined as $c_\beta = c + (1 + B/2A)u = c + \beta u$, where u = particle velocity amplitude and $\beta = 1 + B/2A$ is the nonlinearity parameter for the medium [180]. Nonlinearity causes distortion of the pressure wave shape, resulting in the buildup of higher harmonic frequencies ($2f$, $3f$, $4f$, …) in the acoustic waveform as the distance from the source increases.

The sound wave is attenuated due to the absorption in the medium, scattering from the particles in the medium, and reflection from the acoustic interfaces. If the intensity of the incident wave is I_0, then for the wave propagation path length z, the intensity can be written as $I = I_0 e^{-2\alpha z}$, where α is the amplitude attenuation coefficient (cm^{-1}) that includes the effects of both absorption and scattering. The absorbed component of the wave energy is dissipated to the medium. Neglecting the thermal conduction, the rate of temperature rise due to the absorption can be estimated as $dT/dt = 2\alpha I/(\rho C_P)$, where C_P is the

specific heat capacity (J/kgK) [142]. Sound that is scattered or reflected by particles in the medium will change its direction of propagation, resulting in increased attenuation of the beam. The ultrasound attenuation in soft tissues and trabecular bone increases approximately linearly with frequency up to 2 MHz [105,346].

In materials with low viscosity, such as liquids, the sound absorption causes bulk medium movement known as acoustic streaming. This flow of fluid is due to the Rayleigh radiation pressure within the medium. A simplified equation describing the flow velocity is $v = (2\alpha I/c\nu)d^2Q$, where ν is kinematic viscosity, d is beam diameter, and Q is a system-specific geometric factor. Medical transducers are capable of generating streaming with velocities of several centimeters per second when operated in liquids [304,305].

If the exposed medium contains small gas bubbles or the negative pressure amplitude is high enough to extract gas from the tissue to form bubbles, the bubbles may act as nuclei for acoustic cavitation [180]. The likelihood for cavitation processes increases with increasing negative pressure and with decreasing frequency [8,16]. Acoustic cavitation is generally divided into two different categories: non-inertial (stable) and inertial (transient) cavitation. In non-inertial cavitation, the gaseous inclusion oscillates in the acoustic field [180]. The amplitude and phase of the bubble oscillation depends on its size in respect to the resonant bubble size at the acoustic frequency. For approximately resonant size bubbles, the velocities of bubble motion and forcing pressure field are in-phase and the amplitude of the bubble motion is significantly increased. Depending on the size of the bubbles with respect to the resonance size, the bubbles may attract or repel each other through a radiation force between the bubbles known as the secondary Bjerknes force. When the acoustic pressure is elevated, the bubble oscillation becomes nonlinear. The nonlinearly oscillating bubbles sends sound at the harmonics, ultraharmonics ($3f/2$, $5f/2$, $7f/2$, …) , and subharmonics ($f/2$, $f/3$, $f/4$, …) of the acoustic frequency [234]. If the acoustic amplitude

is sufficiently high, the bubbles may grow due to rectified diffusion [79]. In rectified diffusion, during the rarefactional phase, the bubble in liquid expands. The gas concentration inside the bubble is therefore lowered resulting in a diffusion of gas into the bubble. The opposite happens during the compressional part of the wave. However, the bubble surface area which is available for this flow is larger for the expanded bubble. Thus the net flow of gas during one acoustic cycle is higher into the bubble than from out of it. In addition, the liquid shell around the bubble becomes thinner and thicker during the expansion and contraction phases, respectively. Thus, the gradient of the gas concentration is higher during the expansion-phase resulting in higher gas diffusion into the bubble compared to gas outflow during the contraction-phase. As a result of these effects, the time-average size of the bubble increases.

During bubble growth and oscillation, the bubbles may create local perturbations in the liquid medium resulting in small-scale fluid streams at the periphery of the bubbles. This phenomenon is known as microstreaming [78]. If the amplitude of the pressure source is further elevated and the bubble growth further increased, during the contraction of the bubbles, the inertia of the surrounding medium may become so large that the increasing gas pressure in the bubbles is not able to arrest the compression, resulting in a violent and rapid bubble collapse [84]. The cavitation process that leads to bubble collapse is known as inertial cavitation. During the collapse, the microscopic temperature elevation and pressure rise may be several thousand Kelvins and hundreds of MPas, respectively [84]. Neighboring interfaces may be punctured and eroded due to the high-speed liquid jets, and the formation of chemical free-radicals is possible [64,216]. A suitable bubble size is one of the most important pre-requisites for inertial cavitation. For air bubbles in water, the resonance size for the bubbles can be estimated using Minnaert resonance frequency $f_M = 1/(2\pi R_0)(3\gamma P_o/\rho)^{1/2}$, in which R_0 is the mean bubble radius (m), γ is the polytropic coefficient (1.4 for air), and P_0 is the ambient

pressure [180]. This can be approximated as $f_M R_0$ = 3.3 m/s. Artificial gas bubbles of approximately resonant size and having high echogenity can be administered to achieve and amplify cavitation [331].

When an acoustic wave meets an acoustic interface, part of the wave is reflected (Fig. 2.2). Assuming plane waves, real acoustic impedances (density ρ multiplied with c) and an interface having dimensions much larger than the wavelength, the incidence angle-dependent coefficient for pressure reflection is [161]

$$R = \frac{Z_2 \cos\theta_i - Z_1 \cos\theta_t}{Z_2 \cos\theta_i + Z_1 \cos\theta_t}, \tag{2-1}$$

where $Z_{1,2}$ are the acoustic impedances in media 1 and 2, respectively, and θ_i and θ_t are the incident and transmission angles, respectively.

The coefficient for transmitted pressure at the boundary can be formulated as

$$T = \frac{2Z_2 \cos\theta_i}{Z_2 \cos\theta_i + Z_1 \cos\theta_t}. \tag{2-2}$$

For the transmitted wave intensity and power, the reflected part is $R_I = R^2$ and the transmitted part is

$$T_I = \frac{4Z_1 Z_2 \cos\theta_i \cos\theta_t}{(Z_2 \cos\theta_i + Z_1 \cos\theta_t)^2}. \tag{2-3}$$

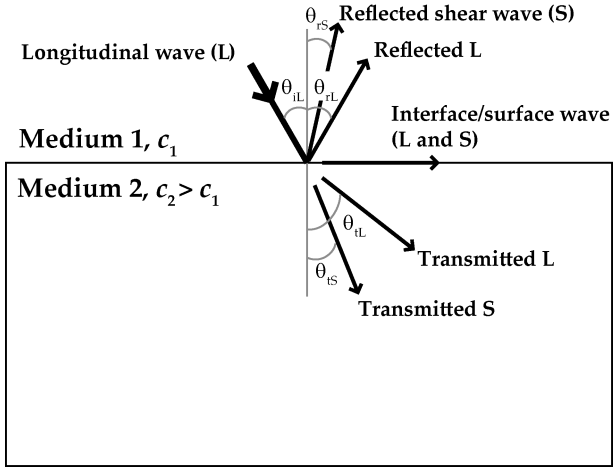

Figure 2.2. *Longitudinal wave reflection and refractive transmission between media 1 and 2. The speed of sound c in medium 1 is lower than the speed of sound in medium 2. L = longitudinal wave, S = shear wave, θ = angle respect to the normal of the interface, i = incident, r = refracted, and t = transmitted. Modified from [271].*

These equations do not take into account the frequency dependency of the transmission in the case of wavelength-scale objects or the generation of shear and surface waves in solids through acoustic wave mode conversion [26,271].

When the reflected wave encounters the incident wave, a standing wave pattern is created [161]. If the incident wave has pressure amplitude of p_0 = 1, the amplitude for this summed incident and reflected wave having an amplitude R can be written

$$p = \left[(1+R)^2 \cos^2(k_1 z) + (1-R)^2 \sin^2(k_1 z)\right]^{1/2}, \tag{2-4}$$

where $k_1 = 2\pi/\lambda_1$ is the wave number in medium 1. In a special case of reflection from water-air interface ($Z_2 << Z_1$, R = -1), the resulting standing wave pressure can be written as

$$p = 2\sin(k_1 z), \tag{2-5}$$

which has the maximum amplitudes, or antinodes, at $p = 2$ at $z = -n\lambda/4$ ($n = 1, 3, 5, \ldots$) relative to the reflecting surface at $z = 0$. Respective pressure minima, or nodes, are at the positions $z = -n\lambda/2$ ($n = 0, 1, 2, 3, \ldots$). Standing wave patterns have distinct pressure antinodes or nodes in $z = \lambda/2$ intervals. When a standing wave is established in a fluid containing particles or gas bubbles, they are affected by a substantial radiation force known as the primary Bjerknes force [180]. This force separates the particles into the pressure antinode or node positions depending on the particle size and the operating frequency. This force is capable of moving and holding cells or cell-size particles inside the blood vessels or in chambers, establishing spatial patterns that replicate the standing wave [47,68,94,95,170].

A steady force originating from the attenuation of the propagating wave on absorbers or reflectors in the beam path due to the transfer of wave momentum is known as Langevin radiation force [307,326,350]. In case of when the sound beam hits a perfect sound absorber, the force on the absorber is $F = W/c$, where W is the acoustic power (W). For targets having absorption α, the generated force is $F = 2\alpha I/c$, where $I = I_{TA}$= the time-average intensity and F is a force per unit volume [237]. For a perfect sound reflector, the force is doubled $F = 2W/c$. Both the absorption and the scattering contribute to the generated force when the target deviates from a perfect absorber or reflector.

2.3 WAVE MODE CONVERSION

When a longitudinal wave propagates through a medium interface, its energy is distributed into longitudinal, shear and surface waves (Fig. 2.2). In fluids such as water, the incident and reflected waves can only be longitudinal, as shear waves are not supported in fluids. The longitudinal speed of sound c, and the shear speed of sound c_S in solids can be calculated using the equations $c = [(K+4/3G)/\rho]^{1/2}$ and $c_S = (G/\rho)^{1/2}$, respectively.

Parameters K and G are the bulk and shear modules, respectively. In hard solids, the shear speed is approximately half of the longitudinal speed of sound, reducing both the wavelength and acoustic impedance. The reflection and refraction angles can be calculated using Snell's law, $c_1\sin(\theta) = c_2\sin(\theta)$. When $c_1 < c_2$, the first critical angle is defined as $\theta_{CR1} = \sin(c_1/c_2)^{-1}$. Ideally at this angle, the longitudinal wave reflects at angle θ and is converted to surface or interface waves in medium 2. Shear waves continue to propagate in medium 2 at angle θ_S. The second critical angle is defined as an incident angle that results in a 90° shear refraction angle $\theta_{CR2} = \sin(c_1/c_{2S})^{-1}$. Above this second critical angle, only surface or interface waves can propagate in medium 2 [271]. Compared to longitudinal wave attenuation, the reported values indicate that shear wave attenuation is approximately twice as high in cortical bovine bone (70 Np/m/MHz vs. 130 Np/m/MHz) [355] and significantly higher in several commercial plastics (approximately 24–64 Np/m/MHz vs. 250–300 Np/m/MHz) [356]. In soft tissues including bovine muscle, the shear attenuation is roughly three to four orders of magnitude higher than the longitudinal attenuation (3–10 Np/m/MHz) [105,142,200].

In addition to mode conversion to shear waves, induction of interface and surface waves is also possible. Several types of acoustic surface waves can propagate along solid isotropic materials. These include Rayleigh surface waves along a free semi-infinite solid interface, Stoneley interface waves along a semi-infinite solid–solid interface, Scholte interface waves along a semi-infinite solid-liquid interface, and Lamb waves along a solid free plate [271]. In a liquid immersed solid, the wave may become leaky, in other words, energy is radiated to the surrounding liquid. Leaky Rayleigh waves having speed c_R can propagate if the bulk shear speed c_S of the solid is nearly equal to or larger than the longitudinal speed of sound c in the surrounding liquid [223], thus limiting their presence in hard solids. Rayleigh speed is generally slightly less than c_S. In the case of a soft solid-liquid interface ($c_S < c$), for example, polymers in water, Scholte waves propagate so that almost all the energy

of the wave is in the solid, resulting in propagation that is sensitive to the properties of the solid [102].

Lamb waves are a result of coupled longitudinal and shear waves, and both symmetric (S) and antisymmetric (A) Lamb wave modes can propagate in free (air) or liquid-immersed plates (Fig. 2.3). Symmetry is defined by the particle displacements with respect to the center of the plate. The Lamb wave excited plate shows both in-plane and out-of-plane particle displacements. For a free plate having a thickness of $2h$, the Rayleigh-Lamb wave dispersion equations can be written as [271]

$$\frac{\tan(qh)}{\tan(sh)} = -\left[\frac{4k^2sq}{\left(q^2-k^2\right)^2}\right]^{\pm 1}, \tag{2-6}$$

where exponents +1 and -1 are for the symmetric and antisymmetric Lamb wave modes, respectively. The actual dispersive Lamb velocity is under the terms $s^2 = (\omega/c)^2 - k^2$ and $q^2 = (\omega/c_S)^2 - k^2$. Here $k = 2\pi f/c_P$, in which c_P is the Lamb wave phase velocity. Several symmetric and antisymmetric modes having different speeds and particle displacement shapes (in-plane and out-of-plane movement) can propagate on the same plate. Starting from the frequency-plate thickness product $fd = 0$, the velocity of the zero-order modes c_P approaches c_R from $c_P < c_R$ (A0) or $c_P > c_R$ (S0) as the fd increases. The higher-order modes $fd > 0$ approach the shear speed c_S from $c_P > c_S$. The fluid loading of a plate has been shown to affect the propagation of Lamb waves especially when c_S and c, and the densities of the plate and liquid are of the same order, respectively [86,270]. Low-frequency guided Lamb waves have been observed through pulse-echo ultrasound in pulsing human heart walls [154], as well as in externally vibrated pig myocardium, spleen phantoms and *in vivo* pig heart [232,233,333]. Lamb waves have been generated in long bones *in vivo* [235] and in bone phantoms [58,263] using ultrasound excitation.

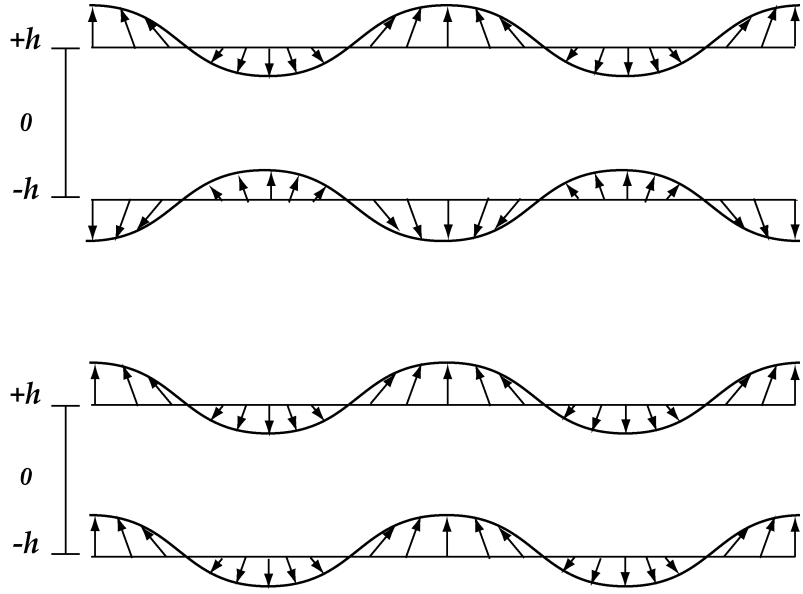

Figure 2.3. *Illustration of symmetric (top) and antisymmetric (bottom) guided Lamb waves propagating in 2h thick plate. The arrows indicate the particle displacements at the plate. Modified from [271].*

3 Therapeutic Ultrasound in Bone and Cartilage

3.1 BONE

Bone is a complex connective tissue that has several important functions in the body [52]. Bones form a structure to which the muscles can attach; they protect the internal organs in the body; they serve as mineral storage; and they are the location for blood cell production. Bone matrix consists mostly of inorganic (hydroxyapatite, 65% of bone mass) and organic (mostly type I collagen) material. Other organic components include proteins such as bone sialoprotein, fibronectin, osteocalcin, osteonectin, osteopontin, enzymes (collagenase, alkaline phosphatase; ALP), growth factors (transforming growth factor-β; TGF-β), and cytokines (prostaglandin E_2; PGE_2, interleukins; IL-1, IL-6).

Bone has two main structural parts. The outer periosteum-covered dense part of the bone is the compact bone. It has concentric ring-like structures known as osteons. In osteons, layers of concentric bone lamellae surround canal-like structures known as Haversian canals. The blood vessels and nerves go inside these canals. Under the compact bone, the structure is highly porous and is called trabecular bone. Trabecular bone forms the medullar cavity which contains the bone marrow. Bone marrow is the source for blood cell production and the location of multipotent stromal (stem) cells that can differentiate to, for example, bone or cartilage cells.

Several different cells are present in bone [52]. Osteoprogenitor (stem) cells are located at the bone periousteum and differentiate to osteoblasts. Osteoblasts, the bone forming cells, are found on the surfaces of the bones. Fully matured osteoblasts transform to osteocytes which are numerously present inside the bone matrix (within lamellae). Osteocytes,

which are connected to each other by tiny canal-like structures (canaliculi), are assumed to play an important role in sensing mechanical perturbations. Osteoclasts are specialized cells which can resorb bone tissue to its basic elements so it can be re-used by the osteoblasts to form new bone. Bone tissue has high capability to regenerate and repair. Normal bone growth (modeling) and bone structure maintenance (remodeling) are both a balanced action and interaction of osteoblasts and osteoclasts. Osteoblasts and osteoclasts create the functional unit of bone known as the basic multicellular unit.

A fractured bone can heal either through direct intramembranous (primary) healing or through indirect (secondary) healing [205]. In direct fracture healing, the fracture gap between the bone ends is filled with bone by the osteoclasts and the osteoblasts, and then remodeled into final lamellar bone. Direct healing is rare without external intervention and requires that the fracture ends are nearly in contact (separation < 1 mm). In addition, the fracture ends must be rigidly fixed, thus eliminating any movement. Therefore, the more common type of fracture healing is indirect healing which can fill larger gaps. Indirect healing also benefits from small mechanical perturbations of the fracture. It encompasses both intramembranous healing and endochondral healing in which cartilage tissue is temporarily constructed and then remodeled into bone tissue.

Indirect healing consists of several different phases [205]. The inflammatory phase occurs immediately after the trauma, creating a haematoma which consist of the cells from blood circulation and bone marrow around the fracture. The haematoma coagulates and creates a loose support around the fracture. During this phase, inflammatory cells such as macrophages secrete tumor necrosis factor-α (TNF-α) and interleukins (IL-1β, IL-6 etc.). Vascular endothelial growth factors which activate the angiogenesis are also induced. Acute inflammatory reaction is highest on the first day and is resolved by one week. In the next phase, granular fibrous tissue, which is formed around the fracture, is transformed into cartilage

through endochondral ossification. First, the mesenchymal stem cells from the surrounding tissue, bone marrow, and possibly systemically from the peripheral circulation, are recruited. The cells are then differentiated to osteogenic cells. This process is orchestrated specifically by bone morphogenetic proteins, such as BMP-2 and BMP-7 and TGF-β proteins. At the end of this process, the fracture is surrounded and supported with hyaline cartilage which expresses high levels of extracellular matrix protein type II collagen and proteoglycans. This structure is known as the soft fracture callus. Simultaneously, intramembraneous ossification generates a hard woven bone callus around the fracture further increasing its rigidity. The cartilaginous appearance peaks around 7 to 9 days post-fracture. Revascularization takes place in the callus. The chondrocytes become hypertrophic, generating calcified mineralized matrix in the callus. This calcified matrix is then resorbed into woven bone through the activation of several proteins such as receptor activator for nuclear factor kappa B ligand (RANKL), osteoprotegerin, and TNF-α. The process of cartilage resorption and hard fracture callus formation peaks at 14 days post-fracture, and shows callus mineralization and presence of type I collagen, osteocalcin, ALP, and osteonectin. The calcified callus is finally transformed into woven bone. In the final stage of fracture healing, the woven bone is remodeled into lamellar bone. This process starts 3 to 4 weeks after trauma and may last for several years.

3.1.1 Wnt/β-catenin signaling in bone

Cellular signaling within single cells and between cells directs the fundamental cellular processes, such as cell development, differentiation, and apoptosis. Specific interest, in the case of bone cell development, has been directed to canonical Wnt/β-catenin which is one of the secreted proteins in the family of Wnt proteins mediating cellular signaling [24]. Wnt/β-catenin signaling has been shown to be activated at different stages of fracture healing [290]. Its induction has been shown to accelerate

fracture healing, while inhibition of this signaling has been shown to induce delayed fracture healing [290].

In Wnt/β-catenin signaling, the Wnt protein binds to the receptors in the plasma membrane of the cell. This initiates an intracellular signaling event in which the phosphorylation of β-catenin protein by glycogen synthase kinase GSK-3β is inhibited, and β-catenin is stabilized. β-catenin levels then rise in the cell cytoplasm and β-catenin is translocated into the cell nucleus. Inside the cell nucleus, it binds to lymphoid-enhancer binding factor (LEF-1) and T-cell transcription factor (TCF). This complex starts then to regulate gene expressions.

3.2 CARTILAGE

Cartilage is a flexible connective tissue found in the ears, nose, skeleton, intravertebral discs, and joints. The types of cartilage found from human body include elastic cartilage, fibrocartilage, and hyaline cartilage.

Articular, hyaline-like cartilage covers the bones at the synovial joints [52,121]. It provides low-friction joint movement and equalizes forces concentrated at the end of the bones. It is nutritioned (mostly) and lubricated by the synovial fluid from the synovial membrane. Articular cartilage is mainly composed of chondrocytes (cartilage cells), collagen fibers (types II, IX, and XI) which form the extracellular matrix, proteoglycans, and water (75-80% of tissue). Proteoglycans consist of glycosaminoglycans (specifically chondroitin-4 and 6-sulfates) connected to a specific protein core. Aggregating proteoglycans bind to hyaluronan chains in a regular pattern. Aggrecan is a specific proteoglycan in cartilage. Proteoglycans are trapped to the extracellular matrix by collagen fibers in complex manner. Negatively charged proteoglycans assist in regulating the water content of the cartilage and in ion binding. Articular cartilage can be divided to four different zones, which from the top to bottom are the superficial or tangential zone, the transitional zone, the deep or radial zone, and the calcified zone above the

subchondral bone. The calcified zone and noncalcified deep zone are separated by a thin undulating layer, termed the tidemark. The calcified zone and tidemark restrict the passage of substances from the subchondral bone into the upper cartilage layers [14].

Articular cartilage is a specialized, avascular, and aneural tissue having very limited healing capacity in cases of injury or deteriorating metabolic disease. Osteoarthritis is the most common joint disease, which slowly but progressively deteriorates the cartilage and underlying bone. Osteoarthritis is characterized by increased proliferative and metabolic chondrocyte activity, by the presence of inflammatory cytokines (interleukins, TNF-α) and collagen-digesting enzymes know as matrix metalloproteinases (e.g. MMP-13), by the dedifferentiation of chondrocytes to fibroblastic cells, and in the final stage, by the formation of osteochondral nodules known as osteophytes on the surface of degenerated cartilage [281].

3.3 CELL-BASED TISSUE ENGINEERING FOR BONE AND CARTILAGE

The principle in tissue engineering is to use methods of biology, chemistry, and physics to replace, repair, and regenerate the tissue and organs in body [177,226]. This can be accomplished using cell, tissue or organ transplants, or by replacing the degenerated tissue with prostheses. In cell-based tissue engineering, cells or specifically stem cells and progenitor cells which have the capability to differentiate into several cell types such as bone and cartilage are harvested, for example, from the cartilage, bone marrow or fat [226]. The cells can be further cultured *in vitro* to advance the cell differentiation and to increase the cell proliferation. The grown cell mass can then be transplanted into the target of treatment for further growth and maturation. The cells can impregnate porous artificial three-dimensional structures known as cell matrices or scaffolds. These structures are engineered to advance tissue growth into it

(osteoconductive/chondroconductive structure). It serves as structural support for the cells enabling extracellular matrix binding, vascularization and fluid flow between the cells. During cell culturing or post-transplantation, the cells can be stimulated to induce cell growth and differentiation using osteoinductive/chondroinductive methods, such as chemical agents (BMP's, growth factors) or external physical stimulants such as ultrasound exposures.

3.4 STIMULATION OF *IN VIVO* BONE

It is estimated that approximately 5% to 10% of the 7.9 million bone fractures occurring annually in the United States suffer from impaired healing [204]. Bone healing can be regarded as normal if healing occurs within three to six months after the fracturing incident. The fracture is defined as a delayed union if it is not united approximately six months after the incident. If the healing has not ended within nine months after the incident and has not shown signs of healing for three consecutive months, the fracture is classified as non-union [236,255]. Several methods have been developed to accelerate bone healing, including ultrasound [75,204].

A set of animal studies was conducted in the 1950s to study the therapeutic effect of ultrasound on bone [9,23,55,201,225]. A few years later, Ardan *et al.* summarized many of these earlier observations and argued that despite all the studies reported, and evidence of some stimulatory effects on bone or bone fracture healing, the results were still inconclusive [10]. In this same study, the authors sonicated dogs having artificial bone defects. Three continuous wave (CW) ultrasound exposures (f = 0.8 MHz) of five minutes in length were delivered, each separated by five minutes of cooling. The spatial-average temporal-average intensity (I_{SATA}) was 0.5 to 2.5 W/cm^2, corresponding to temporal-average acoustic powers (P_{TA}) of 5 to 25 W. The exposures were reported to be either ineffective (at 5 W) or deleterious, causing bone necrosis, fractures, and delayed

bone healing (at 10, 15, 20, and 25 W). The measured maximum temperature elevation in the bone was 31.7°C. Based on current knowledge [283,320,327], this clearly demonstrates that the exposures were causing thermal damage, thus negating any potential beneficial effect. Therefore, it is not a surprise that at the time therapeutic ultrasound was seen to have limited potential to stimulate bone healing. A more extensive review of the early days of therapeutic ultrasound on bone can be found from Schortinghuis *et al.* [286].

In later studies, thermal effects were mitigated through the use of low-intensity CW or pulsed sonications, and positive impacts on fracture healing were reported. The exposure conditions for these studies are detailed in Table 3.1. In 1983, Duarte [59] reported accelerated callus formation and fracture healing in rabbit fibula and femur after pulsed low-power ultrasound exposure. The sonications were executed with short bursts (5 μs) and low (0.5%) duty cycle (dc), and the two tested operating frequencies were equally effective. The measured temperature rise in the bone was only 0.01°C. In that same year, Dyson and Brookes [71] sonicated rat fibula fractures in different stages of healing. The study suggested that ultrasound was the most effective during the inflammatory phase and soft callus formation. This typically translates to treatment given during the first two weeks after the fracture. When the treatment was given only during the hard callus formation stage (weeks three and four), bone healing was impaired and accelerated cartilage formation was observed. Sonications at 1.5 MHz were reported to be more efficient than at 3 MHz (78.6% vs. 56.2% improvement in repair). Acceleration in fracture healing in rabbit legs (17% acceleration, 168 days vs. 203 days) was reported by Klug *et al.* using low intensity CW sonications [162]. A few years later, Pilla *et al.* reported 1.7-fold (17 days vs. 28 days) acceleration in rabbit fracture healing (ultimate bone strength) after low-intensity pulsed ultrasound treatments [257–259]. A temperature rise of 0.1°C was measured from the osteotomy site. In the study by Wang *et al.*, 0.5 MHz and 1.5 MHz operating frequencies were compared in rat femoral

fracture models [338]. The authors reported that pulsed ultrasound treatment with average intensity, I_{SATA} = 30 mW/cm^2, significantly increased (22%) the average maximum torque of the fractures measured 21 days after the operation. Both of the tested operating frequencies were equally effective. However, the stiffness of the fracture site was statistically increased (67%) only at 1.5 MHz. Two years later this same group, using a similar fracture model and ultrasound configuration, reported that at 0.5 MHz statistically significantly increases in the fractures' maximum torque (30%) and maximum stiffness (37%) [357] could be achieved at an intensity of I_{SATA} = 50 mW/cm^2. A higher 100 mW/cm^2 intensity also elevated these parameters, but not in a statistically significant fashion ($p > 0.2$). Furthermore, aggrecan gene expression in ultrasound-stimulated (50 mW/cm^2) fracture calluses was higher than in the non-sonicated calluses seven days after the operation (during the ultrasound treatment period), while it was lower several days after ultrasound treatment had stopped. The authors suggested that the mechanism for improved fracture healing was the acceleration of chondrogenesis and cartilage hypertrophy, resulting in accelerated endochondral ossification.

In 1994, after a decade of studies, the United States Food and Drug Administration approved a clinical device (Exogen®) for the treatment of fresh fractures (treatment initiated within seven days post-fracture) in skeletally mature individuals. In 2000, the device was approved for use with nonunion fractures, excluding skull and vertebrae. The battery-powered and patient-operated device uses the same acoustic parameters that were first introduced by Xavier and Duarte (as cited by [257]) and more generally applied by Pilla *et al.* [257–259]. The current device has a circular planar transducer with an effective radiating area of 3.88 cm^2 and a beam non-uniformity ratio of four [300]. The transducer is directly coupled to skin using acoustic coupling gel, resulting in near-field exposure of the soft tissue–covered bone. The device is generally assumed to have a minimal thermal effect on tissues due to the moderate operating frequency (1.5 MHz), diagnostic level average intensity (I_{SATA} =

30 mW/cm^2 with 1 kHz PRF and 20% duty cycle, 20 minutes daily), and low temperatures measured in *in vivo* animals [259] for a similar device.

Several clinical studies have applied this device. Heckman *et al.* reported 38% acceleration (96 days vs. 154 days) in healing of human tibial cortical fresh fractures [123]. Kristiansen *et al.* reported similar results in human radial cancellous bone fractures [172]. Accelerated healing has been reported also in other bone trauma treatments techniques [62,103,246]. However, sonication has also been reported to be ineffective with fresh fixed tibial fractures [81] and stress fractures [273].

In the case of delayed unions and nonunions, a retrospective analysis of ultrasound-treated patients implied that low-intensity ultrasound could result in up to a 91% success rate for delayed unions and an 86% success rate for nonunions [211]. A recent study from Schofer *et al.* was the first randomized sham-controlled trial dealing with delayed unions and showed a 34% increase in fractured tibial bone mineral density after LIPUS [285].

Further animal studies have provided detailed information about the effects of sonications and have tested new applications for ultrasound bone therapy. The Exogen® device and the acoustic parameters it uses have been studied the most. However, a wide variety of other exposure parameters have been explored as well in numerous studies. The animal and *in vivo* human studies are summarized in Tables 3-1 and 3-2, respectively in chronological, alphabetical order.

Many of the animal studies have provided the foundation for ultrasound-assisted bone healing. The results of these studies have further encouraged the use of this technique for the treatment of various bone diseases and deficiencies and several clinical studies support the use of low-intensity ultrasound intervention for bone fractures. Though the ultrasound-induced fracture-healing acceleration in fresh fractures is significant, perhaps the largest potential for this intervention would be to treat impaired, diseased, or artificially engineered bones. However, recent systematic reviews of human trials concluded

that the evidence is still inadequate and that larger blinded trials, focusing on functional outcomes, that would verify the general efficiency of this fracture treatment modality are needed [28,107]. In Finland, the medical experts have given similar recommendations [3].

Table 3-1. Animal *in vivo* low-intensity ultrasound studies. CW = continuous wave; dc = duty cycle; f = operating frequency; I_{SATA} = spatial-average temporal-average intensity; I_{SATP} = spatial-average temporal-peak intensity; PRF = pulse repetition frequency; T1 = ultrasound sonication time • time span or number of sonications; T2 = time delay between the operation and the start of sonications; ↑ / → / ↓ = ultrasound has stimulating effect / is equally effective / is detrimental respect to the sham treatment or control; ?? = value not clear.

Reference	Sonication parameters	Target of treatment	Main outcome
Ardan *et al.* 1957 [10]	f = 0.8 MHz, CW I_{SATA} = 0.5 to 2.5 W/cm² T1: three 5 min sonications w/ 5 min of cooling T2: 15 min to 2 h	Fractured dog femur	↑→↓ Ineffective (0.5 W/cm²) or deleterious (> 0.5 W/cm²); some neogenesis around the sonications dsite
Duarte 1983 [59]	f = 1.65 or 4.93 MHz PRF = 1 kHz, burst duration 5 µs I_{SATA} = 49.6 (1.65 MHz) or 57 mW/cm² T1: daily for 15 min • 4 to 18 d T2: 24 h	Fractured rabbit tibia or femur	↑ Increased and accelerated callus formation; effect visible after 5 days; no significant difference in operating frequency
Dyson & Brookes 1983 [71]	f = 1.5 or 3 MHz, PRF = 100 Hz, dc = 20 % I_{SATP} = 0.5 W/cm² T1: 5 min/d on 4 consecutive d/wk for 1,2 or 3 wks during 6 wk period T2: 0 to 5 wks	Fractured rat fibula at different stages of healing	↑ 1.5 MHz more effective; should be given during the inflammatory phase and soft callus formation (first two weeks); in later phase cartilage formation
Klug *et al.* 1986 [162]	f = ??, CW I_{SATA} = 0.2 W/cm² T1: 3 min every other day for 8 treatments T2: 14 d	Fractured rabbit lower-leg	↑ Accelerated healing (17%, 168 vs. 203 days)
Pilla *et al.* 1989 [257]	Exogen signal but I_{SATA} = 20 mW/cm² T1: daily for 20 min • up to 28 d T2: 1 d	Fractured rabbit fibula	↑ Accelerated fracture healing
Pilla *et al.* 1990 [258]	Exogen signal but I_{SATA} = 1.5 to 30 mW/cm² T1: daily for 20 min • up to 28 d T2: 1 d	Fractured rabbit fibula	↑ Accelerated fracture healing when I_{SATA} > 1.5 mW/cm²; optimal intensity 30 mW/cm²

Table 3-1 continued

Pilla *et al.* 1990 [259]	Exogen signal T1: daily for 20 min • up to 28 d T2: 1d	Fractured rabbit fibula	↑ Ultimate bone strength comparable to intact bones: ultrasound treated 17 days and control 28 days post-operation
Tsai *et al.* 1992 [327]	f = 1.5 MHz, burst duration = 200 µs I_{SATA} = 0.5 or 1 W/cm² T1: daily for 5, 15 or 25 min • 1 to 4 wks T2: 2 d	Fractured rabbit fibula	↑→↓ Healing is not affected (5 or 15 min) or it is suppressed (25 min) at 1 W/cm²; healing is accelerated at 0.5 W/cm² for all durations while 25 min results in the largest accumulated growth
Wang *et al.* 1994 [338]	Exogen signal but f = 0.5 or 1.5 MHz T1: 15 min/session • 10 sessions during 10 of the first 14 days after the operation T2: 1 d	Fractured rat femora	↑ Increase in maximum torque (22%, both frequencies); fracture stiffness increased significantly only at 1.5 MHz (67%)
Yang *et al.* 1996 [357]	f = 0.5 MHz, PRF = 1 kHz, dc = 20 % I_{SATA} = 50 or 100 mW/cm² T1: 15 min/treatment • 5, 8, 10, or 15 treatments 7, 10, 14, or 21 d after the operation, respectively T2: 1 d	Fractured rat femora	↑ maximum torque and torsional stiffness at 50 mW/cm², statistically insignificant at 100 mW/cm² (after 3 weeks); ultrasound stimulates genes related to cartilage formation
Tanzer *et al.* 1996 [317]	Exogen® T1: daily for 20 min • 2, 3, or 4 wks T2: 1 d	Porous titanium transcortical implants in dog femora	↑ Bone ingrowth to the implants increased by 18%
Spadaro & Albanese 1998 [302]	Exogen® T1: daily for 20 min • 14 or 28 d T2: 3 d	Young rat femur and tibia (intact or periosteal trauma)	→ Ultrasound does not affect bone growth in intact or superficially damaged bone
Shimazaki *et al.* 2000 [297]	Exogen signal T1: daily for 20 min • up to 42 d T2: 7/7 (fast) or 10/17 (normal) days after start of distraction/after operation distraction period 7 d (fast) and 10 d (normal)	Rabbit tibia distraction osteogenesis (fast or normal distraction rate)	↑ Increased hard callus area/bone maturation, mechanical resistance and bone mineral density (normal); bone maturation (fast)
Azuma *et al.* 2001 [15]	Exogen signal T1: daily for 20 min • 8 or 24 d T2: 1, 9, or 17 d	Fractured rat femora (treatments at different phases of healing)	↑ Mechanical torsional properties increased, hard callus or bone mineral content not changed; ultrasound should be given throughout healing process (24 d)

Table 3-1 continued

Takikawa *et al.* 2001 [312]	Exogen signal T1: daily for 20 min • 2, 4, or 6 wks T2: 6 wks after induction of nonunion	Nonunion fracture in rat tibia	↑ Ultrasound healing rate 50% (7/14), 0% in controls (6 weeks)
Tanzer *et al.* 2001 [318]	Exogen® but I_{SATA} = 250 mW/cm² T1: daily for 20 min • 6 wks T2: 1 d	Porous tantalum intramedullary implants in dog ulnae	↑ Bone ingrowth to the implants increased by 119%
Warden *et al.* 2001 [340]	f = 1 MHz, PRF = 1 kHz, dc = 20 % I_{SATA} = 30 mW/cm² T1: 20 min/d, 6 d/wk • 12 wks T2: 0 d after induction of osteoporosis	Intact or osteoporotic rat femur and tibia	→ No effect on intact bone or osteoporotic bone with respect to the bone status (mineral contents, density)
Yang *et al.* 2001 [358]	f = 1 MHz, burst duration = 200 µs, PRF = 1 kHz??, I_{SATA} = 50 mW/cm² T1: daily for 15 min, 6 d/wk • 1, 3, or 5 mo T2: 1 d	Fully defected canine ulna	↑ Accelerated healing in both small and large bone defect groups
Chang *et al.* 2002 [34]	f = 1.5 MHz,PRF = 250 Hz, burst duration = 2 ms I_{SATA}(??) = 0.5 W/cm² T1: daily for 15 min • 1, 2, or 3 wks T2: ??	Fractured rabbit fibula (ultrasound vs. microwave)	↑ Ultrasound having a significant thermal component ($\Delta T_{MAX} \approx$ 10°C) induces new bone growth more efficiently than plain microwave heating
Gebauer *et al.* 2002 [98]	Exogen® T1: daily for 20 min • 2, 4, or 7 d or 6 wks T2: 1 d	Fractured diabetic rat femur	↑ Mechanical properties of fracture calluses are improved (after 6 weeks), proliferation is not affected (2, 4, or 7 days)
Heybeli *et al.* 2002 [125]	f = 7.5 MHz, PRF = 1 Hz, burst duration = 1 ms total output intensity = 11.8 mW/cm² T1: 10 min/treatment • one, five or eight treatments in five day intervals T2: 5 days	Fractured rat femur	↑ Healing accelerated after 5 and 8 sessions
Tis *et al.* 2002 [325]	Exogen® T1: daily for 20 min • 21 d T2: 10/17 days after start of distraction/after operation (distraction period 10 d)	Rabbit tibia distraction osteogenesis	↑ Increased callus size; mechanical properties or bone density not affected

Table 3-1 continued

Eberson *et al.* 2003 [73]	Exogen® T1: daily for 20 min • 5 wks T2: 21/28 days after start of distraction/after operation (distraction period 21 d)	Rat femur distraction osteogenesis	↑ Accelerated bone maturation; changes in bone microarchitecture; no significant effects on mineral contents, density, or mechanical properties
Rawool *et al.* 2003 [264]	Exogen® T1: daily for 20 min • 7 or 11 d T2: 1 d	Fractured dog ulnae (Doppler ultrasound analysis)	↑ Increased vasculature on the fracture site
Carvalho & Cliquet Jr. 2004 [30]	Exogen signal T1: daily for 20 min • 20 d T2: 1/31 days after operation/after induction of osteopenia	Osteopenic rat femur	↑ Indication of new bone formation; less bone deterioration
Hantes *et al.* 2004 [113]	f = 1 MHz, PRF = 1 kHz, dc = 20 % I_{SATA} = 30 mW/cm² T1: 20 min/d, 6 d/wk • 75 or 120 d T2: 1 d	Fractured sheep tibia (transosseous sonication through a pin)	↑Accelerated fracture healing (79 vs. 103 days): increased cortical bone density and ultimate strength (day 75); invasive administration well tolerated
Sakurakichi *et al.* 2004 [280]	Exogen signal T1: daily for 20 min • 7 d T2: -7/0, 0/7, or 7/14 days after start of distraction/after operation (distraction priod 7 d)	Rabbit tibia distraction osteogenesis (different phases of distraction)	↑ Ultrasound is the most effective (mineral content, mechanical strength) when given during the lengthening phase
Yang *et al.* 2005 [359]	f = 1 MHz, CW I_{SATA} = 125 mW/cm² T1: 15 min/d, 5 d/wk • 4 wks T2: 3 d	Neurectomy-induced bone loss in rats	→↓ Ultrasound doesn't prevent bone loss; thinner proliferative zone in tibia growth plate
Chan *et al.* 2006 [33]	Exogen® T1: daily for 20 or 40 min • 6 d T2: 0/7 days after start of distraction/after operation (distraction period 6d)	Rapid rabbit tibia distraction osteogenesis	↑ Larger mineralized tissue volume using the longer 40 min sonication; spatial variation in ossification around the fracture callus
Warden *et al.* 2006 [343]	f = 1 MHz, PRF = 100 Hz, dc = 20 % I_{SATA} = 100 mW/cm² T1: 20 min/d, 5 d/wk • 16 or 27 treatments T2: 1 d	Fractured rat femur	↑ Healing is not accelerated after 16 treatments; bone mineral content, bone area and mechanical strength are increased after 25 treatments
Iwai *et al.* 2007 [147]	Exogen® T1: daily for 20 min • 2 or 3 wks T2: 3 d	Porous hydroxiapatite ceramic implants in rabbit femular condyle	↑ Increased osteoblast number, bone area, and mineralized tissue volume in ceramics

Table 3-1 continued

Li *et al*. 2007 [186]	As Warden *et al*. [343] T1: 20 min/d, 5 d/wk • 2, 4, or 8 wks T2: 1 to 3 hr	Stress fracture in rat ulna ± nonsteroidal anti-inflammatory drug	↑ Ultrasound increases the bone formation rate; no effect on bone resorption; no clear interaction between the ultrasound and drug treatment
Huang *et al*. 2008 [136]	Exogen® T1: daily for 20 min • 3, 7, or 14 d T2: 1 d	Fractured rat tibia (cyclooxgenase-2 enzyme inhibition induced delayed healing)	↑ Ultrasound-improved healing delayed but not blocked in enzyme-inhibited animals; ultrasound interacts also with other pathways
El-Bialy *et al*. 2008 [77]	Exogen®, PRF = 1.12 kHz, dc = 22.4 % or CW at I_{SATA} = 30 mW/cm² T1: daily for 20 min • 5 d or up to 4 wks?? T2: 0/3 days after start of distraction/after operation (distraction period 5 days)	Rabbit mandibular bone osteodistraction	↑ CW ultrasound more effective during the early stages of bone healing (1 to 2 weeks post-distraction), pulsed at the later stage (3 to 4 weeks post-distraction)
Perry *et al*. 2009 [254]	f = 1 MHz, PRF = 100 Hz, dc = 20 % I_{SATA} = 150 mW/cm² T1: 7 min/d on Mon., Wed., and Fri. for two consecutive weeks T2: intact	Intact rat ulna ± mechanical loading	↑ Ultrasound and mechanical loading both induce periosteal bone growth; mechanical loading > concurrent treatment > ultrasound
Warden *et al*. 2009 [344]	As Warden *et al*. [343] T1: 20 min/d, 5 d/week • up to 5 wks T2: 1 d	Fractured rat femur ± parathyroid hormone treatment	→ Additive but not synergistic effects between the treatments suggested; ultrasound induces less mature callus (callus area and cartilage formation ↑, mineral content ↓) with these parameters contrary to parathyroid hormone treatment
Coords *et al*. 2010 [51]	Exogen® Treatments for 4, 7, or 10 days, otherwise as Gebauer et al. [98]	Fractured diabetic rat femur	↑ Enhanced cartilage formation in callus; neovascularization; the diabetic facture group w/ ultrasound started to resemble the non-diabetic group
Lim *et al*. 2010 [191]	Exogen signal T1: 20 min/d, 5 d/wk • 6 wks T2: 52.2% decrease in bone volume fraction	Osteoporotic mouse tibia	↑ Increased trabecular bone formation and cortical bone thickness in the region directly exposed to ultrasound (6 wks); elevated amount of osteocytes in cortical bone
McClure *et al*. 2010 [213]	f = 1.5 MHz PRF = 166.7 Hz / burst duration = 2 ms for two min; PRF = 1 kHz / burst duration = 200 µs for three min; PRF = 833 Hz / burst duration = 400 µs for two min; PRF = 1 kHz / burst duration = 200 µs for three min; this cycle repeated four times for 40 min/d • up to 84 days I_{SATA} = 44 mW/cm² (average) T2: 2 d ??	Fractured horse metacarpal bone	→ No significant effects on bone healing

Table 3-1 continued

Naruse *et al.* 2010 [231]	Exogen signal T1: daily for 20 min • 16 treatments T2: 5 d	Fractured mouse femur (aged cyclooxgenase-2 knockout mice/wild-type mice)	↑ Endochondral phase halved in wild-type mice; endochondral healing is not accelerated in knockout mice; prostaglandin E2 agonist treatment restores the sensitivity to ultrasound; ultrasound induces cyclooxgenase-2
Shakouri *et al.* 2010 [294]	Exogen signal T1: daily for 20 min • 1 mo T2: 4 d	Fractured rabbit tibia	↑ Callus mineral density but not bone strength is increased after the sonications
Woo *et al.* 2010 [353]	Exogen signal T1: 20 min/d, 5d/wk • 6 wks T2: 3 wks after induction of osteoporosis	Osteoporotic mouse tibia	↑ Increased effective structural modulus after 6 weeks of ultrasound stimulations (5.2/4.3/5.6 GPa at weeks 0/3/9, respectively); ultrasound may prevent osteoporotic bone fractures
Cheung *et al.* 2011 [38]	Exogen signal ?? T1: 20 min/d, 5 d/wk • up to 8 wks T2: 0 d/3 months after induction of fracture/osteoporosis	Fractured osteoporotic rat femur	↑ Accelerated endochondral ossification after the sonications (higher cartilage content in fracture callus after 2 to 4 weeks, lower cartilage content after 8 weeks)
Chung *et al.* 2011 [45]	Exogen® T1: 20 min/d, 6 d/wk • up to 8 wks T2: 1 d	Fractured rat femur (angle of sound incidence varied)	↑ Rate of fracture healing may be related to the ultrasound angle of incidence; (rubber wedge attenuation was compensated so that the acoustic power delivered to the treatment site was constant at all angles)
Hsu *et al.* 2011 [132]	f = 1 MHz, PRF = 100 Hz, dc = 20 % or CW I_{SATA}(??) = 50 to 300 mW/cm² T1: daily for 10 min • 20 or 30 d T2: 24 h	Titanium implants placed in rabbit tibia	↑ Enhanced blood flow within implants (day 10, pulsed and CW); elevated levels of periosteal bone (specifically pulsed) and connective tissue in the implants (pulsed and CW)
Hui *et al.* 2011 [138]	Exogen®, two(??) transducers T1: 20 min/d, 5 d/wk • 7 wks T2: 3 d	Mesenchymal stem cell-impregnated calcium phosphate bioceramic in decorticated rabbit spine	↑ Enhanced spinal fusion rate, fusion bone mass and osteochondral bridging
Katano *et al.* 2011 [156]	Exogen signal T1: daily for 20 min • up to 28 d T2: 1 d	Fractured aged mouse femur	↑ Enhanced hard callus bridging and bone remodeling; neovascularization in fibrous tissue comprising the periosteum that surrounds the fracture callus
Lai *et al.* 2011 [176]	f = 0.5, 1, 1.5 or 2 MHz PRF = 100 Hz??, burst duration = 2 ms?? I_{SATP} (??) = 0.5 W/cm² T1: daily for 15 min • up to 3 wks T2: 3 d	Fractured rabbit fibula	↑ New bone formation (1 to 3 weeks) and increased torsional stiffness (2 weeks all frequencies, 3 weeks < 2 MHz); bone growth and torsional stiffness is enhanced also in the contralateral sham-treated fractures compared to nonoperated and nonsonicated controls ?? (systemic effect suggested)

Table 3-1 continued

Fung *et al.* 2012 [90]	Exogen®, 30 or 150 mW/cm^2 T1: daily for 20 min?? • up to 6 wks T2: 2 d	Fractured rat femur	↑ Fracture healing (bone volume, mechanical properties, and woven bone area) is enhanced at 30 mW/cm^2 but not at 150 mW/cm^2
Fung *et al.* 2014 [91]	Exogen® T1: daily for 20 min • 4 or 6 wks T2: 2 d	Fractured rat femur	↑ Rate and type of fracture healing may be related to the axial distance of exposure; (rubber coupler attenuation was compensated so that the acoustic power delivered to the treatment site was constant for all exposure distances)

Table 3-2. Human *in vivo* low-intensity pulsed ultrasound studies. dc = duty cycle; *f* = operating frequency; I_{SATA} = spatial-average temporal-average intensity; PRF = pulse repetition frequency; ↑ / → = ultrasound has stimulating effect / is equally effective respect to the sham treatment or control.

	Reference	Sonication parameters or device	Target of treatment	Main outcome
Fresh fractures (Non-operative)	Pilla *et al.* 1990 [258]	Exogen signal	Colles' and tibia diaphysis fractures	↑Accelerated healing (Colles' fractures by 1.5 fold and tibia diaphysis by 1.6 fold)
	Heckman *et al.* 1994 [123]	Exogen signal	Tibial cortical fractures	↑ Acceleration in healing > 38% (96 vs. 154 days)
	Kristiansen *et al.* 1997 [172]	Exogen®	Radial cancellous fractures	↑ Acceleration in healing 38% (61 vs. 98 days)
	Cook *et al.* 1997 [48]		Data from [123] and [172] re-reported to include impact of smoking	↑ Tibial: smokers 41% (175 vs. 103 days), non-smokers 26% (129 vs. 96 days); radial: smokers 51%, non-smokers 34%
	Rue *et al.* 2004 [273]	Exogen®	Tibial stress fractures	→ Total days of symptoms (active 56.2 days, placebo 55.8 days)
	Lubbert *et al.* 2008 [195]	Exogen®	Fresh clavicle fractures	→ Healing (active 26.77 days, placebo 27.09 days)
Delayed/ nonunions	Mayr *et al.* 2000 [211]	Exogen®	Delayed unions and nonunions (various anatomic locations)	↑ Delayed unions: 91% healing rate (average healing time 129 days); Nonunions: 86% healing rate (152 days)
	Nolte *et al.* 2001 [240]	Exogen®	Nonunions (various anatomic locations)	↑ 86% percent of the nonunions healed during the ultrasound treatment period (mean heal time 152 days, fracture age 61 weeks)
	Gebauer *et al.* 2005 [96]	Exogen®	Nonunions and delayed unions in children	↑ All treated healed (within 3 to 12 months)
	Gebauer *et al.* 2005 [97]	Exogen®	Nonunions (various anatomic locations)	↑ 85% percent of the nonunions healed during the ultrasound treatment period (mean heal time 168 days, fracture age 31.2 months)
	Jingushi *et al.* 2007 [152]	Exogen®	Postoperative delayed union or nonunion (long bones)	↑ Healing rate 75% in all bones; treatment should be started within 6 months after the most recent operation

Table 3-2 continued

	Rutten *et al.* 2007 [275]	Exogen®	Nonunions of the tibia	↑ Healing rate 73% (average healing time 184 days, fracture age 256.8 days)
	Schofer *et al.* 2010 [285]	Exogen®	Delayed unions of the tibia (randomized and sham-controlled trial)	↑ Bone mineral density increased by 34% after the ultrasound treatments (fracture age > 4 months, study limited to 16 weeks)
	Roussignol *et al.* 2012 [272]	Exogen®	Nonunions (various anatomic locations)	↑ Six-month healing rate 88% (fracture age 271 days)
Other (Operative intervention etc., case studies)	Jensen 1998 [149]	Exogen® 3 times/day	Tibial stress fracture (Case report: 14-year old athlete)	↑ Successful implementation; normal radiographs after 3 weeks, full workout after 1 month
	Emami *et al.* 1999 [81]	Exogen®	Intramedullary nail-fixed tibial fractures	→ Healing is not accelerated (active 115 days, placebo 125 days)
	Sato *et al.* 1999 [284]	Exogen®	Leg lengthening: poor callus formation (Case report: 22-year old patient)	↑ Ultrasound may accelerate bone callus formation during and after the leg lengthening period
	Warden *et al.* 2001 [341]	Two transducers f = 1 MHz PRF = 3.3 kHz, dc = 3.3 % I_{SATA} = 30 mW/cm² 20 min/d, 5 d/wk	Prevention of calcaneal osteoporosis after spinal cord injury	→ No signs of prevention after 6 weeks of treatments
	Okada *et al.* 2003 [246]	Exogen®	Congenital pseudoarthrosis: initiation/acceleration of healing (Case report: 16-year old patient)	↑ Callus visible after 6 months, solid fusion after 1 year
	Leung *et al.* 2004 [183]	Exogen®	Postmenopausal bone loss in distal radius (older Chinese women)	→ No significant increase in bone mineral density (3 months of treatments, 6 month follow-up)
	Leung *et al.* 2004 [184]	Exogen®	Complex tibial fracture	↑ Removal time of an external fixator reduced (active 9.9, placebo 17.1 weeks), bone mineral content and alkaline phosphatase levels increased
	Tsumaki *et al.* 2004 [328]	Exogen®	High tibial osteotomy: acceleration of maturation	↑ Increased bone callus mineral density with respect to the control tibia (4 weeks of sonications)

Table 3-2 continued

El-Mowafi & Mohsen 2005 [80]	Exogen®	Tibial distraction osteogenesis: acceleration of bone formation/maturation	↑ External fixation period after distraction reduced (active 30 days/cm, inactive 48 days/cm)
Gold *et al.* 2005 [103]	Exogen®	Bone transports for large segmental tibial defects	↑→ Indication for reduced time for an external fracture fixator (treated 13.91 months, non-treated 16.71 months)
Handolin *et al.* 2005 [111,112]	Exogen®	Bioabsorbable screw-fixed lateral malleolar fractures	→ No changes in bone density, callus formation or healing (up to 12 weeks)
Schortinghuis *et al.* 2005 and 2008 [287,288]	Exogen®	Mandibular bone distraction: stimulation of early bone formation	→ Bone formation is not stimulated during the fracture consolidation period (31 days [287] or 46 days [288])
Dudda *et al.* 2011 [62]	Exogen®	Lower leg distraction: stimulation of osteogenesis	↑→ Indication for shorter external fixation period (218.6 vs. 262.2 days)

3.5 STIMULATION OF *IN VIVO* CARTILAGE

Osteoarthritis is the most common joint disease, which slowly but progressively deteriorates the cartilage and underlying bone [11]. The most common osteoarthritic joint is the knee, and it is estimated that in Finland, the age-adjusted prevalence of knee osteoarthritis in individuals over 30 years of age is approximately 5% in men and 7% in women [2]. Its prevalence increases rapidly with age, being 9.2% and 8.1% for men and women near the age of retirement (55–64 years), respectively. Similar statistics have been reported internationally [11]. Several surgical and tissue engineering-based methods are developed to repair articular cartilage defects [210].

Several animal studies have reported favorable ultrasonic effects on cartilage [49,50,53,65–67,76,109,133,134,227,251,334,366]. Ultrasound bone-healing studies have also noted changes in cartilage and chondrocytes. Dyson *et al.* found an increase in elastic cartilage in rabbit ears using a novel tissue regeneration device [65–67]. The optimal settings induced a 32.5% increase in tissue growth area and were achieved using 3.5 MHz pulsed ultrasound. Continuous wave sonication (I_{SATA} = 0.1 W/cm^2) was nearly equally as effective as this pulsed ultrasound mode. However, sonication using this same temporal-average intensity but higher pulse intensity (increased intensity, decreased PRF and dc) was regeneratively ineffective or even inhibitory. All intensities gave a similar temperature rise (1.3 to 1.6 °C). Following their studies, many animal studies were conducted demonstrating benefits from sonications, particularly on osteoarthritic cartilage. These studies are summarized in Table 3-3. However, in a study by Chow *et al.*, growth and activity in a cartilage cell pellet that was placed to treat a physeal bone fracture was not enhanced after the daily sonications [43]. Further, the results from studies that maturate and grow tissue-engineered chondrocyte constructs *in vivo* have been conflicting [53,61]. This may be explained by the

differences in biological setups and ultrasonic exposure. In a study by Lyon *et al.* [198], the efficacy of therapeutic ultrasound (1 MHz, unspecified intensity 0.5 W/cm^2, pulsed but not specified, 20 min daily for six weeks) and of higher-intensity ultrasound (2.2 W/cm^2) was compared by sonicating the normal cartilaginous growth plate in rabbit knee. The therapeutic level was ineffective. Contrary to this, the higher-intensity experiment showed significant cartilage thickening in the different zones of growth plate even though disorganization of the chondrocytes and bone resorption were also evident. This suggests a difference in effective sonication parameters between cartilage and bone.

Based on the success in the animal experiments, conventional soft-tissue ultrasound physiotherapy (several watts of acoustic power) was used in effort to alleviate the symptoms of osteoarthritis [82]. Based on the acoustic parameters, these exposures are expected to induce at least thermal effects on the innervated subchondral bone, tendons, and cartilage. Recently, human trials have indicated both pain alleviation and functional improvements after CW sonications (1 MHz, 1–2 W/cm^2, intensity not specified, transducer diameter 4–5 cm, five- to ten-minutes-long treatments repeated daily 10 to 24 times) [248,319]. Tascioglu *et al.* further reported that pulsed ultrasound (1 MHz, 2 W/cm^2, PRF not mentioned, dc = 20%) was more therapeutic than CW with 2 W/cm^2 [319]. In a study by Huang *et al.*, pulsed ultrasound (1 MHz, spatial-peak temporal-peak intensity I_{SPTP} = 2.5 W/cm^2, PRF most likely 100 Hz, dc = 25%, five-minutes-long treatments to several locations, three times/week for eight weeks) combined with muscular exercise increased the functional knee parameters more than CW ultrasound (I_{SPTP} = 1.5 W/cm^2) with exercise or exercise alone [135]. The intensity level was adjusted based on the level at which the patients felt warmth or a mild sting. These corresponding temporal-average intensity levels were lower with pulsed ultrasound than CW.

Ultrasound's superior effectiveness over the other physiotherapeutic modalities, such as heat packs or exercise, has not been confirmed in all studies [32,82,330]. Recent reviews

have concluded that there are supportive data on pain and function improvement after the ultrasound intervention but also that the current evidence behind therapeutic ultrasound on knee osteoarthritis is inadequate, requiring controlled methodologically improved studies [192,274]. Recently, the authors of this latter review conducted a double-blinded, sham-controlled, randomized pilot study utilizing pulsed ultrasound (1 MHz, I_{SATA} = 0.2 W/cm^2, PRF not mentioned, dc = 20%, 9.5 minutes three times/week for eight weeks), and reported a statistically significant increase (1700±160 μm vs. 1640±170 μm, mean increase 90 μm) in tibial cartilage thickness but found no effect on pain or physical function among patients suffering from mild or moderate knee osteoarthritis [193].

In general, soft tissue and bone encases the cartilage in the joint and therefore, allows only a limited window for ultrasound to directly propagate into cartilage surface [351]. Planar transducer devices designed for muscle tissue, tendon, or bone healing may not be the optimal configurations to deposit a moderate or low average intensity ultrasound, specifically in cartilage-space. An efficient deposition may require altered sonication parameters, beam steering, beam focusing, and image guidance and/or active control.

Table 3-3. Animal *in vivo* ultrasound studies on cartilage. CW = continuous wave; dc = duty cycle; f = operating frequency; I_{SATA} = spatial-average temporal-average intensity; I_{SAPA} = spatial-average pulse-average intensity; I_{SATP} = spatial-average temporal-peak intensity; PRF = pulse repetition frequency; T1 = ultrasound sonication time • time span or number of sonications; T2 = time delay between the operation and the start of sonications; ↑ / → / ↓ = ultrasound has stimulating effect / is equally effective / is detrimental respect to the sham treatment or control; ?? = value not clear.

Reference	Sonication parameters	Target of treatment	Main outcome
Dyson *et al.* 1968, 1970 [65–67]	f = 3.55 or 3.5 MHz PRF = 12.5 or 100 Hz, dc = 1.25 %, 20 % or CW I_{SAPA} = 0.25 to 8 W/cm², I_{SATA} = 0.1 W/cm² T1: 5 min/d, 3 d/wk • up to 49 d after operation T2: 14 d	Punctured rabbit outer ear	↑Accelerated tissue regeneration: 32.5 % increase (0.5 W/cm² / 100 Hz / 20 %, 21 days), 27% increase (0.1 W/cm² / CW, 42 days); tissue damage (8 W/cm² / 100 Hz / 20 %; decrease in growth (8 W/cm² / 12.5 Hz / 1.25 %, all time points); temperature elevation < 2°C
Vanharanta *et al.* 1982 [334]	f = 1 MHz, CW I_{SATA}(??) = 1 W/cm² T1: daily for 5 min • 5 d T2: intact	Healthy rabbit knee	↑→ Increased metabolic activity in medial collateral ligament but not in articular cartilage
Huang *et al.* 1997 [133]	f = 1 MHz, PRF = 100 Hz, dc = 20 % I_{SATP} = 2.5 W/cm² (maximum beam non-uniformity = 6) T1: 3 times/week for 7 min • 4 wks T2: 1, 2, or 3 weeks after induction of arthritis	Experimental osteoarthritis in rat knee (chemically-induced, several grades of severity)	↑ Deceleration of disease; high likelihood for cartilage repair in case of mild grades of severity
Huang *et al.* 1999 [134]	f = 1 MHz, PRF = ??, dc = 25 % I_{SPTP} = 2.5 W/cm² T1: 3 times/week for 7 min • 4 wks T2: 1 wk	Experimental early osteoarthritis in rat knee (chemically-induced)	↑ Decrease in disease severity; heat-shock protein (Hsp72) is in elevated level in arthritic tissue and is further elevated after the sonications; Hsp72 declines to non-arthritic level in arthritic sonicated samples during the follow-up period; (increased chondrocyte proliferation!)
Cook *et al.* 2001 [49]	Exogen® T1: 5, 10, 20 or 40 min/day, 6 d/wk • up to 52 wks T2: 3 d	Defected cartilage inrabbit patellar groove	↑ Gross and histologic appearance of repair cartilage improved; highest histologic quality when sonication was 40 min long (after 4 weeks)
Lyon *et al.* 2003 [198]	f = 1 MHz, pulsed ?? I_{SATA} (??) = 0.5 or 2.2 W/cm² T1: daily for 20 min • 6 wks T2: intact	Growth plate in rabbit hind knee	↑→↓ Growth plate not affected (0.5 W/cm²); thickening of cartilaginous zones, chondrocyte disorganization, and bone resorption (2.2 W/cm²)
Duda *et al.* 2004 [61]	Exogen® T1: daily for 20 min • up to 12 weeks T2: 2 d	Chondrocytes from bovine articular cartilage loaded in fibrinogen meshes and placed in back of mice	→↓ Cell construct maturation is not accelerated; Young's modulus lower in ultrasound treated constructs: native 1.75 MPa, sham-treated 1.5-1.8 MPa, treated 1.3 MPa (6 and 12 weeks)

Table 3-3 continued

Park *et al.* 2005 [251]	f = 1 MHz, CW I_{SATA}(??) = 0.4 W/cm² T1: once/week for 10 min • 4 wks T2: 4 wks	Osteoarthritic rabbit knee + hyaluronate injection and/or ultrasound (surgically-induced)	↑ Reduced histopathological score; reduced levels of synovial fluid; reduced levels of prostaglandin E2, proteoglycan, collagen II, and matrix metalloproteinase-3 in synovial fluid; especially with hyaluronate + ultrasound
Cui *et al.* 2006 [53]	f = 0.8 MHz, CW I_{SATA}(??) = 0.2 W/cm² T1: twice/day for 10 min • 1, 2, or 3 wks T2: 1 d	Mesenchymal stem cells embedded in polyglycolic acid meshes, cultured in chondrogenic-type medium and then placed in back of mice	↑ Increased levels of total protein, glycosaminoglycan, and collagen (after 4 weeks); increased compressive strength (control 1.85, ultrasound 2.25 MPa)
Cook *et al.* 2008 [50]	Exogen® T1: 20 min/d, 6 d/wk • 6 and 12 wks T2: 3 d	Autologous osteochondral plugs in dog knee	↑ Improved gross (6 weeks) and histologic appearance (6 and 12 weeks)
El-Bialy *et al.* 2010 [76]	Exogen® T1: daily for 20 min • 4 wks T2: immediate ??	Collagen sponge with chondrogenic or osteogenic bone marrow stromal cells placed in rabbit mandibular condyle	↑ Indications of improved chondrogenesis and osteogenesis in scaffolds loaded with cells after 4 weeks of treatments
Gurkan *et al.* 2010 [109]	Exogen® T1: 20 min/d, 5 d/wk • up to 10 mo T2: 2 months (early disase) or 12 months (progressed disease) old animals	Osteoarthritic Hartley guinea-pigs (spontaneous progressive disease)	↑ Reduced histopathological score especially when the treatment is started in early phase of disease; indication of less active endogenous repair after LIPUS (reduced levels of transforming growth factor-β1 and matrix metalloproteinase-13)
Naito *et al.* 2010 [227]	Exogen signal T1: daily for 20 min • up to 28 days T2: 1 d	Osteoarthritic rat knee (surgically-induced)	↑↓ Synthesis of type II collagen is increased in osteoarthritic knee after LIPUS; indication for histopathological score improvement
Chow *et al.* 2011 [43]	Exogen® T1: 20 min/d, 5 d/wk • up to 16 wks T2: 1 d	Rabbit chondrocyte pellets placed in young rabbits physeal femur fractures	→ Bioactivity and growth potential of cartilage pellets is not prolonged after LIPUS exposures
Zeng *et al.* 2012 [366]	f = 1 MHz, PRF = ??, dc = 20% I_{SATA}(??) = 0.3 W/cm² T1: daily for 10 min • 10 d T2: 6 wks	Rabbit knee osteoarthritis (surgery-induced model)	↑→ Reduced histopathological score; level of apoptosis markers (caspase-3 and -8) not reduced

3.6 STIMULATION OF *IN VITRO* BONE AND CARTILAGE

In vitro studies have provided the biological basis for bone and cartilage stimulations. Studies using bone and stem cells have reported elevated levels of collagen, alkaline phosphatase, osteocalcin, and several other bone-specific markers indicating that ultrasound has an enhancing effect on bone cell function and differentiation. More specifically, studies have indicated that ultrasound can influence prostaglandin E_2 and cycloaxygenase-2 levels [165,277,309,310], elevate the levels of nitric oxide [268,337], affect several cytokines [57,337], regulate the cell surface integrins [315,316,360], and activate matrix metalloproteinase's [39,332]. The effect of ultrasound on cell proliferation has been conflicting. Table 3-4 summarizes reported findings. In cartilage and chondrocyte studies, sonications have been reported to stimulate chondrogenic activity, maintain and enhance chondrogenic phenotype, and enhance the differentiation of stem cells to chondrocytes. Parvizi *et al.* have shown that calcium ion influx inside the cells contributes to proteoglycan synthesis and also that presence and release of intracellular Ca^{2+} is required for an increased synthesis in the sonicated chondrocyte monolayer [252]. Mortimer and Dyson, using fibroblastic cells, were the first to report elevated Ca^{2+} levels in cells after ultrasound [222]. In mammalian ovary cells, Kumon *et al.* have shown that signals emanating from the immediately sonoporated cells may activate the adjacent cells for delayed additive Ca^{2+} influxes through so-called "calcium waves" [173,174]. Elevated glycosaminoglycan levels [131,220,250] and cell surface integrin activation [41,42,130] have been reported after the sonications. Table 3-5 summarizes the reported effects on the cartilage cells and cell structures.

Tissue engineering uses chemical and physical stimulations to grow tissues [206]. A recent study that compared ultrasound to a rotating-type bioreactor suggests that ultrasound by itself could serve as a bioreactor [131], or ultrasound could be

implemented as a part in a larger, more complex bioreactor system. Kang *et al.* [155] have tested a system that combines cyclic strain and LIPUS on 3D pre-osteoblast scaffolds. The *in vitro* data can provide information about the optimal sonication parameters, optimal sonication setups, and co-play with the other stimulants for tissue-engineering systems.

Table 3-4. ***In vitro*** **ultrasound studies to stimulate bone formation and osteogenic differentation. Abbreviations:** **dc = duty cycle; *n* = number of repeated sonications (treatments/day); PRF = pulse repetition frequency // A, B, C, D = sub-illustrations in Fig 4.1; FF = acoustic far field; NF = acoustic near field; NF/FF = near-far field transition // BMSC = bone marrow stromal cell; FB = fibroblast; MC = monocyte; OB = osteoblast; OC = osteoclast; OCY = osteocyte // ALP = alkaline phosphatase; ATP = adenosine 5′-triphosphate; BMP = bone morphogenetic protein; BSP = bone sialoprotein; Cbfa-1/Runx2 = core-binding factor α-1; COX-2 = cyclooxygenase-2 (prostaglandin-endoperoxide synthase 2); (c)DNA = (complementary) deoxyribonucleic acid; EGR = early growth response; ERK = extracellular-signal regulated protein kinase; HIF = hypoxia-inducible factor; IGF = insulin-like growth factor; IL = interleukin; MAPK = mitogen-activated protein kinase; MCP = macrophage chemoattranctant protein; MMP = matrix metalloproteinase; NO = nitrite oxide; OCN = osteocalcin; OPN = osteopontin; OPG = osteoprotegerin; PDGF = platelet-derived growth factor; PGE_2 = prostaglandin E_2; RANKL = receptor activator for nuclear factor kappa B; TGF = transforming growth factor; TNF = tumor necrosis factor; VEGF = vascular endothelial growth factor // ↑/↓/→ = ultrasound has stimulating effect/ inhibiting effect/ is equally effective respect to the sham treatment // NR = value not reported; ?? = value not clear.**

Reference	Sonication parameters	Setup type	Coupling	Transmission	US heating	In vitro sample	Main outcome
Example	*operating frequency, PRF, dc* *acoustic intensity* *duration • n = no. of sonications*	*Ref. to Fig. 4.1* *exposure chamber type* *distance (mm) • temperature*	*transducer* *coupling path to* *sample volume*	*sound path after the* *sample transmission*	*measurement point* *temperature value*	*sample* *contact • medium volume*	
Webster *et al.* 1978, 1980 [347,348]	3 MHz, 100 Hz, 20% 0.5 W/cm² (I_{SPTP}) 5 min • *n* = 1	**A** Al tube w/ 0.13mm film window NF/FF (210 mm) • 25°C	water–film	film–water–absorber	NR	human embryonic FB cells suspension • NR	Protein and collagen synthesis ↑; ambient pressure ↑ synthesis ↓
Mortimer & Dyson 1988 [222]	1 MHz, 100 Hz, 20% 0.25 to 1.5 W/cm² (I_{SPPA}) 1 to 20 min • *n* = 1	**A** steel tube w/ thin film window NF/FF (100 mm) • 36°C	water–film	film–water–absorber	medium 0°C	chick embryonic 3T3 FB cells suspension • 4 ml	Transient calcium influx ↑ (peak at 0.75 W/cm²); influx ↑ when sonication time ↑
Wiltink *et al.* 1995 [352]	1 MHz, 100 Hz, 20% and CW 0.1 to 0.77 W/cm² (I_{SATP}) 0.1 and 0.5 W/cm² (I_{SATA} CW) 1 or 5 (CW) or 5 (pulsed) min • *n* = 1	**A** Petriperm dish w/dialysis tube NF/FF (100 mm) • 37°C	extracellular solution–tube	dish–solution–absorber	NR	fetal mouse metatarsal bone rudiments bottom contact • NR	Metatarsal bone growth in 16-day-old rudiments; increase in proliferative cartilage (10%, day 7), not in hypertrophic zone; only with pulsed ultrasound at 0.77 W/cm²; transient longitudinal growth in 17-day-old rudiments (pulsed 0.5 W/cm², post-culture day 3)
Reher *et al.* 1997 [265]	3 MHz, 100 Hz, 20% 0.1 to 2 W/cm² (I_{SATA}) 5 min • *n* = 1	**C** plastic 6-well + plastic ring NF (5 mm) • 19-26°C	medium	well–castor oil–absorber	medium 0 to 1.8°C (3 MHz)	mouse calvaria bone (5-day-old) bottom contact • 5 ml	Collagen and non-collagen ↑ (0.1 W/cm²), ↓ (0.5 – 2 W/cm²)
Reher *et al.* 1998 [266]	1 MHz, 100 Hz, 20% and 45 kHz CW 0.1 to 1 W/cm² (I_{SAPA}) 5 to 50 mW/cm² (I_{SATA} 45 kHz) 5 min • *n* = 1	**C** plastic 6-well NF (5-6 mm) • 37°C	medium	well–water–absorber	NR	human FB or OB cells monolayer • 5 ml	FB, proliferation/collagen ↑, peak: 0.7/0.4 W/cm² (1 MHz), 50/15 mW/cm² (45 kHz) OB, proliferation/collagen ↑, peak: 1.0/0.1 W/cm² (1 MHz), 30/30 mW/cm² (45 kHz)
Sun *et al.* 1999 [309]	1.5 MHz, 250 Hz, 50% 0.32 and 0.77 W/cm² (I_{SATA}??) 15 min • *n* = 7 or 14 (once/day)	**B** Urethane chamber NF/FF (NR) • 37 ± 2°C	water–urethane	medium-urethane–air ??	NR	defected mouse femora bottom contact • NR	Enhanced defect healing and trabecular bone regeneration; PGE_2 levels ↓ after ultrasound; 0.77 W/cm² more effective

Table 3.4 continued

Doan *et al.* 1999 [57] and Reher *et al.* 1999 [267]	1 MHz, 100 Hz, 20% and 45 kHz CW 0.1 to 1 W/cm² (I_{SAPA}) 5 to 50 mW/cm² (I_{SATA} 45 kHz) 5 min • n = 1	**C** plastic 6-well NF (5-6 mm) • 37°C	medium	well–water–absorber	NR	human FB, OB, or MC cells monolayer • 5 ml	FB, proliferation/collagen ↑, peak: 1.0/0.4 W/cm² (1 MHz), 50/15 mW/cm² (45 kHz) OB, proliferation/collagen ↑, peak: 0.7/0.1 W/cm² (1 MHz), 30/15 mW/cm² (45 kHz) Several cytokines *e.g.* IL-1β, VEGF ↑ (optimal intensities and frequencies vary)
Kokubu *et al.* 1999 [165]	1.5 MHz, 1 kHz, 20% 30 mW/cm² (I_{SATA}) 20 min • n = 1	**B** plastic 6-well w/ thin film chamber FF (200 mm) • 37°C	water–well	film–absorber	NR	mouse MC3T3-E1 OB cells monolayer • NR	PGE_2 production ↑ and COX-2 expression ↑ in time-dependent manner; ultrasound induced PGE_2 ↓ when COX-2 inhibited
Ito *et al.* 2000 [145]	1.5 MHz, 1 kHz, 20% 30 mW/cm² (I_{SATA}) 20 min • n = 4 (once/day)	**B** plastic 6-well NF/FF (130 mm) • 37°C	water–well	medium–absorber	NR	co-culture of human SaOS-2 and endothelial cells monolayer • NR	Indication that sonication (n = 4) further elevates vitamin D_3 induced PDGF-AB secretion in co-cultured cells
Naruse *et al.* 2000 [228]	1.5 MHz, 1 kHz, 20% 30 mW/cm² (I_{SATA}) 20 min • n = 1	plastic 6-well NR (NR) • NR	NR	NR	NR	mouse ST2 line BMSC cells monolayer • NR	Expression levels of several genes (c-Fos, TGF-β1, IGF-I, IGF-II, OCN, BSP) elevated after sonication indicating anabolic cell response
Warden *et al.* 2001 [342]	1 MHz, 1 kHz, 20% 30 mW/cm² (I_{SATA}) 20 min • n = 1	**A** PTFE tube w/ thin Mylar window NF/FF (NR) • 37°C	water–Mylar	Mylar–water–absorber	NR	rat UMR-106 cells monolayer • NR	Early response genes (c-Fos, COX-2) ↑; mRNA levels (ALP, OCN) ↑
Harle *et al.* 2001a [115]	3 MHz CW 0.14 to 0.99 W/cm² (I_{SATA}) 5 min • n = 1	**A** plastic chamber flask NF/FF (80 mm) • 37°C	water–well	well–water–absorber	inner flask surface 0.1 to 0.5°C	human MG63 OB-like or periodontal ligament cells monolayer • 40 ml	Both cell types: proliferation →; bone and connective tissue specific protein expressions ↑↓
Harle *et al.* 2001b [114]	3 MHz CW 0.12 to 1.49 W/cm² (I_{SATA}??) 10 min • n = 1	Harle *et al.* 2001a[115]	[115]	[115]	NR	MG63 cells monolayer • NR	ALP/OPN gene expressions ↑/ ↑↓; intensity-dependent expressions
Nolte *et al.* 2001 [239]	1.5 MHz, 1 kHz, 20% 30 mW/cm² (I_{SATA}) 20 min • n = up to 6 (once/day)	**D** plastic 6-well NF (< 2 mm) • 37°C	gel–well	medium-air	NR	fetal mouse metatarsal bone rudiments (17-day-old) bottom contact • 2.54 ml	Ultrasound stimulates endochondral ossification: calcified diaphysis length ↑ ($n \geq 3$), total rudiment length →, bone collar formed around the diaphysis
Sun *et al.* 2001 [310]	1 MHz, ??Hz, ??% 68 mW/cm² (I_{SATA}??) 20 min • n = up to 7 (once /day)	Sun *et al.* 1999 [309] NF/FF (120 mm)	[309]	[309]	NR	co-culture of mouse OB and OC monolayer • NR	OB count ↑, OC count ↓ (n = 7); PGE_2 levels, ALP, and TNF-α ↑ after 4 to 7 sonications.
Li *et al.* 2002 [187]	1 MHz, 100 Hz, 20% 0.15 to 2.4 W/cm² (I_{SATP}) 15 min • n = 1	**B** plastic cell dish w/ absorption chamber FF (240 mm) • 37°C	water–well	film–water–absorber	medium 0.2°C at 2.4 W/cm²	rat calvaria OB cells monolayer • 5 ml	Proliferation rate and PGE_2 synthesis ↑ (0.6 W/cm²)

Table 3-4 continued

Reher *et al.* 2002 [268]	1 MHz, 100 Hz, 20% and 45 kHz CW 0.1 to 1 W/cm² (I_{SAPA}) 5 to 50 mW/cm² (I_{SATA} 45 kHz) 5 min • n = 1	**C** plastic 6-well NF (5-6 mm) • 37°C	medium	well–water–absorber	NR	human OB cells monolayer • 5 ml	NO and PGE_2 ↑; NO/PGE_2 peak: 0.1/0.7 W/cm² (1 MHz), 50/30 mW/cm² (45 kHz).
Li *et al.* 2003 [188]	1 MHz, 100 Hz, 20% 0.6 W/cm² (I_{SATP}) 15 min • n = up to 4 (once/day)	Li *et al.* 2002 [187]	[187]	[187]	[187]	Li *et al.* 2002 [187]	Proliferation ↑ ($n \geq 1$), cytokine regulation: TNF-α ↓ ($n \geq 2$), IL-6 ↓ ($n \geq 3$), and TGF-β1 ↑ ($n \geq 2$)
Naruse *et al.* 2003 [229]	1.5 MHz, 1 kHz, 20% 30 mW/cm² (I_{SATA}) 20 min • n = 1	Naruse *et al.* 2000 [228]	[228]	[228]	[228]	mouse ST2 line BMSC, and rat OB, OCY and BMSC cells monolayer • NR	Intra-cellular calcium influx→; plethora of gene responses (COX-2, c-Fos, IGF-I, OCN, ALP etc.)
Leung *et al.* 2004 [182]	1.5 MHz, 1 kHz, 20% 30 mW/cm² (I_{SATA}) 5, 10, or 20 min • n = 2 or 4 (once/day)	**D** plastic 6-well NF (NR) • ??°C	gel–well	medium–air	NR	human periosteal cells monolayer • NR	Proliferation ↑ (n = 2), viability →, and ALP ↑ ($n \geq 2$), OCN (n = 4), VEGF expression ($n \geq 2$), mineralization ↑, (n = 24). Highest elevations when sonication 20 min long
Korstjens *et al.* 2004 [168]	Nolte *et al.* 2001 [239]	[239]	[239]	[239]	[239]	fetal mouse metatarsal bone rudiments (17-day-old) bottom contact • 2.54 ml	Ultrasound stimulates cell differentiation: calcified diaphysis length → , total rudiment length →, bone collar volume and calcified cartilage ↑
Saito *et al.* 2004a [277]	1.5 MHz, 1 kHz, 20% 30 and 120 mW/cm² (I_{SATA}) 20 min • n = up to 4 (once/day)	Ito *et al.* 2000 [145]	[145]	[145]	Identical with the unexposed	MC3T3-E1 cells monolayer • NR	Collagen contents → (n = 4). COX-2 expression and PGE_2 level ↑; ultrasound induced PGE_2 ↓ when COX-2 inhibited. PGE_2 levels higher when intensity 120 mW/cm². Enzyme activity *e.g.* collagen cross-linking more intense at 30 mW/cm²
Saito *et al.* 2004b [278]	1.5 MHz, 1 kHz, 20% 30 and 120 mW/cm² (I_{SATA}) 20 min • n = up to 21 (once/day)	Ito *et al.* 2000 [145]	[145]	[145]	Identical with the unexposed	Saito *et al.* 2004a [277]	Collagen contents → (n = 4). Calcium accumulation in cell layers ↑ at 30 (n = 11 and 21) and 120 mW/cm² (n = 21). Accumulation and *e.g.* collagen cross-linking more intense at 30 mW/cm²
Wang *et al.* 2004 [337]	1.5 MHz, 1 kHz, 20% 30 mW/cm² (I_{SATA}) 20 min • n = 1	Reher *et al.* 2002 [268]	[268]	[268]	NR	human fetal pre-osteoblastic hFOB 1.19 cells, MG63 or SaOS cells monolayer • NR	Cell proliferation ↑, VEGF-A production ↑, NO production and nuclear HIF-1α activation ↑; VEGF-A expression mediated by NO
Harle *et al.* 2005 [116]	3 MHz CW 0.13 to 1.77 W/cm² (I_{SATA}) 10 min • n = 1	Harle *et al.* 2001a [115]	[115]	[115]	inner flask surface 0.1 to 0.8°C	MG63 cells monolayer • 40 ml	Up-regulation of TGF-β1 and β3 gene expressions; 1.77 W/cm² optimal
Hayton *et al.* 2005 [122]	1.5 MHz, 1 kHz, 20% 30 mW/cm² (I_{SATA}) 40 min • n = 1 (once) or 6 (twice/day)	**C** plastic ø60 mm Petri dish NF (3 mm) • 37°C??	medium	well–air	NR	SaOS-2 cells monolayer • 8 ml	Post-sonication ATP release to culture medium ↑ (n = 1), expression of several genes altered (c-Fos, RANKL, OPG), proliferation ↑ (n = 6); similar stimulations using ATP-impregnated medium

Table 3-4 continued

Sant'Anna *et al.* 2005 [282]	1.5 MHz, 1 kHz, 20% 30 mW/cm² (I_{SATA}) 20 min • n = up to 7 (once/day)	**D** plastic 12-well NF (NR) • 37°C	gel–well	medium–air	NR	rat BMSC cells monolayer • 1 ml	Expression of several genes ↑↓ (Cbfa-1, ALP, OPN, collagen, BMP-2 and 7, TGF-β 1 and 2, VEGF, IGF-1, and their receptors); no synergistic effect with BMP-2 treatment; most changes after three sonications
Sena *et al.* 2005 [292]	1.5 MHz, 1 kHz, 20% 30 mW/cm² (I_{SATA}) 20 min • n = 1	**D** plastic 12-well NF (NR) • 37°C	gel–well	medium–air	medium 36.8 ± 04°C (abs.)	rat BMSC cells monolayer • 2 ml	Several early response/bone differentiation marker genes ↑ (c-Jun, EGR-1, c-Myc, TGF-β stimulated clone-22, COX-2, osteonectin, OPN); Cbfa-1 and ALP →
Yang *et al.* 2005 [360]	1 MHz CW 62.5 to 250 mW/cm² (I_{SATA}) 10 min • n = 1 to 11 (once/day)	**D** plastic 6- and 24-wells, glass coverslips NR (NR) • 37°C	water–well	medium–air	NR	mouse MC3T3-E1, rat primary OB, or rat bone marrow hematopoietic OC cells monolayer • NR	Optimal 125 mW/cm²; MC3T3-E1 and primary OB cells: changes in cell surface integrins (n = 1); MC3T3-E1 cells: collagen, mineralization, and ALP ↑ (n = 11); OC cells: osteoclastogenesis ↓ (n = 5)
Bandow *et al.* 2007 [18]	1.5 MHz, 1 kHz, 20% 30 mW/cm² (I_{SATA}) 20 min • n = 1	Iwabuchi *et al.* 2005 [146]	[146]	[146]	NR	MC3T3-E1 cells monolayer • NR	Expressions of several cytokines ↑ (MCP-1, RANKL, macrophage-inflammatory protein-1β and 2, angiotensin II type I receptor); OB's have different response to ultrasound at different stages of maturation
Gleizal *et al.* 2006 [101]	1 MHz, ??Hz, 20% 0.1 to 0.5 W/cm² (I_{SATA}??) 5 min • n = 1 to 3 (once/day)	**C** plastic 6-wells NF (8 mm) • 37°C	medium	well–water–tank	NR	mouse primary OB cells monolayer • NR	Proliferation rate ↑ (0.1 W/cm²); osteogenesis-related gene expressions ↑ (all intensities)
Ikeda 2006 *et al.* [143]	1.5 MHz, ??Hz, ??% 70 mW/cm² (I_{SATA}) 20 min • n = 1	**C** plastic 6-wells NF (3-4 mm) • ??°C	medium	well–air ??	NR	mouse C2C12 myoblast cells monolayer • NR	mRNA expressions of cell phenotype-specific markers for osteoblasts (*e.g.* Runx2, zinc finger transcription factor AJ18) and chondroblasts (transcription factor Sox-9) ↑, while ↓ for myoblasts and adipocytes; Runx2 protein expression ↑; phosphorylation of ERK 1/2 and p38 MAPK ↑ indicating pathway activation
Li *et al.* 2006 [189]	1 MHz, 100 Hz, 20% 0.6 W/cm² (I_{SATP}) 15 min • n = 1	Li *et al.* 2002 [187]	[187]	[187]	< 0.2°C, [187]	[187]	Cellular viability ↑, viability blockers tested, similar results using a pulsed electromagnetic device administered for 2 hours
Maddi *et al.* 2006 [199]	45 kHz CW 30 mW/cm² (I_{SATA}) 5 min • n = 1	**C** plastic 6-well NF (5 mm) • 37°C	medium	well–water–absorber	NR	MG63 cells monolayer • 5 ml	mRNA expression: ALP ↑, OCN ↑, OPG ↑, RANKL →, TNF-α →; protein levels: OPG ↑, RANKL ↓, TNF-α →
McCormick *et al.* 2006 [214]	1.5 MHz, 1 kHz, 20% 30 mW/cm² (I_{SATA}) 20 min • n = 1	**C** plastic cell slide NF (5 mm) • 37°C	medium	slide–water–absorber	NR	SaOS-2 monolayer • NR	No morphological changes after sonication, cell elongation and cell orientation changes after fluid shear stress (19 dyne/cm²); BMP-4 expression after sonication →, after fluid shear ↓, further decrease after shear stress when pre-sonicated

Table 3-4 continued

Tang *et al.* 2006 [315]	1.5 MHz, 1 kHz, 20% 30 mW/cm² (I_{SATA}) 20 min • n = 1 or 10 (once/day)	**C** plastic 6-well NF (5-6 mm) • ??°C	medium	well–air	NR	MC3T3-E1 or rat primary OB cells monolayer • NR	Cell surface integrin expressions ↑, COX-2 expression and PGE_2 levels ↑; ultrasound induced bone formation through integrin/FAK/PI•K/Akt and ERK pathway
Chiu *et al.* 2008 [39]	1.5 MHz, 1 kHz, 20% 30 mW/cm² (I_{SATA}) 20 min • n = 1	Tang *et al.* 2006 [315]	[315]	[315]	[315]	rat primary OB cells monolayer • NR	MMP-13 ↑ through p38 and JNK pathways
Unsworth *et al.* 2007 [332]	1.5 MHz, 1 kHz, 20% 30 mW/cm² (I_{SATA}) 20 min • n = 1 to 10 (once/day)	**D** plastic 6-well NF (NR) • 37°C	gel–well	medium–air	medium not significant	MC3T3-E1 cells monolayer • 2 ml	ALP enzymatic activity and expression ↑, MMP-13 expression ↑, mineralization ↑, ($n \geq 6$)
Tang *et al.* 2007 [316]	1.5 MHz, 1 kHz, 20% 30 mW/cm² (I_{SATA}) 20 min • n = 1	Tang *et al.* 2006 [315]	[315]	[315]	[315]	MC3T3-E1 cells monolayer • 1 ml	NO formation ↑; ultrasound up-regulates inducible NO synthase involving ILK/Akt and mTOR pathways
Tam *et al.* 2008 [313]	1.5 MHz, 1 kHz, 20% and/or shock-waves 30 mW/cm² (I_{SATA}) 20 min • n = up to 33 (once/day)	**D** plastic 6-well NF (NR) • ??°C	gel–well	medium–air	NR	human periosteal cells monolayer • ~ 0.3 ml (0.27 mm)	Proliferation, viability, ALP ↑ (n = 4), mineralization → (n = 33); no additive effect with shock-waves, shock-waves more effective in later days
Hasegawa *et al.* 2009 [118]	1.5 MHz, 1 kHz, 20% 30 mW/cm² (I_{SATA}) 20 min • n = up to 28 (once/day)	**D** plastic 6-well NF (NR) • 37°C	water (thin)–well	medium–air	NR	human fracture haematoma-derived progenitor cells monolayer • NR	Cells differentiate to osteogenic direction: trend to enhanced proliferation (n = 2, 4, and 7); ALP (after $n \geq 2$), OCN (after $n \geq 4$), mineralization (n = 28) ↑; bone specific gene responses ↑
Hauser *et al.* 2009 [120]	1.5 MHz, 1 kHz, 20% 30 mW/cm² (I_{SATA}) 6 min • n = 2 (twice/day)	**D** plastic 6-well + ø12 mm coverslips NF (NR) • 37°C	gel–well	medium–air	NR	SaOS-2 cells monolayer • 2 ml	Proliferation and mitotic activity ↑; altered cell cytoskeleton structure; post-sonication cell rounding
Hou *et al.* 2009 [129]	1.5 MHz, 1 kHz, 20% 30 mW/cm² (I_{SATA}) 20 min • n = 1	Tang *et al.* 2006 [315]	[315]	[315]	[315]	murine primary OB cells monolayer • NR	BMP-2 expression ↑. BMP-2 expression through PI3K, Akt, c-Fos/c-Jun, and AP-1 pathways
Lu *et al.* 2009 [194]	1.5 MHz, 1 kHz, 20% 30 mW/cm² (I_{SATA}) 20 min • n = 1	**D** plastic 6-well NF (NR) • 37°C	gel–well	medium–air	NR	SaOS-2 cells monolayer • NR	cDNA microarray reporting 165 altered genes in osteoblast-like cells (> 100 not previously reported)
Alvarenga *et al.* 2010 [6]	1.5 MHz, 1 kHz (??), 20% (??) 30 mW/cm² (I_{SATA}) 20 min • n = up to 7 (once/day)	Hayton *et al.* 2005 [122] ??	[122]	[122]	NR	neonatal rat OB cells monolayer • NR	Cell proliferation ↑ ($n \geq 5$); sonication induces ATP/purines; osteoblast proliferation related P2Y receptor presence ↑
Borsje *et al.* 2010 [25]	1.5 MHz, 1 kHz, 20% 30 mW/cm² (I_{SATA}) 10 min, n = 1	**C** plastic 6-well NF (5 mm) • 37°C	medium	well–water–absorber	NR	human SaOS-2 cells monolayer • NR	LIPUS (10 min) or 2 mT pulse electromagnetic field (PEMF) (3h): both quick and delayed OPG and RANKL expressions; OPG protein level ↑ 0 or 4h after LIPUS or 8h after PEMF

Table 3-4 continued

Marvel *et al.* 2010 [208]	1 MHz, 1, 10, or 1000 Hz, 20% 30 mW/cm² (I_{SATA}) 20 min • n = up to 14 (once/day)	**D** plastic BioFlex® plates having flexible membrane bottom NF (NR) • 37°C	direct membrane contact	medium–air??	NR	human adipose and bone marrow stem cells monolayer • NR	proliferation ↓ in both cell types; in bone marrow cells, highest reduction at PRF = 1 kHz; cell calcium accretion per DNA ↑ in adipose cells at PRF = 1 kHz (n = 7), similar trend in mesenchymal cells
Wang *et al.* 2010 [339]	1.5 MHz, 1 kHz, 20% 30 mW/cm² (I_{SATA}) 30, 60 or 180 min, n = 1	**D** plastic 6-well NF (NR) • 37°C	gel–well	medium–air	NR	human U2OS cells monolayer • NR	Superparamagnetic nanoparticle intake in cells (Exogen® device, all durations)
Angle *et al.* 2011 [7]	1.5 MHz, 1 kHz, 20% 2, 15 or 30 mW/cm² (I_{SATA}) 20 min • n = 1 to 24 (once/day)	Sena *et al.* 2005 [292]	[292]	[292]	[292]	rat BMSC monolayer • 2 ml (??)	ostegenic differentiation ↑: p38 MAPK pathway phosphorylation ↑, indication for ERK1/2 phosphorylation (n = 1), ALP activity ↑ (n = 7), indication for mineralization (n = 24). Most effective 30 mW/cm², effects also at 2 and 15 mW/cm²
Hsu *et al.* 2011 [132]	1 MHz, 100 Hz, 20% or CW 50, 150, or 300 mW/cm² (I_{SATP}??) 3 min • n = up to 14 (once/day)	**C** plastic 24- or 12-well NF (18 mm) • 37°C	medium	well–castor oil–rubber	medium < 0.3°C	MG63 OB cells on titanium plate / plate on defected neonatal rat calvaria monolayer/bottom contact • 3 ml	Cell rounding (CW 300 mW/cm², n = 5); cell viability ↑ (pulsed), viability ↓ (CW); ALP activity with/without the titanium plate →/↓; proliferation ↑ (only pulsed at 50 and 150 mW/cm², n = 3); in calvaries (n = 35): enhanced cell alignment and migration; formation of mineralized bone matrix and nodule ↑ (specifically pulsed 300 mW/cm²)
Kang *et al.* 2011 [155]	1 MHz, CW 30 mW/cm² (I_{SATA}) 20 min • n = 1 or 7 (once/day)	**D** plastic 6-well NF/FF (45 mm) • 37°C	water–well	medium-PTFE bar	NR	rat MC3T3 pre-OB scaffold • NR	Ultrasound and/or cyclic strain (10 Hz, 10% ≈ 0.3 mm) treatment on scaffolds: bone-specific marker gene expressions, ALP protein level and Ca^{2+} concentration ↑ with both methods (n = 7 and 14); combination of ultrasound and strain the most effective
Sena *et al.* 2011 [293]	1.5 MHz, 1 kHz, 20% 30 mW/cm² (I_{SATA}) 20 min • n = 1 or 7 (once/day)	Sena *et al.* 2005 [292]	[292]	[292]	[292]	rat BMSC monolayer • 2 ml	Intercellular dye transfer from the donor cells to the acceptor cells in sonicated co-culture; gap junction inhibitor inhibits ERK1/2 and p38 MAPK phosphorylation (n = 1), and ALP activity (n = 7)
Zia Uddin *et al.* 2011 [370]	1 MHz, 1 kHz, 20% + amplitude modulation (45 or 100 kHz) 5 mW/cm² (I_{SATA}??) 15 min • n = up to 18 (once/day)	**D** chamber slide Focal point (16 mm) • 37°C	water–slide	slide–air	NR	MC3T3-E1 OB cells monolayer • 0.75 ml	Enhanced ALP activity and mineralization especially at 100 kHz amplitude modulation.
Jiang *et al.* 2012 [150]	1 MHz, 1 kHz, 20% 100 mW/cm² (I_{SATA}) 8 min • n = up to 21 (once/day)	**D** ø35 mm plastic dishes NF (NR) • 37°C	gel–well	medium–air	NR	rat adipose derived stem cells monolayer • NR	ALP activity (n = 7 and 14) and mineralization (n = 21) ↑; osteogenic gene expressions (Runx2, ALP, BSP, OCN) ↑, collagen I →, (n ≥ 3 or 5); protein expressions (BSP, Runx2) ↑ (n = 7 and 14)

Table 3-4 continued

Li *et al.* 2012 [190]	1.5 MHz, 1 kHz, 20% 30 mW/cm² (I_{SATA}) 20 min • n = 1	**C** plastic 6-well NF (3 mm) • 37°C	medium	well–gel–absorber	NR	murine MLO-Y4 OCY or MC3T3-1 OB cells monolayer • 3 ml	Conditioned medium from the sonicated osteocytes inhibits osteoblast proliferation but enhances osteoblast differentiation; in sonicated osteocytes, PGE_2 and NO production ↑
Man *et al.* 2012a [202]	1 MHz, 63 Hz, 21.6% and 45 kHz CW 250 mW/cm² (I_{SATA}) 25 mW/cm² (I_{SATA} 45 kHz) 30 min • n = 1	**C** plastic 6-well NF (NR) • 37°C	medium	well–water–absorber	medium 3.3°C (45 kHz)[203]	MC3T3-E1 OB cells monolayer • 9 ml	Cell proliferation/scratch-wound assay ↑; 1 MHz and 45 kHz equally effective
Zhang *et al.* 2012 [367]	3.3 MHz, 0.5 Hz, 15% P_{TA} = 0.9 W, p^- = 9.18 MPa 1 min • n = 1	**C** ø35 mm Petri dish with liquid waveguide Focal point (62.6 mm) • 37°C	silicon–medium	dish–air	dish bottom < 0.4°C , 3 minutes sonicated	MC3T3-E1 OB cells monolayer • 4 ml	Cell viability not affected; cytoskeleton arrangement; bending movement of cilia during sonications; calcium influx into cells; cells stimulated through focused transducer-generated radiation force
Fung *et al.* 2014 [92]	1.5 MHz, 1 kHz, 20% 30 mW/cm² (I_{SATA}) 20 min • n = 1	**D** ø35 mm culture dish NF, mid-NF and FF (0, 60 and 130 mm) • 37°C	(rubber)–gel–well	medium–air	NR	murine MLO-Y4 OCY or MC3T3-1 OB cells monolayer • 2 ml	Osteocytes: β-catenin nuclear translocation → (0 mm), ↑ (60 and 130 mm); Osteoblasts cultured in conditioned medium from the sonicated osteocytes: wound healing assay ↑, proliferation ↓, calcium nodules ↑ and NO ↑; far field distance 130 mm is the most effective on osteocyte stimulation and osteocyte–osteoblast mechanotransduction

Table 3-5. ***In vitro*** **ultrasound studies to stimulate chondrocyte formation and chondrogenic differentation. Abbreviations**: **dc = duty cycle; *n* = number of repeated sonications (treatments/day); PRF = pulse repetition frequency // A, B, C, D = sub-illustrations in Fig. 4.1; FF = acoustic far field; NF = acoustic near field; NF/FF = near-far field transition // BMSC = bone marrow stromal cell; CC = chondrocyte; FC = fibrocyte; MSC = mesenchymal stem cell // BMP = bone morphogenetic protein; COX-2 = cyclooxygenase-2 (prostaglandin-endoperoxide synthase 2); ERK = extracellular-signal regulated protein kinase; GAG = glycosaminoglycans; MMP = matrix metalloproteinase; NO = nitric oxide; TGF = transforming growth factor; VEGF = vascular endothelial growth factor // ↑/↓/→ = ultrasound has stimulating effect/ inhibiting effect/ is equally effective respect to the sham treatment // NR = value not reported; ?? = value not clear.**

Reference	Sonication parameters	Setup type	Coupling	Transmission	US heating	In vitro sample	Main outcome
Example	*operating frequency, PRF, dc* *acoustic intensity* *duration • n = no. of sonications*	*Ref. to Fig. 4.1* *exposure chamber type* *distance (mm) • temperature*	*transducer* *coupling path to sample volume*	*sound path after the sample transmission*	*measurement point* *temperature value*	*sample* *contact • medium volume*	
Parvizi *et al.* 1999 [252]	1 MHz, 1 kHz, 20% 50 and 120 mW/cm² (I_{SATA}) (230 and 360 kPa average peak pressures) 10 min • *n* = up to 5 (once/day)	**D** plastic 6-well NF (3-4 mm) • 37°C	water (3mm)–well	medium (2mm)–air	estimated ≈ 1°C	neonatal rat CC cells monolayer • NR	Trend for increased cell number and proliferation; cell detachment at 360 kPa (*n* = 1); type I and II collagen expression →; aggrecan expression ↑ (*n* = 3 and 5);proteoglycan synthesis ↑ (230 and 250%, *n* = 3 and 5)
Nishikori *et al.* 2002 [238]	1.5 MHz, 1 kHz, 20% 30 mW/cm² (I_{SATA}) 20 min • *n* = 6 (once/day, twice/week)	**D** ø27 mm plastic dish NF (NR) • 37°C??	gel–dish	medium–air	NR	rabbit CC cells embedded in Atelocollagen® gel bottom contact • 2 ml	Cell number →; chondroitin sulfates C6S, C4S, and ratio C6S/C4S ↑; gel stiffness ↑
Parvizi *et al.* 2002 [253]	1 MHz, 1 kHz, 20% 88-556 kPa pressure from 2 s up to 10 min • *n* = 1 or 3	Parvizi *et al.* 1999 [252] ?? • 37°C	[252]	[252]	medium ≈ 0°C (preliminary)	neonatal rat CC cells monolayer • NR	Intracellular calcium ↑: rapid and transient at 175-320 kPa (peak 222 kPa), rapid and sustained at 350-500 kPa; proteoglycan synthesis ↑ (2.5-fold at 222 kPa, *n* = 3); synthesis → when intra-/extracellular calcium chelated/depleted
Zhang *et al.* 2002 [368]	1.5 MHz, 1 kHz, 20% 30 mW/cm² (I_{SATA}) 20 min • *n* = up to 7 (once/day)	**C** ø35 mm plastic dish with Parafilm NF (5 mm) • 37°C??	gel–film	dish–absorber ??	NR	sterna from 16-day-old chick embryo bottom contact • NR	Proximal part of sterna: collagen II ↑ (*n* ≥ 3), type X collagen and aggrecan ↑ (*n* ≥ 1); distal part of sternum: collagen II ↑ (*n* ≥ 3), aggrecan ↑ (*n* ≥ 1), collagen X →; ultrasound induces hypertrophy in proximal part; ultrasound doesn't induce hypertrophy in distal hyaline-like cartilage but induces both aggrecan and collagen II
Zhang *et al.* 2003 [369]	1.5 MHz, 1 kHz, 20% 2 or 30 mW/cm² (I_{SATA}) 20 min • *n* = up to 7 (once/day)	**C** ø35 mm plastic dish with Parafilm (0.127 mm); at 2 mW/cm² 120 mm thick attenuator included NF or FF (3 or 123 mm) • 37°C??	(gel–attenuator–) gel–film	dish–absorber ??	NR	CC cells from 16-day-old chick embryo distal sterna embedded in alginate bead bottom contact • NR	Viability→; proliferation ↑↓→: *n* = 1, 3 or 7 at 30 mW/cm² ↓, *n* = 3 at 2 mW/cm² ↑; immunohistochemistry staining: collagen II ↑ (*n* = 7, specifically 2 mW/cm²) and collagen X ↓, aggrecan →; mRNA expressions: collagen II ↑, X ↓ (*n* = 7, specifically 2 mW/cm²), aggrecan ↓ (*n* = 1 and 3)

Table 3-5 continued

Ebisawa *et al.* 2004 [74]	1 MHz, 1 kHz, 20% 15 to 120 mW/cm² (I_{SATA}) 20 min • n = 10 (once/day)	**D** polypropylene tube (15 ml) NF (NR) • 37°C	gel ??–tube	medium–air	NR	human MSC pellet bottom contact • 2 ml	Aggrecan synthesis in TGF-β treated pellets ↑ at 30, 60, and 120 mW/cm², highest at 30 mW/cm²; protein amount and proliferation → (only 30 mW/cm² tested); aggrecan in pellet (30 mW/cm²): sonication with TGF-β ↑, without TGF-β →; optimal matrix formation on the pellet side close to the transducer
Argadine *et al.* 2005 [12]	1.5 MHz, 1 kHz, 20% and 1 kHz square wave 30 mW/cm² (I_{SATA})/displacement 4 nm 20 min • n = up to 12 (once/day)	**D** plastic 6-well NF (NR) • 37°C	gel–well	medium–air	NR	mouse ATDC5 CC cells monolayer • NR	Chondrogenesis (Alcian-blue staining of cartilage nodules) ↑: more staining with 1 kHz sound; more treatments results more staining; later the treatments after plating started more intense the staining
Iwabuchi *et al.* 2005 [146]	1.5 MHz, 1 kHz, 20% 30 mW/cm² (I_{SATA}) 20 min • n = up to 4 (once/day)	**B** plastic 6-well with silicon chamber NF/FF (130 mm) • 37°C	water–well	medium–absorber	NR	rat intraverbereal disc tissue samples bottom contact • NR	Ultrasound accelerates herniated disc resorption (apoptosis ↑, n = 4); resorption activated through MMP-3 via TNF-α and MCP-1 pathways; no effect on normal intraverbereal disc
Miyamoto *et al.* 2005 [221]	1.5 MHz, 1 kHz, 20% 30 mW/cm² (I_{SATA}) 20 min • n = up to 20 (once/day)	**D** plastic 24-well NF (NR) • 37°C??	gel–well	medium–air	NR	bovine CC-like, FC-like, or intermediate-like cells in alginate beads bottom contact • NR	Cell viability and proliferation →; proteoglycan synthesis ↑ (n= 20); collagen synthesis ↑ ($n \geq 10$); proteoglycan accumulation in beads having FC-like and intermediate-like cell ↑ ($n \geq 10$)
Mukai *et al.* 2005 [224]	1.5 MHz, 1 kHz, 20% 30 mW/cm² (I_{SATA}) 20 min • n = up to 10 (once/day)	**A** plastic culture tube NF (30 mm) • 37°C	water–tube	medium–plastic–water absorber	NR	neonatal rat CC cell aggregate monolayer • 0.2 ml ??	Collagen X expression ↓ (n = 5); collagen II and aggrecan expressions ↑ (n = 10); proliferation ↑, and ALP/DNA ratio ↓ (n = 7); both TGF-β1 expression and protein production ↑ (n = 1); anti-TGF-β1 inhibits ultrasound effects
Argadine *et al.* 2006 [13]	Argadine *et al.* 2005 [12]	[12]	[12]	[12]	NR	[12]	Study in Ref. [12] repeated: cells unresponsive; this cell line cells have lost their capability to differentiate
Choi *et al.* 2006 [40]	1 MHz, CW 100 to 300 mW/cm² (I_{SATA}) 10 min • n = up to 15 (once/day)	**D** ø60 mm culture dish NF (NR) • room temperature??	gel–dish	medium–air	NR	human articular CC cells in alginate bead bottom contact • NR	Viability ↑, peak at 200 mW/cm² (n = 15); proliferation → (n = 7); proteoglycan and collagen II synthesis ↑, peak at 200 mW/cm² (n = 7); expression of several genes *e.g.* MMP-1 ↓ (n = 7)
Hsu *et al.* 2006 [131]	1 MHz, 100 Hz, 20%, 50% or CW 17 to 100 mW/cm² (I_{SPTA}) 10 min • n = up to 49 (once/day)	**D** plastic 24-well FF (120 mm) • 37°C	water–well	medium–air	unchanged	human articular CC cells in polyester composite scaffold or cell monolayer bottom contact/monolayer • 1 ml	Optimization, monolayer (n = 6): proliferation ↑ (only at 100 Hz, dc = 20%, 67 mW/cm²), GAG production per cell →; NO in medium or per cell ↓ (on all parameters); Scaffold sonications (100 Hz, dc = 20%, 67 mW/cm²) : cell number ↑ (n = 7 and 28), → (n = 42 or 49); GAG ↑ (only n = 28); collagen II ↑ (only n = 28); NO per cell ↓ (only n = 28); neocartilage-stimulating effect on ultrasound is shorter (28 days) than in rotating-type bioreactor (42 days)

Table 3-5 continued

Iwashina *et al.* 2006 [148]	1.5 MHz, 1 kHz, 20% 7.5 to 120 mW/cm² (I_{SATA}) 20 min • n = up to 12 (once/day)	**B** plastic 6-well w/ absorption chamber NF (NR) • 37°C??	gel–well	medium–chamber	NR	rabbit CC-like or FC-like cells embedded in alginate bead bottom contact • 4.5 ml ??	Cell proliferation ↑: both cell types at 7.5 mW/cm² (n = 5 and 12); proteoglycan synthesis ↑: both cell types at 30, 60, and 120 mW/cm² (n = 5 and 12); Proteoglycan content ↑: CC-like cell at 30 and 120 mW/cm² (n = 12), FC-like cells at 30, 60, and 120 mW/cm² (n = 5 and 12)
Lee *et al.* 2006 [178]	1 MHz, CW 200 mW/cm² (I_{SATA}) 10 min • n = 14 or 28 (twice/day)	**D** ø60 mm culture dish NF (NR) • room temperature??	gel ??–dish	medium–air	NR	rabbit CC cells in alginate bead or monolayer bottom contact/monolayer • NR	Alginates: expression of proteoglycan and collagen II ↑ (with or without TGF-β3 co-treatment, n = 12 and 28); chondrogenic marker expressions *e.g.* Sox-9 ↑; Cells from the sonicated (n = 14) beads replated as monolayers: proliferation rate ↑; chondrogenic marker expressions ↑
Min *et al.* 2006 [220]	1 MHz, CW 40 to 700 mW/cm² (I_{SATA}) 10 min • n = 7 (once/day)	**D** plastic 4-well NF (local maxima,60 mm) • 37°C	water–well	medium–air	circulating water inhibited heating	human articular CC cells monolayer • 3 ml/g tissue	proliferation → (all intensities); proteoglycan synthesis ↑ (200 mW/cm²), ↓ (500 and 700 mW/cm²); proteoglycan amount: ↑ (200 mW/cm²), ↓ (700 mW/cm²);); collagen II synthesis ↑ (200 mW/cm²), ↓ (500 and 700 mW/cm²); histologies after 200 mW/cm² sonications: GAG and collagen II ↑, collagen X ↓
Schumann *et al.* 2006 [289]	1.5 MHz, 1 kHz, 20% 30 mW/cm² (I_{SATA}) 20 or 40 min, n = 7 (once/day)	**D** plastic 6-well NF (< 2 mm) • 37°C	gel–well	medium–air	NR	human bone marrow MSC cell aggregate or scaffold bottom contact • 2.5 ml	Aggregates: expression of aggrecan, type I, II, and X collagen ↓ (20 min sonication); all ↑ when sonicated for 40 minutes; proteoglycan and collagen contents ↑ (40 min); Scaffolds (40 min): collagen II expression ↑, aggrecan and collagen I →; proteoglycan and collagen content ↑
Choi *et al.* 2007 [41]	1 MHz, CW 200 mW/cm² (I_{SATA}) 5, 10, 15, or 20 min • n = 1	**D** ø60 mm culture dish with/without ø12 mm coverslip NF (NR) • room temperature??	gel–well	medium–air	heat effect is not likely	human C-28/12 CC cells monolayer • NR	Aggrecan and collagen II mRNA levels highest when sonicated for 15 minutes; ultrasound signal mediated through stretch-activated channels and integrins, and JNK and ERK pathways.
Cui *et al.* 2007 [54]	0.8 MHz, CW 200 mW/cm² (I_{SATA}) 20 min • n = 7 (once/day)	Lee *et al.* 2006 [178]	gel–dish	[178]	NR	rabbit MSC cells in polyglycolic acid scaffold monolayer • NR	Ultrasound or sham pre-treated scaffolds were subcutaneously implanted in mice. Analysis of retrieved (4 and 6 weeks post-implantation) scaffolds indicated higher volume, increased cartilage-specific extracellular matrix accumulation, delayed ostegenesis, increased type II collagen level, and decreased mechanical strength (control 25 MPa, ultrasound 16 MPa, native 4 MPa) for the sonicated scaffolds

Table 3-5 continued

Hsu *et al.* 2007 [130]	1.5 MHz, 1 kHz, 20% 30 mW/cm² (I_{SATA}) 20 min • n = 1	Tang *et al.* 2006 [315]	[315]	[315]	NR	human articular CC cells monolayer • NR	Expression of PGE_2 ↑; expression and protein levels of COX-2 ↑; COX-2 expression is activated through cell membrane integrins, ILK, Akt, NF-κB and p300 pathway
Lee *et al.* 2007 [179]	1 MHz, CW 200 mW/cm² (I_{SATA}) 20 min • n = 7 or 14 (once/day)	?? ø35 mm culture dish NF (NR) • 37°C	gel??–dish	medium–air??	NR	human bone marrow MSC cells in alginate layer bottom contact • NR	Cell viability ↑, inhibits cell damage and apoptosis respect to the TGF-β1 treated or control cells (n = 7 and 14); chondrogenic markers (Sox-9, aggrecan, collagen II) ↑ with/without TGF-β1
Noriega *et al.* 2007 [242]	1.5, 5 or 8.5 MHz (5 MHz transducer), CW estimated < 30 mW/cm² (I_{SATA}) 161, 51, or 24 s • n = 20 (twice/day)	**C** plastic 12-well NF (8.5 mm) • ??	medium	well–air	?? 0.5 to 1 °C	human cartilage CC cells in chitosan scaffold bottom contact • NR (10.2 mm)	DNA content and total collagen amount ↑ (5 MHz); viability ↑ (all frequencies); morphological changes (5 and 8.5 MHz); expressions of aggrecan and collagen II ↑ (5 and 8.5 MHz)
Park *et al.* 2007 [250]	1.5 MHz, 1 kHz, 20% 30 mW/cm² (I_{SATA}) 10 to 50 min (50 min cycled) • n = 5 (once/day)	**D** plastic 24-well NF (NR) • 37°C	gel–well	medium–air	medium above physiological level	porcine osteoarthritic articular cartilage CC cell pellet bottom contact • 2 ml??	Cell proliferation and viability in IL-1β pre-treated pellets →; GAG deposit in constructs ↑ (50 min only), loss in the medium →; GAG and collagen in constructs through histology ↑ (50 min); gene expressions: collagen II/I ratio ↓, MMP-1 ↓ while MMP-13 and TGF-β1/3 → after 50 min sonication; when the ultrasound setup was modified to curb the heating, GAG levels in constructs lower than using the original setup
Korstjens *et al.* 2008 [169]	1.5 MHz, 1 kHz, 20% 30 mW/cm² (I_{SATA}) 20 min • n = 6 (once/day)	Nolte *et al.* 2001 [239]	[239]	[239]	NR	human osteoarthritic/non-osteoarthritic cartilage sample or CC monolayer bottom contact/monolayer • 2.54 ml	^{35}S incorporation of proteoglycans ↑ in arthritic and non-arthritic monolayers, change higher in degenerated cells; explants: incorporation → in both explants; incorporation ↑ in arthritic explants when analyzed through autoradiographs; indications for CC proliferation and matrix production (histologies)
Tien *et al.* 2008 [324]	1 MHz, 1 kHz, 20% 18 to 98 mW/cm² (I_{SPTP}??) 20 min • n = up to 14 (once/day)	**D** plastic 48-well FF (150 mm) • 37°C	water–well	medium–air	NR	human child articular cartilage CC cells in agarose gel bottom contact • 1 ml	Time-dependent elevation of aggrecan synthesis (98 mW/cm², up to n = 14); optimal intensity to induce the aggrecan synthesis is ≥ 48 mW/cm² (n = 14); collagen II synthesis ↑ at 48 mW/cm² higher than at 18 mW/cm² (n = 14); proliferation → (all intensities, n = 14); aggrecan response from a 1-year-old donor stronger and faster than from a 10-year-old donor (48 mW/cm²)
Takeuchi *et al.* 2008 [311]	1.5 MHz, 1 kHz, 20% 30 mW/cm² (I_{SATA}) 20 min • n = up to 14 (once/day)	**A** plastic 24-well NF (NR) • 37°C??	silicon rubber–gel-well	medium–air	NR	pig articular cartilage CC cells in type I collagen sponges bottom contact • 2 ml ??	Proliferation ↑ (n = 14); protein levels *e.g.* type IX collagen, cyclin B_1, cydin D_1 ↑; collagen II →; activation of integrin/phosphatidylinositol 3-OH kinase/Akt pathway

Table 3-5 continued

Kobayashi *et al.* 2009 [163]	1.5 MHz, 1 kHz, 20% 7.5 to 120 mW/cm² (I_{SATA}) 20 min • n = up to 12 (once/day)	**B** Iwabuchi *et al.* 2005 [146] NF (NR) • room temperature	gel–well	medium–abs. chamber	NR	human CC-like cells embedded in alginate bead bottom contact • 4 ml	Proliferation ↑ (60 and 120 mW/cm², n = 5); cell number ↑ (only 120 mW/cm², n = 5 and 12); proteoglycan synthesis ↑ (all intensities, n = 5 and 12); cDNA array indicate several up-regulated genes *e.g.* growth factors BMP-2, TGF-β1 receptor, and VEGF (only 30 mW/cm² was tested, n = 3)
Naruse *et al.* 2009 [230]	1.5 MHz, 1 kHz, 20% 30 mW/cm² (I_{SATA}) 20 min • n = up to 15 (once/day)	**D** plastic 6-well with metal clip to fix the sample NR (NR) • ??	NR	medium–air	NR	rat bilateral femora bottom contact • NR	Cartilage directly unresponsive to ultrasound: diaphyseal and condular length, proteoglycan synthesis, and histologic features of cartilage → (all time points); periosteum responsive: extended mineralization and periosteum calcification only at the entry side of ultrasound beam
Yoon *et al.* 2009 [363]	40 kHz, ??Hz, 50% 25-35 mW/cm² (NR) 50 to 600 s • n = 1 or 2	conical culture tube (15 ml) NR (NR) • NR	NR	NR	NR	human umbilical cord cells monolayer • NR	Sonication increases MSC amount derived from the cord explants (50s, n = 1); isolated MSc's: viability → (100s, n = 1) and ↓ (300 and 600s) ; proliferation ↑ (100s, n = 1), ↓ (100s, n = 2) ; adherent post-sonicated cells express osteogenic and chondrogenic differentiation potential
Lai *et al.* 2010 [175]	1 MHz, 100 Hz, 20% 200 mW/cm² (I_{SATP}) 20 min • n = up to 28 (once/day)	Li *et al.* 2002 [187]	[187]	[187]	[187]	human bone marrow MSC cells monolayer • NR	Morphology: sonicated cells grow in lower cell density and cell shape rectangular/cuboidal (with/without dexamethasone/TGF-β1 or BMP-2 co-treatment, n = up to 28); mRNA expressions: ultrasound enhances dexamethasone/TGF-β1 induced chondrogenic markers; ultrasound alone enhances ostegenic markers but doesn't amplify the BMP-2 induction
Uenaka *et al.* 2010 [329]	1.5 MHz, 1 kHz, 20% 30 mW/cm² (I_{SATA}) (70 kPa average pressure) 20 min • n = up to 35 (once/day)	**D** plastic 6-well with inner ring having porous (0.2 µm) membrane NF (NR) • 37°C	gel–well	medium–air	NR	rat chondrocytes inoculated on porous membrane bottom contact • 12 ml	Cell density relevant: 1.0, 2.0 and 4.0 ·10⁷ cell/cm² tested, significant effects only when the density is 2.0·10⁷ cell/cm²; aggrecan and GAG ↑, collagen I and II → after sonications; histologies indicate that collagen II and proteoglycan ↑
Vaughan *et al.* 2010 [335]	1.5 MHz, 1 kHz, 20% 30 to 300 mW/cm² (I_{SATA}) 20 min • n = up to 15 (once/day)	**D** plastic 6-well NF (NR) • 37°C	gel–well	medium–air	NR (possible heating speculated)	steer CC cells embedded in agarose scaffold or monolayer bottom contact • 6.6 or 6 ml	Scaffold cell viability (n = 9): at 30 to 100 mW/cm² →, at 200 and 300 mW/cm² ↓ (loss of viability highest close to the well bottom); GAG synthesis in scaffolds: sporadic ↑↓ (30 and 100 mW/cm² tested, n = 15); no synthesis in monolayers observed
Hasanova *et al.* 2011 [117]	5 MHz, CW 114 mW/cm² (I_{SPTP}??) 51 s • n = 10 to 80 (once, twice, four times or eight times/day for ten days)	**C** plastic 6-well NF (10.5 mm) • ??	medium	well–air	medium no discernible	calf CC cells in chitosan scaffold bottom contact • NR (12 mm)	Cell viability ↑ (4 times/day); proliferation ↑ (4 and 8 times /day); Gene expressions: collagen I and II ↑ (4 and 8 times/day); Sox-5 and 9 up-regulated; MMP-3 and COX-2→; several integrins ↑↓ (4 and 8 times/day)

Table 3-5 continued

Choi *et al.* 2011 [42]	1 MHz, CW 100 mW/cm² (I_{SATA}) 10 min • *n* = 6 (once/day)	**D** ø60 mm culture dish NF (NR) • 37°C??	gel–well	medium–air	Min *et al.* 2006 [220]	rat bone marrow MSC cells monolayer • NR	Number of MSC colonies in wells ↑, cell attachment to well including expression of integrins α1, β1, and fibronectin ↑; cell doubling time →; phenotype not changed after sonications, multi-potent differentiation capability (e.g. chondrogenic) not affected
Subramanian *et al.* 2013 [308]	5 MHz, CW peak pressure 14 or 60 kPa 51 or 180 s • *n* = several times per day up to ten days	**D** plastic 6-well NF (23 mm) • 37°C	water-well	medium–air	target non-detectable	calf CC monolayer / chitosan scaffold bottom contact • 5–8 ml	Multi-transducer bioreactor introduced: several chondrogenic responses ↑ (viability, proliferation, collagen II expression, protein expressions)

4 Ultrasound Exposures: In Vitro *Bone and Cartilage Studies*

4.1 ULTRASOUND INTERACTIONS

As introduced in Chapter 2, ultrasound can affect cells and tissue via various thermal and mechanical, non-thermal mechanisms. Mechanical interactions include radiation force through sound absorption or reflection, acoustic cavitation, acoustic streaming, standing-wave induced radiation forces, and microstreaming. Additional interactions include mode-converted waves, in the case of acoustic discontinuities; electromagnetic effects, in the case of electrically active targets; and the presence of electromagnetic interference. These interactions are dependent on the amplitude, frequency, and geometry of the acoustic beam and physical properties of the target tissue. In this section, specific effects induced by the various mechanisms are reviewed.

4.1.1 Temperature elevation

One of the physical changes associated with ultrasound exposure is temperature elevation. Elevated temperature resulting from ultrasound exposure has been extensively studied, especially in the case of fetal diagnostic ultrasound due to possible adverse teratogenic effects [1,4]. Ultrasound-induced hyperthermia, alone or in combination with other therapies, is an efficient method to generate cell-destructive responses [56].

Based on current knowledge, it has been stated that *in vivo* temperature elevations less than or equal to 2°C above body temperature, for up to 50 hours, are safe in postnatal subjects [243].

It has been known for a long time that small temperature changes (1–2°C) can alter the human fibroblast collagenase enzyme activity *in vitro* [349]. Moderate temperature elevation and resulting heat stress have also been reported to cause beneficial effects on various cell types [249]. Studies have indicated beneficial responses of bone and cartilage cells after mild heat exposure. Transient exposure to mild hyperthermia has been reported to induce cyclin D1 synthesis in fibroblasts (39–43°C for 40 minutes) [110], enhance differentiation of bone marrow stromal cells and human osteoblastic MG-63 cells (39–41°C for 60 minutes) [298], and enhance differentiation of human mesenchymal stem cells to osteoblasts (41–42.5°C for 60 minutes) [241]. In chondrocytes or chondrocyte-like cells, mild (39–41°C for 15 or 30 minutes) hyperthermia has been reported to improve cell viability and proteoglycan synthesis [128], while higher level (48°C for 10 minutes) [362] hyperthermia has been reported to impair these. Culture media conditioned by heat-shocked (42°C for 60 minutes) human fetal osteoblasts induced osteogenesis of rabbit bone marrow–derived mesenchymal stromal cells [361]. Thermal stress conditioning (four or eight minutes at 44°C) of pre-osteoblastic cells prior to the administration of osteoinductive growth factors has been reported to stimulate several bone-specific markers and up-regulate vascular endothelial growth factor protein levels [44].

In a recent study utilizing human mesenchymal stem cells, the cells were seeded inside a 3D cell matrix and placed inside a heated (41°C) cell culture incubator for one hour once a week, for up to four weeks [35]. These heated-air hyperthermia treatments were found to both accelerate stem cell differentiation towards bone cells, and also to enhance the maturation of these cells to bone cells.

It is believed that heat shock factors and heat shock proteins (HSP) have an important role in these effects [249]. These

proteins are formed when the cells are subjected to stresses, including heat, and protect the cells from protein unfolding. There are also indications that HSPs serve as thermosensitive markers on the cell membrane and take part in increased plasma membrane fluidity. The HSPs that seem to be activated without protein denaturation are considered possible therapeutic targets [301]. In the study by Huang *et al.*, the calming and repairing effect of repeated ultrasound exposures on early-stage osteoarthritic rat cartilage was linked to elevated levels of stress protein after the treatment [134]. Proteins aided the viable chondrocytes to survive resulting in chondrocyte proliferation at the follow-up period, and which was deduced to improve the condition of arthritic cartilage.

In the case of *in vitro* sonications, ultrasound wave energy is absorbed mostly in the cell culture vessel structures, which are normally made of plastic materials (usually polystyrene or polypropylene). On a microscopic level, cells or collagen-rich tissue samples may also absorb the sound and contribute to elevated temperatures.

4.1.2 Radiation force–based momentum transfer and motion

Direct evidence of a radiation force–induced bioeffect came from a study by Mihran *et al.* [215]. In the study, relatively short (500 μs) high-intensity (100–800 W/cm^2) ultrasound (2, 4, and 7 MHz) bursts were focused on excised frog sciatic nerve placed in an *in vitro* exposure chamber. The single bursts were observed to either temporally enhance or suppress the nerve action potentials. Similar effects were seen using a direct mechanical stimulus having comparable duration and amplitude. Displacement amplitudes may be estimated to be on the order of micrometers [237]. The nerve bulk heating was estimated to be insignificant. The exposure was more effective at higher operating frequencies (given constant energy and burst length). The bioeffect was frequency-independent when the results were calculated as a function of energy attenuated in the target at each frequency. A 2 MHz electrical RF pre-stimulus had no effect. Thus, it was suggested that the bioeffect on nerve

action potentials is due to the radiation force acting on stretch-sensitive ion channels of the nerve membrane.

In the LIPUS treatments, a dynamic force is created at the PRF, which is conventionally 100 Hz or 1 kHz. The amplitude of the particle motion for Exogen® LIPUS parameters is on the order of a nanometer (particle velocity 1–1.2 μm/s) in the edges of bone fractures and approximately four-times larger in tissue/fluid space between the fracture ends [106]. The values were measured in a fractured cadaveric human forearm using a laser vibrometer (fractured arm between the transducer and vibrometer). In a recent review, radiation force was suggested as the likely mechanism behind bone fracture healing [46].

There is a relatively limited amount of data that directly compares the different pulse parameters in tissue regeneration. In an early study of Dyson *et al.*, CW sonications and pulsed sonications at 100 Hz were compared (I_{TA} constant) [65]. Both modes were found to regenerate rabbit ear tissue, while pulsed sonications were marginally more effective. In other *in vivo* studies [59,259], the pulsed mode was chosen and applied, as it is less likely to cause heating or cavitation compared to CW.

In vitro studies of Wiltink *et al.* [352], Hsu *et al.* [131], and Hsu *et al.* [132] have used pulsed and CW modes and reported that pulsed (PRF = 100 Hz) sonications are more effective in stimulating bone-length growth, increasing chondrocyte number, and forming higher mineralized bone matrix and denser mineralized nodules in neonatal rat calvarial tissue, respectively. Argadine *et al.* have shown that 20% duty cycle 1 kHz sonic square waves that were generated using acoustic speakers resulted in similar chondrocyte stimulation as the Exogen® signal [12]. The authors further reported that the amplitude of the motion was 4 nm for both devices, in a near-field setup. This strongly suggests that radiation force is one of the cell stimulating mechanisms. As noted by Marvel *et al.* [208], the current commercial systems are not flexible enough to vary and compare the different pulsing parameters. In his study, three different PRF frequencies at a constant 20% duty cycle were compared using a custom-made ultrasound device and

stem cells in a near-field configuration. The authors reported that a PRF of 1 kHz was more effective than 100 Hz or 1 Hz.

4.1.3 Cavitation

A myriad of studies have shown ultrasound cavitation–induced bioeffects. Extensive reviews of bioeffects, setups, and parameters affecting inertial cavitational effects can be found from Miller *et al.* [217]. Apfel and Holland, and recently Bader and Holland, have created models to estimate the thresholds for cavitation [8,16]. The threshold for inertial cavitation in the presence of free bubbles is given by mechanical index (MI), that is defined: $MI = p_-/f^{1/2}$ where p_- is the peak rarefactional pressure in MPa and f, the frequency in MHz. The cavitation index (I_{CAV}) for stable cavitation (bubble rupture and subharmonic emissions) in the presence of contrast agents, is defined as: $I_{CAV} = p_-/f$.

As indicated by Miller *et al.*, (inertial) cavitation is a highly variable effect, affected by many parameters [217]. Sacks *et al.* have found that cells in spheroids are more tolerant to cavitational effects than cells in a monolayer [276]. In blood, tonicity and dissolved gas contents have been found to affect blood cell hemolysis [218,219]. Sonoporation of mammalian cells is more efficient at body temperature than at room temperature [159,364]. Temperature elevation (from 37 up to 45°C) has been found to induce cell-type dependent variations in sonoporation efficiency in cells exposed to high-pressure laser-induced stress waves [322].

Forbes *et al.* have shown that inertial cavitation is not required to sonoporate ovary cells in presence of gas bubbles [85]. Sonoporation is assumed to be due to the stable, linear and/or nonlinear bubble oscillations that result in microstreaming. Krasovitsky *et al.* have suggested a cell model that could explain many of the ultrasound bioeffects at low pressures, and in the absence of contrast agents [171]. In this bilayer sonophore model, the space between cell membranes expands and contracts in phase with the ultrasound wave generating small-amplitude motion inside the cells.

Evidence that cavitation has a role in therapeutic activity can be found from studies of Webster *et al.* [347,348]. Fibroblastic cell suspensions were sonicated with or without elevated ambient overpressure. Artificial bubbles were not used. When the pressure of the cell chamber was at normal ambient pressure, the protein synthesis of treated cells was 127.2% compared to sham-sonicated cells (100%). When the ambient pressure was elevated by 2 atm, the syntheses were 109.7% and 111.8% for the sonicated and sham-sonicated cells, respectively, relative to control cells at normal ambient pressure. Wang *et al.* have found an increase in silica-coated 8 nm nanoparticle intake by osteosarcoma cells after the Exogen® treatment [339]. The intake increased when the sonication time was extended (3 h > 1 h > 0.5 h). Harle *et al.* measured the presence of subharmonic noise during the bone cell exposures using a hydrophone as a passive cavitation detector [116]. Their data indicated that the subharmonic emissions ($f/2$ = 1.5 MHz) were present only at the highest intensity level (3 MHz, I_{SATA} = 1.78 W/cm^2, CW). The highest therapeutic effects were also evident at this level. However, the gene expressions were also elevated with lower intensities, which excluded the subharmonic emissions, indicating that cavitation above the detection of sub-harmonic signals is not the sole cause for stimulation.

Though ultrasound contrast agents are not used in studies of this field, the presence of natural air bubbles in the culture medium is likely, as the medium is not routinely degassed before sonications. In the study by Zhang *et al.*, water inside an acoustic waveguide as well as the medium covering the bone cells were both degassed before exposing osteoblastic cells to low PRF (0.5 Hz) high-pressure bursts (f = 3.3 MHz, burst duration = 300 ms, p^- = 9.18 MPa) using a novel optical microscope setup [367]. Degassing may have been one important factor in this experiment that enabled a stimulatory effect on cells without inducing cell death, despite the substantially high negative pressure and long burst duration.

4.1.4 Standing waves

The two commonly applied temporal sonication modes in LIPUS studies are PRF = 100 Hz at 1 MHz operating frequency and PRF = 1 kHz at 1.5 MHz operating frequency, with both using a constant 20% duty cycle. These result in temporal burst lengths of 2 ms and 200 μs, respectively. In water these correspond to single-burst spatial lengths of 3 m and 0.3 m, respectively. In a standard six-well cell plate (area = 9.62 cm^2) one milliliter of medium volume equals approximately 1 mm medium column height. Therefore, in the majority of the *in vitro* configurations (Tables 3-4 and 3-5), the sonication is effectively a near-field CW sonication.

Kinoshita and Hynynen [160] conducted a controlled *in vitro* sonoporation using several experiments in which the standing wave was either induced or eliminated. The study indicated that ultrasound standing waves are required for high cell sonoporation efficiency with cells in monolayer. In earlier work, the cell viability in a cell monolayer seeded in a commercial polystyrene flask was regulated by placing the cells in either nodal or antinodal positions [256]. Thus, standing wave formation may be used to improve the sonoporation efficiency. In two recent papers from Garvin *et al.*, spatial controlling of cells using standing waves has been applied for the purpose of tissue engineering [94,95]. In this method, cells in a suspension are collected and organized inside an extracellular matrix using standing waves. The cells are collected to the node positions due to the standing wave–generated radiation force on the cells. This matrix is then cured while maintaining the generated 3D structure. These continuous wave sonications are conducted using a configuration that is optimized for standing waves but resembles the setups that are routinely used in *in vitro* cell stimulations. Culture medium column height (5 mm) and acoustic pressure levels (100 kPa) are comparable to many LIPUS studies.

4.1.5 Streaming

Evidence of the non-thermal effects of ultrasound can been found in *in vitro* studies that combine non-lethal ultrasound treatment and hyperthermic temperature, and result in increased cell death compared to hyperthermia alone [185,321]. Dunn [63] found similar cell survival curves as ter Haar *et al.* [321] when the cells were exposed to combined elevated temperature and shear stresses (0.7 to 8 dyn/cm^2). Thus, bulk acoustic streaming was suggested as a non-thermal mechanism. Dyson *et al.* [66] suggested that the non-thermal mechanism behind tissue regeneration of *in vivo* rabbit ears was cycle-averaged fluid movement. Harle *et al.* [116] have found elevated transforming growth factor gene levels in osteoblastic MG-63 cells using a far-field configuration. The acoustic streaming ranged from 4 mm/s to 194 mm/s when I_{SATA} ranged from 130 mW/cm^2 to 1770 mW/cm^2 (3 MHz, CW). The gene inductions, which were observed with all intensities, were suggested to be due to the acoustic streaming. In a study by McCormick *et al.*, bone cells were first exposed to Exogen® LIPUS-treatment and then to a physiological level (19 dyn/cm^2) shear stress in a near-field setup [214]. The ultrasound treatment had an insignificant effect on bone markers (bone morphogenetic factor-4), cell morphology, or cell alignment. Shear stress was found to elongate the cells, change their orientation, and decrease the level of bone marker. However, when the shear stress was applied after LIPUS treatments, further decrease in bone marker level was observed.

4.1.6 Wave mode conversion

Mode conversion of longitudinal ultrasound waves to shear or surface waves occurs when the original wave meets an acoustic boundary. Several studies have shown that Lamb-type waves propagate at the surface of bone. Lamb waves have been generated in long bones *in vivo* [235] and in bone phantoms [58,263] using broadband ultrasound excitation. Propagation properties of these waves are studied as a diagnostic means to quantify bone status. In a recent study by Chung *et al.*, which

applied the Exogen® system, the authors sonicated fractured bones of living rats at different angles of incident [45]. Fresh fracture healing and bone mechanical properties were significantly accelerated when the sonications were conducted at an angle of 35° instead of at the routinely applied normal angle of incidence (0°). The authors concluded that this angle (midpoint of θ_{CR1} = 22° and θ_{CR2} = 48°) enabled optimal shear wave induction and transmission to bone. *In vitro*, observations from Hensel *et al.* [124] indicate that mode conversion at the cell culture well walls occurs when the transducer diameter is larger than the well diameter. As a result, the generated shear waves sum up at the center of the well, creating a local pressure peak.

4.1.7 Electrical perturbations

The work of Duarte [59], which forms the experimental framework for the LIPUS techniques in bone, suggests that the primary mechanism behind fracture healing is the direct piezoelectricity of bone (collagen) [89]. He theorized that ultrasound waves induce, through piezoelectricity, small electric voltages in the bone that stimulate the bone cells. Dry bone exhibits clear piezoelectricity but the electrical properties of wet (*in vivo*) bone and cartilage, which lacks the similar-patterned collagen structure of bone, have been under debate [5]. It is suggested that the bone electricity, or strain, generated potentials could be a combination of fluid streaming potentials and piezoelectricity [5]. Pilla has observed that ultrasound induces altered ionic permeability in bone cells [257]. The bone cell impedance was found to be altered after an ultrasound exposure comparable to that of the Exogen® system. He has suggested that the microstreaming of ionic fluids could result in streaming potentials inside the bone structures and in cells, creating an endogenous electric field [260]. This could explain the similarities among the bioeffects and temporal wave characteristics of ultrasound and electric/electromagnetic treatments (≈ mT magnetic flux bursts consisting of high frequency content repeated at tens or hundreds of Hz). However, few studies have actually compared electromagnetic

and LIPUS stimulations [25,189]. These *in vitro* studies have indicated a fairly similar response in bone cells, though the electrical methods have required much longer (2–3 h) exposure times.

Several commercial plastic materials can generate measurable voltages under elongation or bending, including polystyrene and polypropylene [93]. In a method called acoustically stimulated electromagnetic (ASEM) response, an electromagnetic signal is generated on a sample that is probed with short broadband ultrasound pulses and picked up by an external RF-antenna [144,245]. Small signals have been received from wet bone and a thin polystyrene plate. Substantially stronger (≈ ×250) electric signals are found when the probed sample is a piezoelectric crystal. In a silicon plate the signal is absent. Studies further indicate that the strongest electromagnetic pulses are generated when the transducer is switched on, or when the reflection of the sound from the sample returns to the sonicating transducer, indicating transducer generated electrical signals. The impact of these transducer generated electrical signals were investigated by Dyson *et al.* [65], who commented that the electromagnetic interference significantly complicated the temperature measurements during CW *in vivo* tissue regeneration. In the study by Pilla *et al.* possible effect on bone fractures of electric noise from the transducer at Exogen® parameters was directly explored [258]. By replacing the acoustic gel coupling layer with an air layer, the acceleration of rabbit fracture healing was lost. This indicates that ultrasound needs to enter tissue to have an effect, and that the electromagnetic signal alone does not have a noticeable impact on healing. As suggested by Dyson *et al.* [65], the possibility of RF pick-up could be eliminated by using RF-shielding of the transducer and driving electronics [314].

4.2 *IN VITRO* EXPOSURE CONFIGURATIONS

Among the *in vitro* studies, the ultrasound exposure configurations have varied substantially, as indicated in Tables 3-4 and 3-5. To simplify the overview of these setups, the applied ultrasound systems are categorized into four generalized types (Fig. 4.1). Similar classification can be found in the review by Miller *et al.* [217] and in the study by Hensel *et al.* [124].

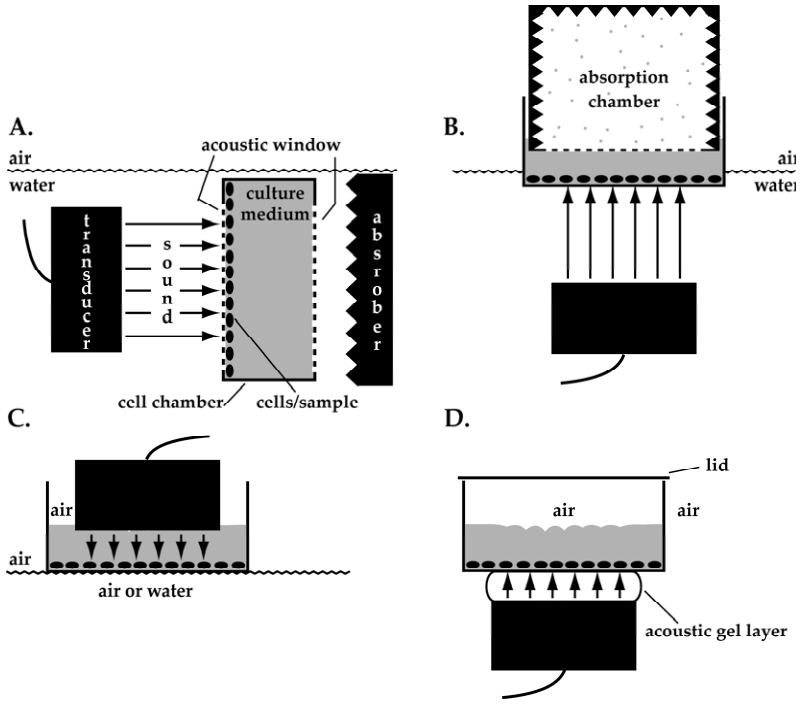

Figure 4.1. *A schematic illustration representing four different ultrasound exposure systems applied in vitro: (a) immersed transducer and sample, (b) immersed transducer with absorption chamber, (c) transducer in the sample volume, and (d) sample on top of the transducer.*

4.2.1 Immersed transducer and sample

In the first experimental setup (Fig. 4.1A), the cell chamber containing the biological sample and the transducer are both immersed in water. This type of setup with cells in suspension was used in studies [222,347,348], which inspired many later

ultrasound *in vitro* studies in this field. This setup has many favorable aspects. First, the transducer-sample distance can be set so that cells are exposed in a uniform and repeatable acoustic field. Second, to exclude standing waves, the cell chamber faces can be made acoustically transparent using thin plastic films. After passing the sample volume, the transmitted sound can be effectively silenced by simply covering the water tank walls with rubber mats or specialized acoustic absorbers. Due to the lack of strongly reflecting interfaces, these setups have the lowest radiation force momentum change and motion. Third, full immersion enables accurate temperature control and efficient removal of ultrasound-induced heat from the chamber. Therefore, the reported temperature elevations have been less than 1°C [115,187,222,342].

A similar design was later used by Wiltink *et al.* [352] with rat bones, Warden *et al.* [342] with a bone cell monolayer adhered to a 19 μm thick Mylar sheet window, and Sun *et al.* [309,310] with rat bones and bone cells placed inside a urethane chamber.

Cells in commercial cell chambers have also been exposed using this setup. Harle *et al.* [114–116] have used polystyrene cell bottles without modifications and Mukai *et al.* [224] used plastic cell tubes containing the cell aggregate at the conical tip of this tube. The latter system consisted of six transducers and six tubes placed 3 cm from the transducers.

Though having several advantages, this type of setup has been used in only a few studies. There may be several reasons for this. First, a cell chamber that is completely or nearly completely immersed has an elevated risk for cell contamination during exposure. Second, the configuration requires larger culture medium and reagent volumes than normal culturing, making it costly. Third, to enable optimal sound transmission, the cell chamber must be modified by making acoustic windows. Finally, the acoustic window may not be an optimal surface for cell adhesion.

Repeatable acoustic exposures are also possible by using special sound absorption chambers (Fig. 4.1B). By placing the

chamber directly into the culture volume, the standing waves within the exposure volume can be significantly reduced [175,187–189]. As with type A setups, studies using absorption chambers have reported low temperature elevations after ultrasound treatments. In the setup, a liquid-filled chamber containing small absorption particles is coupled to culture medium using a thin film window. The transducer positioned in far-field is rotated to increase the exposure area and eliminate standing waves between the transducer and plate. Solid, silicone-based chambers, for example, have also been introduced [18,145,146,148,163,165]. This setup type shares many advantages and disadvantages with the immersion-type systems (Fig. 4.1A).

4.2.2 Transducer in the sample volume

Perhaps the most intuitive way to sonicate the cells would be to immerse the transducer directly into the liquid sample volume (Fig. 4.1C). This technique also minimizes transmission losses between the transducer and cells. Therefore, it is no surprise that transducer immersion has been used in multiple studies (Tables 3-4 and 3-5; 'C'). For example, a UK research group has used this approach in several studies [57,199,266–268]. The studies have experimented with MHz- and kHz-range ultrasound exposures. The transducer immersion into the cell chamber is a common feature among the studies, but several differences are also evident. For example, in the kHz-range studies, the well plates floated on the surface of temperature-regulated water. In some studies, the cell chambers are exposed to air [6,122]. In the other the transmitted sound has been absorbed in castor oil–embedded absorbers [132,265], absorbers placed under the chamber [190,368,369], or reflected from the air under the well [242,315].

This sonication method is simple but it requires careful transducer sterilization before immersion. To eliminate the direct cell volume contact, Zhang *et al.* [368,369] have applied Parafilm membranes between the medium and transducer. Standing wave regulation is also challenging. A sub-wavelength

thick plastic membrane placed between the transducer and radiation force balance has been shown to cause errors in acoustic power measurements in general [21], and a shift in the resonance frequency [196] and acoustic output of physiotherapy transducers [212]. Therefore, standing waves present in a setup can directly regulate the sound amplitude that is delivered to the target. In addition, the absolute calibration of these configurations is highly demanding and in most cases has been inadequate. The in-situ calibrations using invasive hydrophones are susceptible to standing wave artifacts [140,167], which further complicates near-field calibrations.

One significant obstacle is that in the case of large transducers [266] or small chambers, the complete transducer surface may be difficult to place in full liquid contact. In the case of a geometrically focusing (large aperture) transducer, a special waveguide [367] or high liquid layer above the plate is required. Some type of waveguide is also usually required to expose the sample to a spatially uniform acoustic far-field. In type C configurations, the temperature elevations have been found to be small, at least at lower acoustic intensities [132,242,265]. This configuration is, however, susceptible to heating due to the multiple reflections between the transducer surface and culture well bottom. A transducer that has a diameter comparable to the well diameter can also effectively block cooling from the free liquid surface. A specific low-frequency and low-intensity device (45 kHz and 25 mW/cm^2) has been reported to generate substantial heating [203]. In this case, the source for heating may not be direct ultrasound absorption in the cell culture but the transducer surface heating [166,354].

4.2.3 Sample on top of the transducer

During routine use of the Exogen® fracture treatment system, the transducer is coupled to the skin using acoustic coupling gel. In many ways, the *in vitro* exposure configuration illustrated in Fig. 4.1D is similar to the *in vivo* setup. This is also the most frequently applied *in vitro* ultrasound configuration (Tables 3-4 and 3-5; 'D'), especially in recent studies. In some studies, a thin

water layer has been used to couple the transducer to the cell chamber bottom [118,252,360], but in the vast majority of the studies, the transducer and the well have been coupled using an acoustic gel layer. In a recent study by Fung *et al.*, rubber-gel blocks (c = 1400 m/s, otherwise unspecified) were placed between the transducer and the cell well with an acoustic gel layer between the transducer-rubber complex and the well [92]. In these experiments, the length of rubber block was varied from zero to 130 mm, which corresponded to the farfield distance for their system. The intensity of the exposure was calibrated so that it was constant (I_{SATA} = 30 mW/cm^2) at the location of the cell well regardless of the rubber thickness. This study found the highest bone cell-stimulating efficiency when the well was in the transducer farfield.

This setup type is perhaps the most vulnerable to heating due to sound reflections, small culture medium volumes, and a limited cooling capacity. Few studies have reported insignificant culture medium temperature elevations with respect to the control cells in a setup using gel coupling [292,332]. Park *et al.*, using the Exogen® device, have commented that with culture wells smaller than the transducer, the temperature was elevated above the physiological level, which increased the level of glycosaminoglycan staining of cell constructs mimicking an osteoarthritic tissue [250].

The most complex radiation force movement is generated in these setups. Commercial well plates have substantial acoustic attenuation, resulting in direct vibrations of the adhered cells at the burst repetition frequency. A large liquid movement is generated at the acoustically soft liquid-air interface. Reflections and the resulting standing wave fields within the exposure volume can further modify the radiation force and induced motion [21]. Hensel *et al.* [124] have reported that in a type D setup, a medium volume variation of 2.56% (total volume 13 ml) can change the pressure at the cell layer by a factor of two.

The type D setup, having a low culture medium column with standing waves, may form favorable circumstances for cavitation by enabling the bubbles to be close to the cells.

Kodama *et al.* transfected reporter genes in hamster cells using near-field standing wave sonications with gas bubbles (1 MHz, p_- = 0.23 MPa, PRF = 100 Hz, dc = 20%) [164]. The highest luciferase activity and the lowest survival fraction were observed when the culture medium height was 1 to 2 mm, which correlated well with the wavelength of 1.5 mm.

Though acoustic streaming varies substantially in the acoustic near-field, it is concentrated to the transducer focal area [305]. Direct measurements from Spengler *et al.* [303] indicate that acoustic streaming can be attenuated if the free liquid volume is limited by using acoustically transparent films. Successful cell manipulation using standing waves further indicates that standing wave-generated microstreaming may dominate over bulk acoustic streaming in these setups (also in type C). Consequently, there may be a large variation in acoustic streaming values among experiments, depending on the acoustic parameters and the setup details.

Though the acoustic exposure is difficult to calibrate in this configuration due to the potential for various sound interactions (Fig. 4.2), it is simple, rapid to adopt in routine cell culturing protocols, and presents perhaps the lowest cell contamination risk.

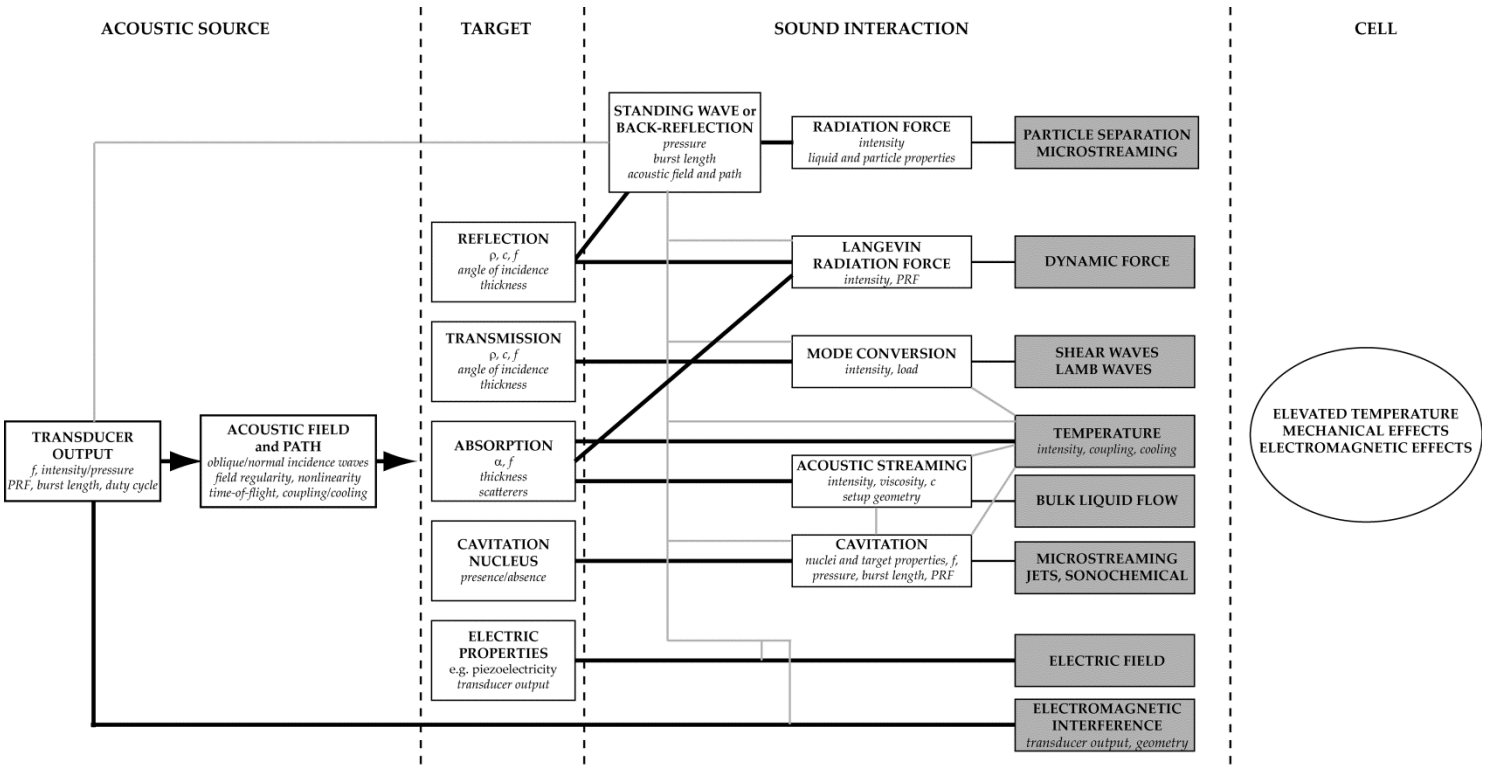

Figure 4.2. *A simplified chart indicating the different ultrasound-induced mechanisms present in typical in vitro ultrasound configurations. The grey lines illustrate the interactions between the mechanisms.*

5 Summary of the Publications

The main results of publications **I to V** are summarized in this chapter. The applied *Materials and Methods* can be found in the original publications.

Publication **I**. The efficacy of ultrasound (setup type A, f = 1 MHz, dc = 20%, PRF = 1 kHz, I_{SATA} = 580 mW/cm^2, 10 minutes daily for 1–5 days) to increase proteoglycan synthesis in bovine primary chondrocyte monolayer was studied. The contribution of ultrasound-induced temperature elevation (mean ± SD = 6.9 ± 0.1 °C) to the synthesis was investigated using a water bath to heat the monolayer by the same amount, but in the absence of ultrasound. Proteoglycan synthesis was increased approximately twofold after three to four daily ultrasound exposures, staying at that level until day five. Temperature elevation alone did not increase proteoglycan synthesis. Ultrasound treatment did not induce Hsp70, while heating alone caused a slight heat stress response. The cells from one donor out of five were non-responsive to ultrasound.

Publication **II**. Human osteoblastic MG-63 cells were sonicated (f = 1.035 MHz, dc = 20%, PRF = 1 kHz, 30 minutes) using setup type B. The temperature elevations were 0.05, 0.18, and 0.72°C at acoustic pressures of 128, 256, and 510 kPa, respectively. Using genome-wide microarray screening, altogether 377 genes were found to be ultrasound-regulated at least by twofold. Ultrasound affected genes are involved with cellular membranes, regulation of transcription, plasma membrane solute carriers, and several transcription factors belonging to the zinc finger proteins.

Publication **III**. From Publication II, it was observed that ultrasound impacts Wnt/β-catenin, which is a regulator of osteoblastogenesis. To further study the effect of ultrasound on Wnt/β-catenin signaling in MG-63 cells, the cells were exposed to several ultrasound intensities (setup type D, f = 1.035 MHz, dc =

20%, PRF = 1 kHz, P_{TA} = 0.2 to 2 W, 10 minutes), heat alone, and ultrasound at a lower baseline temperature. At P_{TA} = 2 W activity was significantly stimulated (6 fold), while also resulting in an average temperature elevation to 47.6 ± 0.9 °C in the cell well. Thermal exposures between 46 and 48°C alone increased the Wnt activity by 5 to 18 fold. The activity was lowered at 49°C (< 5 fold). Sonication at the same intensity but having a lower baseline temperature (average maximum peak temperature reached 40.9 ± 0.7°C) showed stimulation of Wnt activity by 2.6 fold. The induction of Wnt in chemically pre-activated (lithium-chloride) cells was further stimulated by ultrasound by 2.7 fold and by thermal exposure alone at 47°C by 4.2 fold. However, the ultrasound exposure at the low baseline temperature did not stimulate the cells that were pre-activated. The level of HSP70 was elevated after ultrasound treatments at normal baseline temperature and thermal exposure treatments.

Publication **IV**. The temperature elevation in the setup used in publication **III** was measured using fine–wire thermocouples and infrared imaging. The measurements in a standard 24-well plate showed that temperature accumulation was highest at the polystyrene well walls, including the walls of the neighboring, non-sonicated wells. The heating in the centrally located well was higher than in the peripherally located wells. Wnt-specific TOPflash reporter activity in MG-63 cells after ultrasound treatment was significantly higher in the centrally located wells (6.3- to 11.5-fold induction) compared to the peripherally located wells (1.9 to 1.8 fold).

Publication **V**. The acoustic and thermal exposure in the type D setup was characterized using pulse-echo ultrasound, optical methods, and thermocouples. Pulse-echo measurements indicated that the commercial polystyrene 6-well plate is susceptible to frequency-sensitive transmission (resonance frequency 938 ± 9 kHz at 37°C). According to the laser Doppler vibrometer measurements, 1-kHz PRF-induced radiation force displacements were significantly smaller (2–3 nm) but less frequency dependent than the displacements at the operating frequency (5–35 nm at 1.035, 1.625, and 3.35 MHz). Wave mode conversion occurs on the plate, and Lamb waves having phase speeds 1111, 1110, and 1077 m/s at 1.035, 1.625, and 3.35 MHz, respectively, propagate on the plate. Nanometer-scale vibrations are coupled to the non-sonicated neighboring wells. Acousto-optic Schlieren measurements indicated that standing waves are formed inside the cell well,

resulting in up to a nearly 200 % variation in acoustic pressure amplitude in a well. An exposure of cells in a D-type setup with typical LIPUS parameters caused a temperature elevation of 2.7 ± 0.3°C when using commercial acoustic gel coupling and 0.3 ± 0.2°C with circulating water coupling.

6 Discussion

6.1 PUBLICATION I

The proteoglycan synthesis of bovine primary chondrocytes after ultrasound treatment exhibited approximately a twofold increase relative to the controls. This finding indicates that ultrasound may be a feasible method to increase extracellular matrix production in cultured chondrocytes. There was a significant (6–7 °C) ultrasound-induced temperature increase inside the sonicated cell wells, but an induction of proteoglycan synthesis was not evident after the heat treatment mimicking this ultrasound-induced temperature elevation. Activation of Hsp70 was not observed after ultrasound treatment, but a slight increase was observed after hyperthermia treatment. Since the heat treatment alone did not increase proteoglycan synthesis in chondrocytes, our results indicate that in order to increase proteoglycan synthesis with ultrasound, some effect of ultrasound other than temperature rise is required.

The level of the thermal exposure can be an important factor for proteoglycan synthesis. A one-time hyperthermia treatment at 48°C (approx. 4°C higher than in this study) for ten minutes causes apoptosis and suppression of proteoglycan synthesis in rat articular cartilage [362]. Hyperthermia treatment of HCS-2/8 chondrosarcoma cells (41°C for 15 or 30 minutes) was found to have a positive effect on both the cell viability and proteoglycan synthesis rate, while the cell viability and metabolism were decreased after exposing the cells to 43°C or higher for 30 minutes [128]. In our study, the cells experienced temperatures of 43°C or higher for only five minutes.

Although the acoustic field distribution in the cell culture well was found to be non-uniform, the temperature values inside the well were relatively even. Multiple reflections from the liquid-air interface, and heat conduction, most likely

smoothed the temperature rise inside the well. The ultrasound-induced temperature rise is fast and a similar temperature profile is difficult to create, for example, using a water bath. The water bath temperature profile used in our experiments was higher at all time points, but the difference was always under 1°C. The difference in Hsp70 response between the hyperthermia and ultrasound treatments could potentially be explained by this difference in temperature.

Chondrocytes collected from a single bovine were found to be unresponsive to ultrasound. A variation in responses has also been reported by others [13,169] and may further complicate cell manipulations.

6.2 PUBLICATION II

Previous studies investigating ultrasound interactions in bone cells have focused on a small group of genes or proteins. In this study, the first attempt was made to reveal whole genome-wide transcriptional events occurring in bone cells under certain types of ultrasound exposure. In addition, the cells were exposed using an ultrasound setup that enables the ultrasound exposures to be quantified while minimizing ultrasound induced temperature elevations in the cell culture medium.

In the experiments, the cells were located in the acoustic far-field beyond z_{LAM}. The reflections between the cell plate and transducers were minimized using an absorption chamber, favorable transducer orientation, and continuous transducer movement. The ultrasound device geometry improved acoustical field uniformity, enabling more accurate ultrasound field calibrations and resulting in more repeatable cell exposures.

One possible artifact in thermocouple measurements is the viscous heating of the thermocouple probe [87,88,141]. In this case the real medium temperature is overestimated due to a friction-generated rapid local temperature rise. The real temperature rise is thus likely smaller than the measured

temperature elevation of 0.4°C. Therefore, it is very likely that such a small temperature increase is not the primary bone cell stimulating factor in this study.

The largest groups of affected genes were plasma membrane proteins and transporters, and transcription factors, especially zinc finger proteins. One explanation for changes in expressions of solute transporters could be a formation of pores on the plasma membrane, affecting the intracellular ion balance. Zinc has been shown to increase the activity of vitamin D-dependent promoters in osteoblasts [197], and a number of zinc finger proteins appear to be involved in osteoblastic differentiation [153]. Microarray analysis introduced several interesting ultrasound-regulated candidate genes that have a role in bone cell metabolism. Only a few studies can be found in the literature on BMP-2-Inducible Kinase (BIK or BMP2K), which has been shown to attenuate osteoblast differentiation [157]. A high expression of plasma membrane protein CD151 in chondrocytes has been shown to be a marker for high chondrogenic capacity [108]. Enhancer of zeste homolog 2 (EZH2) [296], Homeobox B8 (Hoxb8a) [279], and low density lipoprotein receptor-related protein 5 (LRP5) [17,100] have been previously connected to the Wnt/β-catenin signaling pathway, an important regulator of bone metabolism.

This study suggests that plasma membrane proteins and transporters, and a group of zinc finger proteins, are most sensitive to ultrasound-induced transcriptional regulation. This information may be important, uncovering the mechanisms of how ultrasound stimuli transmit their effects on the bone cells.

6.3 PUBLICATION III

To study the effects of ultrasound stimulation in bone cells, activation of bone-essential Wnt signaling pathway [37,99] was measured. To distinguish the thermal signal induction from the other ultrasound mechanisms, hyperthermia exposures using a

heated water bath and ultrasound exposures in a cooled water bath were conducted.

The TOPflash reporter gene assays showed that ultrasound exposure activated the Wnt signaling pathway in human osteoblastic cells. Nuclear accumulation of β-catenin in ultrasound-treated cells very shortly after the exposure was further evident and confirmed the activation of the canonical Wnt pathway. When LiCl was added to pre-activate the pathway pharmacologically, a synergistic effect of ultrasound and LiCl was observed. Previously, Wnt target genes have been shown to be up-regulated to a greater extent by mechanical loading when the canonical Wnt pathway was pre-activated by the addition of Wnt ligand Wnt3A or by inhibiting GSK3β [269].

When the cells were exposed to hyperthermia, Wnt signaling activity showed systematic temperature dependence. Approximately half of the maximal induction could be inhibited by the Wnt co-receptor blocker, Dkk-1. As with the ultrasound treatments, a synergistic effect of LiCl and heat was observed. To the best of our knowledge, there are no previous reports on the heat-induction of Wnt signaling in bone.

When the water temperature in the ultrasound bath was lowered to 30°C, the thermal dose was drastically lowered and the maximum temperature was less than 41°C at the highest acoustic power. With this cooled setup, the Wnt signaling pathway was again significantly activated. Since hyperthermia, with or without LiCl additions, could not induce Wnt activation until the temperature rose up to 44.7°C, the Wnt activation was not due to the temperature rise, but to some other mechanisms of ultrasound. However, ultrasound exposure excluding the thermal component and including LiCl pre-activation did not result in the synergistic effect, indicating a more likely co-modifying role of ultrasound. Supporting our results, Takeuchi *et al.* also observed a small but significant increase in the nuclear β-catenin level in ultrasound-exposed articular cartilage [311].

Despite the substantially elevated temperatures in ultrasound and hyperthermia experiments, the integrity of cell membranes was not compromised and the apoptotic markers did not

respond markedly at time points or conditions showing the Wnt activation. The observed induction of Hsp70 also indicates a normal stress response of the cells to the applied exposures. Some cell rounding was observed at higher temperatures. In MG-63 cells, hydrostatic pressure (4 MPa for 20 min) has been reported to cause recoverable cell rounding and Hsp70 induction, but not cell death [119].

In this study, the highest ultrasound intensity (407 mW/cm^2) was found to be the most efficient. This is in contrast to many previous studies showing the best results with lower intensities, ranging from 30 to 50 mW/cm^2. The lower intensities (41–326 mW/cm^2) also slightly increased the Wnt activity, but it is possible that the administered short, single burst sonication was not sufficient for higher stimulation.

The exact knowledge of how the ultrasound or thermal signals are mediated in the bone cells is not available. In our experiments, where the specific protein kinase inhibitors were used, the activity of TOPflash reporter suggested that both the PI3K/Akt and mTOR signaling cascades were, at least in some efficiency, involved in mediating the stimulatory effect of the ultrasound exposure, as well as hyperthermia in human MG-63 cells. This agrees with the results of Takeuchi *et al.*, who reported that ultrasound effects are mediated via PI3K/ Akt pathway in chondrocytes [311]. In general, in mammalian cells, Wnt signaling has been shown to proceed via components of the PI3K/Akt and mTOR signaling cascades [151]. The precise regulation of β-catenin is known to be required for fracture healing, as many Wnt ligands and receptors have been found to be selectively up-regulated during bone healing [36,299]. In patients with hypertrophic non-unions, osteoblasts showed down regulation of multiple vital signaling pathways, including Wnt pathway [127].

To conclude, this is the first study to report that ultrasound exposure activates Wnt signaling pathway in human osteoblastic cells. Specifically, this study suggests that Wnt signaling can be activated through temperature elevation using, for example, ultrasound energy deposition but also through

some ultrasound induced non-thermal mechanism. Our observations support the earlier hypothesis that ultrasound-induced mild hyperthermia is a potential technique to stimulate bone tissue. A few *in vivo* animal studies have indicated that continuous (≈ 40°C for up to 44 days) or intermittent (43°C for 45 minutes once or twice a week) hyperthermia has a favorable impact on bone growth after trauma [72,181]. The need for non-invasive *in vivo* temperature evaluation should not limit its applicability. Specifically, soft tissue temperature adjacent to bone could be controlled using a magnetic resonance imaging–based thermography [306].

6.4 PUBLICATION IV

Ultrasound-induced temperature elevation is present to some extent in most *in vitro* setups. Infrared and fine-wire thermocouple temperature measurements indicate that the polystyrene chamber wall is the most susceptible to have increases in temperature during ultrasound exposures. In our measurements, the size of the transducer was larger than the diameter of the exposed chamber (also in Refs. [221,250,360]); therefore, the plastic chamber wall was directly exposed to the ultrasound field. This is analogous to the configurations in which the exposure area inside a larger vessel is decreased using a polystyrene ring to fix and immobilize the biological sample [265]. This is also representative of the setup where a polypropylene cell tube with a narrowing conical end contains a small cell pellet at the cone tip and is exposed to a wide ultrasound field [74]. There are many factors that may influence the temperature elevation. Another possible source of increased heating is when an efficient acoustic absorber is placed close to the cells. This type of absorber is typically placed on top of the cells, inside the well chamber, to attenuate standing wave formation [146,163]. If it is placed close to the cells it can be another possible source for increased heating. If sound cannot propagate freely after travelling through the biological sample,

the formed reflections between the transducer and well bottom, and transducer and reflecting surface (air), will amplify this heating. Therefore, even if the intrinsic sound absorption and resulting temperature effects of relatively thin-walled (≈ 1 mm) polystyrene plastic cell culture plates may be generally small, the type of ultrasound setup may change this dramatically.

Furthermore, different plastic materials have different ultrasound-loss factors. For example, polypropylene cell tubes may be less suitable exposure chambers due to the higher acoustic attenuation in polypropylene compared with, for example, polystyrene (21–41 Np/m vs. 59–210 Np/mm at 5 MHz) [291].

The floor structure of a commercial cell plate may not be a continuous flat plate, as the edges of the plates may contain open cavities. These cavities may be partly or completely filled with water. As a consequence, the wells located at the edges of the plate will have water in contact with their walls, but the center wells will only have contact to the water through their bottoms. The IR images demonstrated that the peripheral wells that experienced the greatest cooling had lower temperature elevations than the centrally located wells. In our setup this temperature variation resulted in unequal biological activation in different well chambers.

Infrared imaging is a spatially accurate, non-invasive, and fast method to characterize complex ultrasound configurations, with respect to induced temperature elevations. The largest limitation is that the liquid immersed interfaces are not observed, only the superficial layer. If the exposure system is closed (*i.e.*, requires opening before imaging), as in our case, convection through moving air and evaporation will lower the absolute temperatures. Different materials also have different emissivity factors, which affect the absolute temperature accuracy [247]. Therefore, using IR-imaging together with thermocouple probes creates an efficient method to characterize *in vitro* ultrasound systems.

Perhaps the most widely utilized commercial ultrasound apparatus applied in the field of ultrasound tissue engineering

research is the Exogen® fracture healing device. This device, as well as corresponding manufacturer modified research devices, has been used in many studies, indicating similarity among studies with respect to ultrasound exposure level and its interpretation. The literature indicates that within studies, the nominal, undisturbed ultrasound output intensities [335,369] and exposure times [182,289] have varied. The level of culture medium inside the well insert may also influence the temperature rise through acoustic field alteration and the cooling effect of the liquid. Very low culture medium levels [313], "normal" levels [168,332], and high levels with varying sonication direction [368,369] have been applied. Considering this heterogeneity in parameters and setups, our results from this study imply that a simple temperature rise per acoustic intensity relationship cannot be given. Unfortunately, very little or no information regarding ultrasound-induced temperature rise is usually reported for experiments.

As confirmed in our study, the variation in the temperature of the ultrasound-exposed cells can, indeed, reflect directly on the biological outcome. Therefore, in light of our results, we believe that to apply repeatable stimulations to biological tissue engineering material, a detailed temperature characterization and systematic exposure protocol are a necessity for *in vitro* ultrasound exposures.

6.5 PUBLICATION V

In publication **V**, several non-invasive measurement methods were applied to study the interactions within the sonicated plastic cell culturing plate.

Commercial polystyrene culture plate wells are usually thin, and it can be estimated that sound loss in a 1.22 mm thick plate is approximately 4% (frequency range from 1–3 MHz) [345]. Respectively, the measured bulk reflection coefficient for polystyrene is 0.214 [139], indicating that the reflection of sound is the dominant cause for sound attenuation in polystyrene

culture plate. However, as our measurements confirm, the culture wells, and other wavelength-scale layers, have very strong frequency-dependent reflection coefficients. This further complicates the quantification of reflection-induced acoustic output variations. More importantly, frequency-selective transmission is present even if the reflections between the target and transducer are eliminated. The load inside the well, level of acoustic pressure, plate thickness variation, and structure of acoustic field will have an effect, especially in near-field exposures, on the reflections. The effect of a temperature increase from 20 to 37°C was found to have an approximately 1% effect on resonance frequency. Our results suggest that the resonance effect may also be present with the cell culture inserts and should be analyzed to obtain accurate exposure conditions. Furthermore, with biological targets in contact with the plate bottom, at plate resonance frequencies the resonating bottom may, at least in theory, be a stimulating factor. To decrease the sound reflection (and absorption), thin-bottomed culture plates could be used [208]. Despite the fact that frequency-dependent transmission is well known and applied to measure the density of the liquids [126], to our knowledge the issue is not widely taken into account in *in vitro* ultrasound setups.

Particle velocity profiles with three different operating frequencies were all found to be irregular in shape but relatively similar in magnitude. However, this similarity is partly misleading, as the corresponding particle displacements are inversely related to operating frequency and are largest at the lowest operating frequency. Contrary to this, the PRF-induced motions were nearly equal for all three operating frequencies. Although they were smaller than the operating frequency displacements, they were more uniform. The measured 2 to 3 nm displacements are comparable with the 4 nm value reported for the Exogen® bone healing device [12]. The magnitude of the PRF-induced motion was found to be directly related to acoustic power. This motion is most likely induced by the radiation force mechanism. By comparison, with the PRF velocity profiles at the two other frequencies, the PRF velocity profile at 1.035 MHz

was more center-weighted and uneven. As 1.035 MHz is close to the resonant frequency of the well, while 1.625 and 3.35 MHz are close to antiresonance frequencies (frequencies with maximum reflection), our data proposes that the operating frequency may be an important factor in the distribution of radiation force–based PRF movement in cell culture plates.

Both the laser vibrometer and Schlieren measurements verified that a standing wave is formed inside a sonicated cell culture well when a liquid-air interface acts as a reflecting surface. It was also observed that the liquid layer height cannot be used to directly compensate for the change in transducer-well separation or vice versa (constant water path length is maintained). The tomographic images also indicate that the radial structure of the acoustic field is different between the node-antinode positions in the near field. Therefore, our measurements suggest that the setups commonly used with *in vitro* studies are susceptible to large variations in ultrasound exposure.

The laser vibrometer measurements indicated that transverse acoustic waves propagate across the well. Equations for shear and Rayleigh speeds [26], give values of 1128 m/s and 1055 m/s, respectively. Our measurements indicated phase speeds between these theoretically estimated speeds, and group speeds close to the Rayleigh speed when the wave propagation was recorded in an empty well. Therefore, the measured wave speeds and the wavelength-order thickness of the culture well imply that Lamb waves are generated at the well bottom when the directly sonicated well is water filled and the waves propagate along the bottom to the neighboring wells.

To test if the transverse waves could propagate when the plate is under water, a similar measurement at 1.035 MHz was made by immersing the 6-well plate in approximately 130 mm of water. According to our measurements, a wave packet having group and phase speeds of 915 and 949 m/s, respectively propagated in the plate. At the center of the non-sonicated well, the displacement amplitude was calculated to be 3.0 nm. Therefore, our data indicates that the transverse surface waves

are generated from the immersed plate and propagate with significant amplitudes underwater. The transversely propagating burst experienced frequency dependent modulation. This modulation could be due to the interference of two different Lamb waves [323]. To our knowledge, the existence of guided Lamb waves in the cell culture plates has not been reported before.

It was also shown that the cells in a well can be indirectly stimulated with different waves, *i.e.*, radiation force–based PRF movement and surface wave movement. Using continuous wave sonications the dynamic radiation force–based PRF motion can be eliminated, leaving only the surface wave component. Our data also highlights that the control wells must not be positioned on the same plate as the sonicated wells due to the "acoustic coupling" between the wells.

Temperature measurements at the bottom of the cell well indicate that the combination of near field sonication, strong ultrasound reflections from liquid-air interface and ultrasound gel coupling is the most vulnerable to ultrasound induced heating. The acoustic power (120 mW), used in this study produced I_{SATA} of approximately 32 mW/cm^2 and resulted in a 3°C temperature rise. This is a large enough temperature rise to potentially induce biologic effects on the cell culture. The acoustic power delivered to the target or the temperature rise in the tissue may depend on the thickness of the gel layer [31,262]. We believe that the large temperature rise difference between the acoustic coupling methods is due to the inferior heat transfer properties of surrounding air compared with circulating water.

This study demonstrates that simple ultrasound *in vitro* setups are very susceptible to large variations in acoustic exposure.

7 Summary and Conclusions

The following points summarize the main observations of this thesis related to the aims set in the Introduction. For future work, some conclusive remarks are given.

- The increase in proteoglycan synthesis in bovine primary chondrocytes after ultrasound exposures implies that ultrasound, either independent of temperature elevation or co-operatively with hyperthermia, augments extracellular matrix production in chondrocyte monolayers.
- Whole genome-wide microarray analysis of sonicated MG-63 osteoblastic cells indicated altered responses specifically on cell membrane-related genes. Most likely, these changes do not originate from the thermal ultrasound effects.
- In osteoblastic cells, both thermal and non-thermal activation of Wnt signaling after ultrasound exposure was observed. Ultrasound activation showed a synergistic effect with the chemical pathway activator. Activation of this route forms new insight into the physical and molecular basis behind the ultrasound stimulation.
- Cell culture chamber walls having substantial sound absorption and poor heat conduction are locations for the highest heating. Standing waves further increase the heating. The type of acoustic coupling may have significant impact on temperature rise.
- At the worst, temperature variation within the exposure chamber may result in uneven cell stimulation. Multiple point temperature measurements and/or thermal imaging may be required for adequate characterization of the *in vitro* setups.

- Many *in vitro* ultrasound setups are vulnerable to frequency-dependent sound transmission, standing waves, and wave mode conversion. These complicate the calibration of the ultrasound wave and reduce the repeatability of the acoustic exposures.
- Radiation force–based displacement on the cell plate is generated at the frequency of PRF.
- Lamb waves are generated on the culture plates. These guided waves are potential cell-stimulating factors. Lamb waves and PRF-induced radiation force vibrations can also couple to the other wells on the same plate.

Focused ultrasound sources could outperform the planar sources used in this work and most other studies of this field. Geometrically focused transducers form a well-defined acoustic focal area. Thus, they allow a spatially localized, shorter exposure distance without strong non-linear harmonic build-up. To treat larger samples, the focal point could be moved mechanically or electrically.

Glass-bottom cell vessels having low acoustic absorption but high reflectivity could be used instead of plastic ones. One should however, be aware that the high speed of sound in glass and thin structure increase the plate resonance frequencies and may cause large uncertainties if not properly accounted for. Culture chambers made of thin, flexible plastic membranes may allow an optimal implementation for exclusion of standing waves and minimization of thermal effects. With adherent samples, minimal interaction with sound and low response of membrane may reduce the radiation force effect.

There is a rich body of published *in vitro* works that show the efficiency of therapeutic ultrasound in regenerative medicine and tissue engineering. Our *in vitro* observations should aid in efforts estimating the role of the various physical factors impacting the cells during these studies. Our results may also be helpful when this technique is further developed for tissue engineering.

Bibliography

[1] "Ultrasound. Update on thermal bioeffects issues," *Ultrasound Med Biol* **24 Suppl 1**, S1-10 (1998).

[2] "Musculoskeletal diseases. Working group for musculoskeletal diseases," in *Health and functional capacity in Finland: Baseline results of the Health 2000 health examination survey,* A. Aromaa and S. Koskinen, eds. (Publications of the National Public Health Institute, 2004) .

[3] Tibial shaft fractures (online). Current Care Guideline. Working group appointed by the Finnish Medical Society Duodecim and the Finnish Orthopaedic Association. 2011; Available at: http://www.kaypahoito.fi/web/kh/suositukset/naytaartikkeli/tunnus/nak07597. Accessed 10/9, 2014.

[4] J. S. Abramowicz, S. B. Barnett, F. A. Duck, P. D. Edmonds, K. H. Hynynen, and M. C. Ziskin, "Fetal thermal effects of diagnostic ultrasound," *J Ultrasound Med* **27**, 541-59; quiz 560-3 (2008).

[5] A. C. Ahn and A. J. Grodzinsky, "Relevance of collagen piezoelectricity to "Wolff's Law": a critical review," *Med Eng Phys* **31**, 733-741 (2009).

[6] E. C. Alvarenga, R. Rodrigues, A. Caricati-Neto, F. C. Silva-Filho, E. J. Paredes-Gamero, and A. T. Ferreira, "Low-intensity pulsed ultrasound-dependent osteoblast proliferation occurs by via activation of the P2Y receptor: role of the P2Y1 receptor," *Bone* **46**, 355-362 (2010).

[7] S. R. Angle, K. Sena, D. R. Sumner, and A. S. Virdi, "Osteogenic differentiation of rat bone marrow stromal cells by various intensities of low-intensity pulsed ultrasound," *Ultrasonics* **51**, 281-288 (2011).

[8] R. E. Apfel and C. K. Holland, "Gauging the likelihood of cavitation from short-pulse, low-duty cycle diagnostic ultrasound," *Ultrasound Med Biol* **17**, 179-185 (1991).

[9] N. I. Ardan Jr, J. M. Janes, and J. F. Herrick, "Changes in bone after exposure to ultrasonic energy," *Minn Med* **37**, 415-420 (1954).

[10] N. I. Ardan Jr, J. M. Janes, and J. F. Herrick, "Ultrasonic energy and surgically produced defects in bone," *J Bone Joint Surg Am* **39-A**, 394-402 (1957).

[11] N. Arden and M. C. Nevitt, "Osteoarthritis: epidemiology," *Best Pract Res Clin Rheumatol* **20**, 3-25 (2006).

[12] H. M. Argadine, R. R. Kinnick, M. E. Bolander, and J. F. Greenleaf, "1 kHz low power ultrasound stimulates ATDC5 chondrocytes," *Proc IEEE Ultrason Symp* **2**, 996-998 (2005).

[13] H. M. Argadine, M. E. Bolander, and J. F. Greenleaf, "Stimulation of proteoglycan synthesis with low-intensity 1 kHz vibration," *Proc IEEE Ultrason Symp* **2**, 849-851 (2006).

[14] K. P. Arkill and C. P. Winlove, "Solute transport in the deep and calcified zones of articular cartilage," *Osteoarthritis Cartilage* **16**, 708-714 (2008).

[15] Y. Azuma, M. Ito, Y. Harada, H. Takagi, T. Ohta, and S. Jingushi, "Low-intensity pulsed ultrasound accelerates rat femoral fracture healing by acting on the various cellular reactions in the fracture callus," *J Bone Miner Res* **16**, 671-680 (2001).

[16] K. B. Bader and C. K. Holland, "Gauging the likelihood of stable cavitation from ultrasound contrast agents," *Phys Med Biol* **58**, 127-144 (2013).

[17] W. Balemans and W. Van Hul, "The genetics of low-density lipoprotein receptor-related protein 5 in bone: a story of extremes," *Endocrinology* **148**, 2622-2629 (2007).

[18] K. Bandow, Y. Nishikawa, T. Ohnishi, K. Kakimoto, K. Soejima, S. Iwabuchi, et al., "Low-intensity pulsed ultrasound (LIPUS) induces RANKL, MCP-1, and MIP-1beta expression in osteoblasts through the angiotensin II type 1 receptor," *J Cell Physiol* **211**, 392-398 (2007).

[19] S. Bao, B. D. Thrall, and D. L. Miller, "Transfection of a reporter plasmid into cultured cells by sonoporation in vitro," *Ultrasound Med Biol* **23**, 953-959 (1997).

[20] C. A. Bassett, S. N. Mitchell, and S. R. Gaston, "Treatment of ununited tibial diaphyseal fractures with pulsing electromagnetic fields," *J Bone Joint Surg Am* **63**, 511-523 (1981).

[21] K. Beissner, "The influence of membrane reflections on ultrasonic power measurements," *Acustica* **50**, 194-200 (1982).

[22] R. Bekeredjian, S. Chen, P. A. Frenkel, P. A. Grayburn, and R. V. Shohet, "Ultrasound-targeted microbubble destruction can repeatedly direct highly specific plasmid expression to the heart," *Circulation* **108**, 1022-1026 (2003).

[23] L. F. Bender, J. M. Janes, and J. F. Herrick, "Histologic studies following exposure of bone to ultrasound," *Arch Phys Med Rehabil* **35**, 555-559 (1954).

[24] P. V. N. Bodine, J. A. Robinson, R. A. Bhat, J. Billiard, F. J. Bex, and B. S. Komm, "The role of Wnt signaling in bone and mineral metabolism," *Clin Rev Bone Miner Metab* **4**, 73-96 (2006).

[25] M. A. Borsje, Y. Ren, H. W. de Haan-Visser, and R. Kuijer, "Comparison of low-intensity pulsed ultrasound and pulsed electromagnetic field treatments on OPG and RANKL expression in human osteoblast-like cells," *Angle Orthod* **80**, 498-503 (2010).

[26] L. M. Brekhovskikh, *Waves in layered media* (Academic Press, New York, USA, 1960).

[27] C. T. Brighton and S. R. Pollack, "Treatment of recalcitrant non-union with a capacitively coupled electrical field. A preliminary report," *J Bone Joint Surg Am* **67**, 577-585 (1985).

[28] J. W. Busse, J. Kaur, B. Mollon, M. Bhandari, P. Tornetta 3rd, H. J. Schunemann, et al., "Low intensity pulsed ultrasonography for fractures: systematic review of randomised controlled trials," *BMJ* **338**, b351 (2009).

[29] M. J. Callam, D. R. Harper, J. J. Dale, C. V. Ruckley, and R. J. Prescott, "A controlled trial of weekly ultrasound therapy in chronic leg ulceration," *Lancet* **2**, 204-206 (1987).

[30] D. C. Carvalho and A. Cliquet Junior, "The action of low-intensity pulsed ultrasound in bones of osteopenic rats," *Artif Organs* **28**, 114-118 (2004).

[31] R. A. Casarotto, J. C. Adamowski, F. Fallopa, and F. Bacanelli, "Coupling agents in therapeutic ultrasound: acoustic and thermal behavior," *Arch Phys Med Rehabil* **85**, 162-165 (2004).

[32] N. Cetin, A. Aytar, A. Atalay, and M. N. Akman, "Comparing hot pack, short-wave diathermy, ultrasound, and TENS on isokinetic strength, pain, and functional status of women with osteoarthritic knees: a single-blind, randomized, controlled trial," *Am J Phys Med Rehabil* **87**, 443-451 (2008).

[33] C. W. Chan, L. Qin, K. M. Lee, W. H. Cheung, J. C. Cheng, and K. S. Leung, "Dose-dependent effect of low-intensity pulsed ultrasound on callus formation during rapid distraction osteogenesis," *J Orthop Res* **24**, 2072-2079 (2006).

[34] W. H. Chang, J. S. Sun, S. P. Chang, and J. C. Lin, "Study of thermal effects of ultrasound stimulation on fracture healing," *Bioelectromagnetics* **23**, 256-263 (2002).

[35] J. Chen, Z. D. Shi, X. Ji, J. Morales, J. Zhang, N. Kaur, et al., "Enhanced osteogenesis of human mesenchymal stem cells by periodic heat shock in self-assembling peptide hydrogel," *Tissue Eng Part A* **19**, 716-728 (2013).

[36] Y. Chen, H. C. Whetstone, A. C. Lin, P. Nadesan, Q. Wei, R. Poon, et al., "Beta-catenin signaling plays a disparate role in different phases of fracture repair: implications for therapy to improve bone healing," *PLoS Med* **4**, e249 (2007).

[37] Y. Chen, H. C. Whetstone, A. Youn, P. Nadesan, E. C. Chow, A. C. Lin, et al., "Beta-catenin signaling pathway is crucial for bone morphogenetic protein 2 to induce new bone formation," *J Biol Chem* **282**, 526-533 (2007).

[38] W. H. Cheung, S. K. Chow, M. H. Sun, L. Qin, and K. S. Leung, "Low-intensity pulsed ultrasound accelerated callus formation, angiogenesis and callus remodeling in osteoporotic fracture healing," *Ultrasound Med Biol* **37**, 231-238 (2011).

[39] Y. C. Chiu, T. H. Huang, W. M. Fu, R. S. Yang, and C. H. Tang, "Ultrasound stimulates MMP-13 expression through p38 and JNK pathway in osteoblasts," *J Cell Physiol* **215**, 356-365 (2008).

[40] B. H. Choi, J. I. Woo, B. H. Min, and S. R. Park, "Low-intensity ultrasound stimulates the viability and matrix gene expression of human articular chondrocytes in alginate bead culture," *J Biomed Mater Res A* **79**, 858-864 (2006).

[41] B. H. Choi, M. H. Choi, M. G. Kwak, B. H. Min, Z. H. Woo, and S. R. Park, "Mechanotransduction pathways of low-intensity ultrasound in C-28/I2 human chondrocyte cell line," *Proc Inst Mech Eng H* **221**, 527-535 (2007).

[42] W. H. Choi, B. H. Choi, B. H. Min, and S. R. Park, "Low-intensity ultrasound increased colony forming unit-fibroblasts of mesenchymal stem cells during primary culture," *Tissue Eng Part C Methods* **17**, 517-526 (2011).

[43] S. K. Chow, K. M. Lee, L. Qin, K. S. Leung, and W. H. Cheung, "Restoration of longitudinal growth by bioengineered cartilage pellet in physeal injury is not affected by low intensity pulsed ultrasound," *J Biomed Mater Res B Appl Biomater* **99**, 36-44 (2011).

[44] E. Chung and M. N. Rylander, "Response of preosteoblasts to thermal stress conditioning and osteoinductive growth factors," *Cell Stress Chaperones* **17**, 203-214 (2012).

[45] S. L. Chung, N. M. Pounder, F. J. de Ana, L. Qin, K. Sui Leung, and W. H. Cheung, "Fracture healing enhancement with low intensity pulsed ultrasound at a critical application angle," *Ultrasound Med Biol* **37**, 1120-1133 (2011).

[46] C. C. Church, E. L. Carstensen, W. L. Nyborg, P. L. Carson, L. A. Frizzell, and M. R. Bailey, "The risk of exposure to diagnostic ultrasound in postnatal subjects: nonthermal mechanisms," *J Ultrasound Med* **27**, 565-92; quiz 593-6 (2008).

[47] W. T. Coakley, D. W. Bardsley, M. A. Grundy, F. Zamani, and D. J. Clarke, "Cell manipulation in ultrasonic standing wave fields," **44**, 43-62 (1989).

[48] S. D. Cook, J. P. Ryaby, J. McCabe, J. J. Frey, J. D. Heckman, and T. K. Kristiansen, "Acceleration of tibia and distal radius fracture healing in patients who smoke," *Clin Orthop Relat Res* **337**, 198-207 (1997).

[49] S. D. Cook, S. L. Salkeld, L. S. Popich-Patron, J. P. Ryaby, D. G. Jones, and R. L. Barrack, "Improved cartilage repair after treatment with low-intensity pulsed ultrasound," *Clin Orthop Relat Res* **391 Suppl**, S231-43 (2001).

[50] S. D. Cook, S. L. Salkeld, L. P. Patron, E. S. Doughty, and D. G. Jones, "The effect of low-intensity pulsed ultrasound on autologous osteochondral plugs in a canine model," *Am J Sports Med* **36**, 1733-1741 (2008).

[51] M. Coords, E. Breitbart, D. Paglia, N. Kappy, A. Gandhi, J. Cottrell, et al., "The effects of low-intensity pulsed ultrasound upon diabetic fracture healing," *J Orthop Res* **29**, 181-188 (2011).

[52] R. S. Cotran, T. Collins, and V. Kumar, *Robbins pathologic basis of disease* (Saunders, USA, 1999).

[53] J. H. Cui, K. Park, S. R. Park, and B. H. Min, "Effects of low-intensity ultrasound on chondrogenic differentiation of mesenchymal stem cells embedded in polyglycolic acid: an in vivo study," *Tissue Eng* **12**, 75-82 (2006).

[54] J. H. Cui, S. R. Park, K. Park, B. H. Choi, and B. H. Min, "Preconditioning of mesenchymal stem cells with low-intensity ultrasound for cartilage formation in vivo," *Tissue Eng* **13**, 351-360 (2007).

[55] R. De Nunno, "Effect of ultrasonics on ossification; experimental studies," *Ann Ital Chir* **29**, 211-220 (1952).

[56] C. J. Diederich and K. Hynynen, "Ultrasound technology for hyperthermia," *Ultrasound Med Biol* **25**, 871-887 (1999).

[57] N. Doan, P. Reher, S. Meghji, and M. Harris, "In vitro effects of therapeutic ultrasound on cell proliferation, protein synthesis, and cytokine production by human fibroblasts, osteoblasts, and monocytes," *J Oral Maxillofac Surg* **57**, 409-19; discussion 420 (1999).

[58] S. P. Dodd, J. L. Cunningham, A. W. Miles, S. Gheduzzi, and V. F. Humphrey, "Ultrasonic propagation in cortical bone mimics," *Phys Med Biol* **51**, 4635-4647 (2006).

[59] L. R. Duarte, "The stimulation of bone growth by ultrasound," *Arch Orthop Trauma Surg* **101**, 153-159 (1983).

[60] F. A. Duck, A. C. Baker, and H. C. Starritt, *Ultrasound in medicine* (Institute of Physics Publishing, London, UK, 1998).

[61] G. N. Duda, A. Kliche, R. Kleemann, J. E. Hoffmann, M. Sittinger, and A. Haisch, "Does low-intensity pulsed ultrasound stimulate maturation of tissue-engineered cartilage?" *J Biomed Mater Res B Appl Biomater* **68**, 21-28 (2004).

[62] M. Dudda, J. Hauser, G. Muhr, and S. A. Esenwein, "Low-intensity pulsed ultrasound as a useful adjuvant during distraction osteogenesis: a prospective, randomized controlled trial," *J Trauma* **71**, 1376-1380 (2011).

[63] F. Dunn, "Cellular inactivation by heat and shear," *Radiat Environ Biophys* **24**, 131-139 (1985).

[64] A. P. Duryea, A. D. Maxwell, W. W. Roberts, Z. Xu, T. L. Hall, and C. A. Cain, "In vitro comminution of model renal calculi using histotripsy," *IEEE Trans Ultrason Ferroelectr Freq Control* **58**, 971-980 (2011).

[65] M. Dyson, J. B. Pond, J. Joseph, and R. Warwick, "The stimulation of tissue regeneration by means of ultrasound," *Clin Sci* **35**, 273-285 (1968).

[66] M. Dyson, J. B. Pond, J. Joseph, and R. Warwick, "Stimulation of tissue regeneration by pulsed plane-wave ultrasound," *IEEE Trans Sonics Ultrason* **SU-17**, 133-139 (1970).

[67] M. Dyson and J. B. Pond, "The effect of pulsed ultrasound on tissue regeneration," *Physiotherapy* **56**, 136-142 (1970).

[68] M. Dyson, B. Woodward, and J. B. Pond, "Flow of red blood cells stopped by ultrasound," *Nature* **232**, 572-573 (1971).

[69] M. Dyson, C. Franks, and J. Suckling, "Stimulation of healing of varicose ulcers by ultrasound," *Ultrasonics* **14**, 232-236 (1976).

[70] M. Dyson and J. Suckling, "Stimulation of tissue repair by ultrasound: a survey of the mechanisms involved," *Physiotherapy* **64**, 105-108 (1978).

[71] M. Dyson and M. Brookes, "Stimulation of bone repair by ultrasound," *Ultrasound Med Biol* **Suppl 2**, 61-66 (1983).

[72] W. M. Eagleson, K. I. Deckert, E. E. Townsend, and J. R. Arnott, "The effect of heat on the healing of fractures: a preliminary experimental report," *Can Med Assoc J* **97**, 274-280 (1967).

[73] C. P. Eberson, K. A. Hogan, D. C. Moore, and M. G. Ehrlich, "Effect of low-intensity ultrasound stimulation on consolidation of the regenerate zone in a rat model of distraction osteogenesis," *J Pediatr Orthop* **23**, 46-51 (2003).

[74] K. Ebisawa, K. Hata, K. Okada, K. Kimata, M. Ueda, S. Torii, et al., "Ultrasound enhances transforming growth factor beta-mediated chondrocyte differentiation of human mesenchymal stem cells," *Tissue Eng* **10**, 921-929 (2004).

[75] T. A. Einhorn, "Enhancement of fracture-healing," *J Bone Joint Surg Am* **77**, 940-956 (1995).

[76] T. El-Bialy, H. Uludag, N. Jomha, and S. F. Badylak, "In vivo ultrasound-assisted tissue-engineered mandibular condyle: a pilot study in rabbits," *Tissue Eng Part C Methods* **16**, 1315-1323 (2010).

[77] T. H. El-Bialy, R. F. Elgazzar, E. E. Megahed, and T. J. Royston, "Effects of ultrasound modes on mandibular osteodistraction," *J Dent Res* **87**, 953-957 (2008).

[78] S. A. Elder, "Cavitation microstreaming," *J Acoust Soc Am* **31**, 54-64 (1958).

[79] A. Eller and H. G. Flynn, "Rectified diffusion during nonlinear pulsations of cavitation bubbles," *J Acoust Soc Am* **37**, 493-503 (1965).

[80] H. El-Mowafi and M. Mohsen, "The effect of low-intensity pulsed ultrasound on callus maturation in tibial distraction osteogenesis," *Int Orthop* **29**, 121-124 (2005).

[81] A. Emami, M. Petren-Mallmin, and S. Larsson, "No effect of low-intensity ultrasound on healing time of intramedullary fixed tibial fractures," *J Orthop Trauma* **13**, 252-257 (1999).

[82] J. Falconer, K. W. Hayes, and R. W. Chang, "Effect of ultrasound on mobility in osteoarthritis of the knee. A randomized clinical trial," *Arthritis Care Res* **5**, 29-35 (1992).

[83] M. Fechheimer, J. F. Boylan, S. Parker, J. E. Sisken, G. L. Patel, and S. G. Zimmer, "Transfection of mammalian cells with plasmid DNA by scrape loading and sonication loading," *Proc Natl Acad Sci U S A* **84**, 8463-8467 (1987).

[84] H. G. Flynn, "Generation of transient cavities in liquids by microsecond pulses of ultrasound," *J Acoust Soc Am* **72**, 1926-1932 (1982).

[85] M. M. Forbes, R. L. Steinberg, and W. D. O'Brien Jr, "Examination of inertial cavitation of Optison in producing sonoporation of chinese hamster ovary cells," *Ultrasound Med Biol* **34**, 2009-2018 (2008).

[86] A. Freedman, "Effects of fluid-loading on Lamb mode spectra," *J Acoust Soc Am* **99**, 3488-3496 (1996).

[87] W. J. Fry and R. B. Fry, "Determination of absolute sound levels and acoustic absorption coefficients by thermocouple probes - experiment," *J Acoust Soc Am* **26**, 311-317 (1952).

[88] W. J. Fry and R. B. Fry, "Determination of absolute sound levels and acoustic absorption coefficients by thermocouple probes - theory," *J Acoust Soc Am* **26**, 294-310 (1954).

[89] E. Fukada and I. Yasuda, "On the piezoelectric effect of bone," *J Phys Soc Jpn* **12**, 1158-1162 (1957).

[90] C. H. Fung, W. H. Cheung, N. M. Pounder, F. J. de Ana, A. Harrison, and K. S. Leung, "Effects of different therapeutic ultrasound intensities on fracture healing in rats," *Ultrasound Med Biol* **38**, 745-752 (2012).

[91] C. H. Fung, W. H. Cheung, N. M. Pounder, F. J. de Ana, A. Harrison, and K. S. Leung, "Investigation of rat bone fracture healing using pulsed 1.5 MHz, 30 mW/cm^2 burst ultrasound--axial distance dependency," *Ultrasonics* **54**, 850-859 (2014).

[92] C. H. Fung, W. H. Cheung, N. M. Pounder, A. Harrison, and K. S. Leung, "Osteocytes exposed to far field of therapeutic ultrasound promotes osteogenic cellular activities in pre-osteoblasts through soluble factors," *Ultrasonics* **54**, 1358-1365 (2014).

[93] T. Furukawa, Y. Uematsu, K. Asakawa, and Y. Wada, "Piezoelectricity, pyroelectricity, and thermoelectricity of polymer films," *J Appl Polym Sci* **12**, 2675-2689 (1968).

[94] K. A. Garvin, D. C. Hocking, and D. Dalecki, "Controlling the spatial organization of cells and extracellular matrix proteins in engineered tissues using ultrasound standing wave fields," *Ultrasound Med Biol* **36**, 1919-1932 (2010).

[95] K. A. Garvin, D. Dalecki, and D. C. Hocking, "Vascularization of three-dimensional collagen hydrogels using ultrasound standing wave fields," *Ultrasound Med Biol* **37**, 1853-1864 (2011).

[96] D. Gebauer and J. Correll, "Pulsed low-intensity ultrasound: a new salvage procedure for delayed unions and nonunions after leg lengthening in children," *J Pediatr Orthop* **25**, 750-754 (2005).

[97] D. Gebauer, E. Mayr, E. Orthner, and J. P. Ryaby, "Low-intensity pulsed ultrasound: effects on nonunions," *Ultrasound Med Biol* **31**, 1391-1402 (2005).

[98] G. P. Gebauer, S. S. Lin, H. A. Beam, P. Vieira, and J. R. Parsons, "Low-intensity pulsed ultrasound increases the fracture callus strength in diabetic BB Wistar rats but does not affect cellular proliferation," *J Orthop Res* **20**, 587-592 (2002).

[99] D. A. Glass 2nd and G. Karsenty, "Molecular bases of the regulation of bone remodeling by the canonical Wnt signaling pathway," *Curr Top Dev Biol* **73**, 43-84 (2006).

[100] D. A. Glass 2nd and G. Karsenty, "In vivo analysis of Wnt signaling in bone," *Endocrinology* **148**, 2630-2634 (2007).

[101] A. Gleizal, S. Li, J. B. Pialat, and J. L. Beziat, "Transcriptional expression of calvarial bone after treatment with low-intensity ultrasound: an in vitro study," *Ultrasound Med Biol* **32**, 1569-1574 (2006).

[102] C. Glorieux, K. Van de Rostyne, K. Nelson, W. Gao, W. Lauriks, and J. Thoen, "On the character of acoustic waves at the interface between hard and soft solids and liquids," *J Acoust Soc Am* **110**, 1299-1306 (2001).

[103] S. M. Gold and R. Wasserman, "Preliminary results of tibial bone transports with pulsed low intensity ultrasound (Exogen)," *J Orthop Trauma* **19**, 10-16 (2005).

[104] A. E. Goodship and J. Kenwright, "The influence of induced micromovement upon the healing of experimental tibial fractures," *J Bone Joint Surg Br* **67**, 650-655 (1985).

[105] S. A. Goss, R. L. Johnston, and F. Dunn, "Comprehensive compilation of empirical ultrasonic properties of mammalian tissues," *J Acoust Soc Am* **64**, 423-457 (1978).

[106] J. F. Greenleaf, R. R. Kinnick, J. T. Bronk, and M. E. Bolander, "Ultrasound induced tissue motion during fracture treatment," *Poster presentation at Orthopaedic Research Society Annual Meeting, Washington, Washington D C , USA* (2005).

[107] X. L. Griffin, N. Smith, N. Parsons, and M. L. Costa, "Ultrasound and shockwave therapy for acute fractures in adults," *Cochrane Database Syst Rev* **doi: 10.1002/14651858.CD008579.pub2.** (2012).

[108] S. P. Grogan, A. Barbero, J. Diaz-Romero, A. M. Cleton-Jansen, S. Soeder, R. Whiteside, et al., "Identification of markers to characterize and sort human articular chondrocytes with enhanced in vitro chondrogenic capacity," *Arthritis Rheum* **56**, 586-595 (2007).

[109] I. Gurkan, A. Ranganathan, X. Yang, W. E. Horton Jr, M. Todman, J. Huckle, et al., "Modification of osteoarthritis in the guinea pig with pulsed low-intensity ultrasound treatment," *Osteoarthritis Cartilage* **18**, 724-733 (2010).

[110] S. I. Han, S. Y. Oh, W. J. Jeon, J. M. Kim, J. H. Lee, H. Y. Chung, et al., "Mild heat shock induces cyclin D1 synthesis through multiple Ras signal pathways," *FEBS Lett* **515**, 141-145 (2002).

[111] L. Handolin, V. Kiljunen, I. Arnala, M. J. Kiuru, J. Pajarinen, E. K. Partio, et al., "Effect of ultrasound therapy on bone healing of lateral malleolar fractures of the ankle joint fixed with bioabsorbable screws," *J Orthop Sci* **10**, 391-395 (2005).

[112] L. Handolin, V. Kiljunen, I. Arnala, J. Pajarinen, E. K. Partio, and P. Rokkanen, "The effect of low intensity ultrasound and bioabsorbable self-reinforced poly-L-lactide screw fixation on bone in lateral malleolar fractures," *Arch Orthop Trauma Surg* **125**, 317-321 (2005).

[113] M. E. Hantes, A. N. Mavrodontidis, C. G. Zalavras, A. H. Karantanas, T. Karachalios, and K. N. Malizos, "Low-intensity transosseous ultrasound accelerates osteotomy healing in a sheep fracture model," *J Bone Joint Surg Am* **86-A**, 2275-2282 (2004).

[114] J. Harle, V. Salih, J. C. Knowles, F. Mayia, and I. Olsen, "Effects of therapeutic ultrasound on osteoblast gene expression," *J Mater Sci Mater Med* **12**, 1001-1004 (2001).

[115] J. Harle, V. Salih, F. Mayia, J. C. Knowles, and I. Olsen, "Effects of ultrasound on the growth and function of bone and periodontal ligament cells in vitro," *Ultrasound Med Biol* **27**, 579-586 (2001).

[116] J. Harle, F. Mayia, I. Olsen, and V. Salih, "Effects of ultrasound on transforming growth factor-beta genes in bone cells," *Eur Cell Mater* **10**, 70-76; discussion 76 (2005).

[117] G. I. Hasanova, S. E. Noriega, T. G. Mamedov, S. Guha Thakurta, J. A. Turner, and A. Subramanian, "The effect of ultrasound stimulation on the gene and protein expression of chondrocytes seeded in chitosan scaffolds," *J Tissue Eng Regen Med* **5**, 815-822 (2011).

[118] T. Hasegawa, M. Miwa, Y. Sakai, T. Niikura, M. Kurosaka, and T. Komori, "Osteogenic activity of human fracture haematoma-derived progenitor cells is stimulated by low-intensity pulsed ultrasound in vitro," *J Bone Joint Surg Br* **91**, 264-270 (2009).

[119] C. L. Haskin, K. A. Athanasiou, R. Klebe, and I. L. Cameron, "A heat-shock-like response with cytoskeletal disruption occurs following hydrostatic pressure in MG-63 osteosarcoma cells," *Biochem Cell Biol* **71**, 361-371 (1993).

[120] J. Hauser, M. Hauser, G. Muhr, and S. Esenwein, "Ultrasound-induced modifications of cytoskeletal components in osteoblast-like SAOS-2 cells," *J Orthop Res* **27**, 286-294 (2009).

[121] D. W. Hayes Jr, R. L. Brower, and K. J. John, "Articular cartilage. Anatomy, injury, and repair," *Clin Podiatr Med Surg* **18**, 35-53 (2001).

[122] M. J. Hayton, J. P. Dillon, D. Glynn, J. M. Curran, J. A. Gallagher, and K. A. Buckley, "Involvement of adenosine 5'-triphosphate in ultrasound-induced fracture repair," *Ultrasound Med Biol* **31**, 1131-1138 (2005).

[123] J. D. Heckman, J. P. Ryaby, J. McCabe, J. J. Frey, and R. F. Kilcoyne, "Acceleration of tibial fracture-healing by non-invasive, low-intensity pulsed ultrasound," *J Bone Joint Surg Am* **76**, 26-34 (1994).

[124] K. Hensel, M. P. Mienkina, and G. Schmitz, "Analysis of ultrasound fields in cell culture wells for in vitro ultrasound therapy experiments," *Ultrasound Med Biol* **37**, 2105-2115 (2011).

[125] N. Heybeli, A. Yesildag, O. Oyar, U. K. Gulsoy, M. A. Tekinsoy, and E. F. Mumcu, "Diagnostic ultrasound treatment increases the bone fracture-healing rate in an internally fixed rat femoral osteotomy model," *J Ultrasound Med* **21**, 1357-1363 (2002).

[126] M. Hirnschrodt, A. von Jena, T. Vontz, B. Fischer, R. Lerch, and H. Meixner, "Time domain evaluation of resonance antireflection (RAR) signals for ultrasonic density measurement," *IEEE Trans Ultrason Ferroelectr Freq Control* **47**, 1530-1539 (2000).

[127] A. Hofmann, U. Ritz, M. H. Hessmann, C. Schmid, A. Tresch, J. D. Rompe, et al., "Cell viability, osteoblast differentiation, and gene expression are altered in human osteoblasts from hypertrophic fracture non-unions," *Bone* **42**, 894-906 (2008).

[128] T. Hojo, M. Fujioka, G. Otsuka, S. Inoue, U. Kim, and T. Kubo, "Effect of heat stimulation on viability and proteoglycan metabolism of cultured chondrocytes: preliminary report," *J Orthop Sci* **8**, 396-399 (2003).

[129] C. H. Hou, S. M. Hou, and C. H. Tang, "Ultrasound increased BMP-2 expression via PI3K, Akt, c-Fos/c-Jun, and AP-1 pathways in cultured osteoblasts," *J Cell Biochem* **106**, 7-15 (2009).

[130] H. C. Hsu, Y. C. Fong, C. S. Chang, C. J. Hsu, S. F. Hsu, J. G. Lin, et al., "Ultrasound induces cyclooxygenase-2 expression through integrin, integrin-linked kinase, Akt, NF-kappaB and p300 pathway in human chondrocytes," *Cell Signal* **19**, 2317-2328 (2007).

[131] S. H. Hsu, C. C. Kuo, S. W. Whu, C. H. Lin, and C. L. Tsai, "The effect of ultrasound stimulation versus bioreactors on neocartilage formation in tissue engineering scaffolds seeded with human chondrocytes in vitro," *Biomol Eng* **23**, 259-264 (2006).

[132] S. K. Hsu, W. T. Huang, B. S. Liu, S. M. Li, H. T. Chen, and C. J. Chang, "Effects of near-field ultrasound stimulation on new bone formation and osseointegration of dental titanium implants in vitro and in vivo," *Ultrasound Med Biol* **37**, 403-416 (2011).

[133] M. H. Huang, H. J. Ding, C. Y. Chai, Y. F. Huang, and R. C. Yang, "Effects of sonication on articular cartilage in experimental osteoarthritis," *J Rheumatol* **24**, 1978-1984 (1997).

[134] M. H. Huang, R. C. Yang, H. J. Ding, and C. Y. Chai, "Ultrasound effect on level of stress proteins and arthritic histology in experimental arthritis," *Arch Phys Med Rehabil* **80**, 551-556 (1999).

[135] M. H. Huang, Y. S. Lin, C. L. Lee, and R. C. Yang, "Use of ultrasound to increase effectiveness of isokinetic exercise for knee osteoarthritis," *Arch Phys Med Rehabil* **86**, 1545-1551 (2005).

[136] T. H. Huang, C. H. Tang, H. I. Chen, W. M. Fu, and R. S. Yang, "Low-intensity pulsed ultrasound-promoted bone healing is not entirely cyclooxgenase 2 dependent," *J Ultrasound Med* **27**, 1415-1423 (2008).

[137] P. E. Huber, M. J. Mann, L. G. Melo, A. Ehsan, D. Kong, L. Zhang, et al., "Focused ultrasound (HIFU) induces localized enhancement of reporter gene expression in rabbit carotid artery," *Gene Ther* **10**, 1600-1607 (2003).

[138] C. F. Hui, C. W. Chan, H. Y. Yeung, K. M. Lee, L. Qin, G. Li, et al., "Low-intensity pulsed ultrasound enhances posterior spinal fusion implanted with mesenchymal stem cells-calcium phosphate composite without bone grafting," *Spine (Phila Pa 1976)* **36**, 1010-1016 (2011).

[139] B. N. Hung and A. Goldstein, "Acoustic parameters of commercial plastics," *IEEE Trans Sonics Ultrason* **SU-30**, 249-254 (1983).

[140] T. Huttunen, J. P. Kaipio, and K. Hynynen, "Modeling of anomalies due to hydrophones in continuous-wave ultrasound fields," *IEEE Trans Ultrason Ferroelectr Freq Control* **50**, 1486-1500 (2003).

[141] K. Hynynen and D. K. Edwards, "Temperature measurements during ultrasound hyperthermia," *Med Phys* **16**, 618-626 (1989).

[142] K. Hynynen, "Biophysics and technology of ultrasound hyperthermia," in *Methods of external hyperthermia heating, clinical thermology series, subseries thermotherapy,* M. Gautherie, ed. (Springer-Verlag, Heidelberg, Germany, 1990), pp. 61-116.

[143] K. Ikeda, T. Takayama, N. Suzuki, K. Shimada, K. Otsuka, and K. Ito, "Effects of low-intensity pulsed ultrasound on the differentiation of C2C12 cells," *Life Sci* **79**, 1936-1943 (2006).

[144] K. Ikushima, S. Watanuki, and S. Komiyama, "Detection of acoustically induced electromagnetic radiation," *Appl Phys Lett* **89**, 194103 (2006).

[145] M. Ito, Y. Azuma, T. Ohta, and K. Komoriya, "Effects of ultrasound and 1,25-dihydroxyvitamin D3 on growth factor secretion in co-cultures of osteoblasts and endothelial cells," *Ultrasound Med Biol* **26**, 161-166 (2000).

[146] S. Iwabuchi, M. Ito, J. Hata, T. Chikanishi, Y. Azuma, and H. Haro, "In vitro evaluation of low-intensity pulsed ultrasound in herniated disc resorption," *Biomaterials* **26**, 7104-7114 (2005).

[147] T. Iwai, Y. Harada, K. Imura, S. Iwabuchi, J. Murai, K. Hiramatsu, et al., "Low-intensity pulsed ultrasound increases bone ingrowth into porous hydroxyapatite ceramic," *J Bone Miner Metab* **25**, 392-399 (2007).

[148] T. Iwashina, J. Mochida, T. Miyazaki, T. Watanabe, S. Iwabuchi, K. Ando, et al., "Low-intensity pulsed ultrasound stimulates cell proliferation and proteoglycan production in rabbit intervertebral disc cells cultured in alginate," *Biomaterials* **27**, 354-361 (2006).

[149] J. E. Jensen, "Stress fracture in the world class athlete: a case study," *Med Sci Sports Exerc* **30**, 783-787 (1998).

[150] T. Jiang, T. Xu, F. Gu, A. Chen, Z. Xiao, and D. Zhang, "Osteogenic effect of low intensity pulsed ultrasound on rat adipose-derived stem cells in vitro," *J Huazhong Univ Sci Technolog Med Sci* **32**, 75-81 (2012).

[151] T. Jin, I. George Fantus, and J. Sun, "Wnt and beyond Wnt: multiple mechanisms control the transcriptional property of beta-catenin," *Cell Signal* **20**, 1697-1704 (2008).

[152] S. Jingushi, K. Mizuno, T. Matsushita, and M. Itoman, "Low-intensity pulsed ultrasound treatment for postoperative delayed union or nonunion of long bone fractures," *J Orthop Sci* **12**, 35-41 (2007).

[153] D. C. Jones, M. N. Wein, M. Oukka, J. G. Hofstaetter, M. J. Glimcher, and L. H. Glimcher, "Regulation of adult bone mass by the zinc finger adapter protein Schnurri-3," *Science* **312**, 1223-1227 (2006).

[154] H. Kanai, "Propagation of spontaneously actuated pulsive vibration in human heart wall and in vivo viscoelasticity estimation," *IEEE Trans Ultrason Ferroelectr Freq Control* **52**, 1931-1942 (2005).

[155] K. S. Kang, S. J. Lee, H. S. Lee, W. Moon, and D. W. Cho, "Effects of combined mechanical stimulation on the proliferation and differentiation of pre-osteoblasts," *Exp Mol Med* **43**, 367-373 (2011).

[156] M. Katano, K. Naruse, K. Uchida, Y. Mikuni-Takagaki, M. Takaso, M. Itoman, et al., "Low intensity pulsed ultrasound accelerates delayed healing process by reducing the time required for the completion of endochondral ossification in the aged mouse femur fracture model," *Exp Anim* **60**, 385-395 (2011).

[157] A. E. Kearns, M. M. Donohue, B. Sanyal, and M. B. Demay, "Cloning and characterization of a novel protein kinase that impairs osteoblast differentiation in vitro," *J Biol Chem* **276**, 42213-42218 (2001).

[158] A. Khanna, R. T. Nelmes, N. Gougoulias, N. Maffulli, and J. Gray, "The effects of LIPUS on soft-tissue healing: a review of literature," *Br Med Bull* **89**, 169-182 (2009).

[159] H. J. Kim, J. F. Greenleaf, R. R. Kinnick, J. T. Bronk, and M. E. Bolander, "Ultrasound-mediated transfection of mammalian cells," *Hum Gene Ther* **7**, 1339-1346 (1996).

[160] M. Kinoshita and K. Hynynen, "Key factors that affect sonoporation efficiency in in vitro settings: the importance of standing wave in sonoporation," *Biochem Biophys Res Commun* **359**, 860-865 (2007).

[161] L. E. Kinsler and A. R. Frey, *Fundamentals of acoustics* (John Wiley & Sons, Inc., New York, USA, 1962).

[162] W. Klug, W. G. Franke, and H. G. Knoch, "Scintigraphic control of bone-fracture healing under ultrasonic stimulation: an animal experimental study," *Eur J Nucl Med* **11**, 494-497 (1986).

[163] Y. Kobayashi, D. Sakai, T. Iwashina, S. Iwabuchi, and J. Mochida, "Low-intensity pulsed ultrasound stimulates cell proliferation, proteoglycan synthesis and expression of growth factor-related genes in human nucleus pulposus cell line," *Eur Cell Mater* **17**, 15-22 (2009).

[164] T. Kodama, Y. Tomita, K. Koshiyama, and M. J. Blomley, "Transfection effect of microbubbles on cells in superposed ultrasound waves and behavior of cavitation bubble," *Ultrasound Med Biol* **32**, 905-914 (2006).

[165] T. Kokubu, N. Matsui, H. Fujioka, M. Tsunoda, and K. Mizuno, "Low intensity pulsed ultrasound exposure increases prostaglandin E2 production via the induction of cyclooxygenase-2 mRNA in mouse osteoblasts," *Biochem Biophys Res Commun* **256**, 284-287 (1999).

[166] C. Kollmann, G. Vacariu, O. Schuhfried, V. Fialka-Moser, and H. Bergmann, "Variations in the output power and surface heating effects of transducers in therapeutic ultrasound," *Arch Phys Med Rehabil* **86**, 1318-1324 (2005).

[167] J. A. Kopechek, H. Kim, D. D. McPherson, and C. K. Holland, "Calibration of the 1-MHz Sonitron ultrasound system," *Ultrasound Med Biol* **36**, 1762-1766 (2010).

[168] C. M. Korstjens, P. A. Nolte, E. H. Burger, G. H. Albers, C. M. Semeins, I. H. Aartman, et al., "Stimulation of bone cell differentiation by low-intensity ultrasound--a histomorphometric in vitro study," *J Orthop Res* **22**, 495-500 (2004).

[169] C. M. Korstjens, R. H. van der Rijt, G. H. Albers, C. M. Semeins, and J. Klein-Nulend, "Low-intensity pulsed ultrasound affects human articular chondrocytes in vitro," *Med Biol Eng Comput* **46**, 1263-1270 (2008).

[170] T. Kozuka, T. Tuziuti, H. Mitome, and T. Fukuda, "Non-contact micromanipulation using an ultrasonic standing wave field," *Micro Electro Mechanical Systems, 1996, MEMS '96, Proceedings An Investigation of Micro Structures, Sensors, Actuators, Machines and Systems IEEE, The Ninth Annual International Workshop on* , 435-440 (1996).

[171] B. Krasovitski, V. Frenkel, S. Shoham, and E. Kimmel, "Intramembrane cavitation as a unifying mechanism for ultrasound-induced bioeffects," *Proc Natl Acad Sci U S A* **108**, 3258-3263 (2011).

[172] T. K. Kristiansen, J. P. Ryaby, J. McCabe, J. J. Frey, and L. R. Roe, "Accelerated healing of distal radial fractures with the use of specific, low-intensity ultrasound. A multicenter, prospective, randomized, double-blind, placebo-controlled study," *J Bone Joint Surg Am* **79**, 961-973 (1997).

[173] R. E. Kumon, M. Aehle, D. Sabens, P. Parikh, D. Kourennyi, and C. X. Deng, "Ultrasound-induced calcium oscillations and waves in Chinese hamster ovary cells in the presence of microbubbles," *Biophys J* **93**, L29-31 (2007).

[174] R. E. Kumon, M. Aehle, D. Sabens, P. Parikh, Y. W. Han, D. Kourennyi, et al., "Spatiotemporal effects of sonoporation measured by real-time calcium imaging," *Ultrasound Med Biol* **35**, 494-506 (2009).

[175] C. H. Lai, S. C. Chen, L. H. Chiu, C. B. Yang, Y. H. Tsai, C. S. Zuo, et al., "Effects of low-intensity pulsed ultrasound, dexamethasone/TGF-beta1 and/or BMP-2 on the transcriptional expression of genes in human mesenchymal stem cells: chondrogenic vs. osteogenic differentiation," *Ultrasound Med Biol* **36**, 1022-1033 (2010).

[176] C. H. Lai, C. C. Chuang, J. K. Li, S. C. Chen, and W. H. Chang, "Effects of ultrasound on osteotomy healing in a rabbit fracture model," *Ultrasound Med Biol* **37**, 1635-1643 (2011).

[177] R. Langer and J. P. Vacanti, "Tissue engineering," *Science* **260**, 920-926 (1993).

[178] H. J. Lee, B. H. Choi, B. H. Min, Y. S. Son, and S. R. Park, "Low-intensity ultrasound stimulation enhances chondrogenic differentiation in alginate culture of mesenchymal stem cells," *Artif Organs* **30**, 707-715 (2006).

[179] H. J. Lee, B. H. Choi, B. H. Min, and S. R. Park, "Low-intensity ultrasound inhibits apoptosis and enhances viability of human mesenchymal stem cells in three-dimensional alginate culture during chondrogenic differentiation," *Tissue Eng* **13**, 1049-1057 (2007).

[180] T. G. Leighton, *The acoustic bubble* (Academic Press, Inc., San Diego, USA, 1994).

[181] S. A. Leon, S. O. Asbell, H. H. Arastu, G. Edelstein, A. J. Packel, S. Sheehan, et al., "Effects of hyperthermia on bone. II. Heating of bone in vivo and stimulation of bone growth," *Int J Hyperthermia* **9**, 77-87 (1993).

[182] K. S. Leung, W. H. Cheung, C. Zhang, K. M. Lee, and H. K. Lo, "Low intensity pulsed ultrasound stimulates osteogenic activity of human periosteal cells," *Clin Orthop Relat Res* **418**, 253-259 (2004).

[183] K. S. Leung, W. S. Lee, W. H. Cheung, and L. Qin, "Lack of efficacy of low-intensity pulsed ultrasound on prevention of postmenopausal bone loss evaluated at the distal radius in older Chinese women," *Clin Orthop Relat Res* **427**, 234-240 (2004).

[184] K. S. Leung, W. S. Lee, H. F. Tsui, P. P. Liu, and W. H. Cheung, "Complex tibial fracture outcomes following treatment with low-intensity pulsed ultrasound," *Ultrasound Med Biol* **30**, 389-395 (2004).

[185] G. C. Li, G. M. Hahn, and L. J. Tolmach, "Cellular inactivation by ultrasound," *Nature* **267**, 163-165 (1977).

[186] J. Li, L. J. Waugh, S. L. Hui, D. B. Burr, and S. J. Warden, "Low-intensity pulsed ultrasound and nonsteroidal anti-inflammatory drugs have opposing effects during stress fracture repair," *J Orthop Res* **25**, 1559-1567 (2007).

[187] J. G. Li, W. H. Chang, J. C. Lin, and J. S. Sun, "Optimum intensities of ultrasound for PGE_2 secretion and growth of osteoblasts," *Ultrasound Med Biol* **28**, 683-690 (2002).

[188] J. K. Li, W. H. Chang, J. C. Lin, R. C. Ruaan, H. C. Liu, and J. S. Sun, "Cytokine release from osteoblasts in response to ultrasound stimulation," *Biomaterials* **24**, 2379-2385 (2003).

[189] J. K. Li, J. C. Lin, H. C. Liu, J. S. Sun, R. C. Ruaan, C. Shih, et al., "Comparison of ultrasound and electromagnetic field effects on osteoblast growth," *Ultrasound Med Biol* **32**, 769-775 (2006).

[190] L. Li, Z. Yang, H. Zhang, W. Chen, M. Chen, and Z. Zhu, "Low-intensity pulsed ultrasound regulates proliferation and differentiation of osteoblasts through osteocytes," *Biochem Biophys Res Commun* **418**, 296-300 (2012).

[191] D. Lim, C. Y. Ko, D. H. Seo, D. G. Woo, J. M. Kim, K. J. Chun, et al., "Low-intensity ultrasound stimulation prevents osteoporotic bone loss in young adult ovariectomized mice," *J Orthop Res* **29**, 116-125 (2011).

[192] A. Loyola-Sanchez, J. Richardson, and N. J. MacIntyre, "Efficacy of ultrasound therapy for the management of knee osteoarthritis: a systematic review with meta-analysis," *Osteoarthritis Cartilage* **18**, 1117-1126 (2010).

[193] A. Loyola-Sanchez, J. Richardson, K. A. Beattie, C. Otero-Fuentes, J. D. Adachi, and N. J. MacIntyre, "Effect of low-intensity pulsed ultrasound on the cartilage repair in people with mild to moderate knee osteoarthritis: a double-blinded, randomized, placebo-controlled pilot study," *Arch Phys Med Rehabil* **93**, 35-42 (2012).

[194] H. Lu, L. Qin, K. Lee, W. Cheung, K. Chan, and K. Leung, "Identification of genes responsive to low-intensity pulsed ultrasound stimulations," *Biochem Biophys Res Commun* **378**, 569-573 (2009).

[195] P. H. Lubbert, R. H. van der Rijt, L. E. Hoorntje, and C. van der Werken, "Low-intensity pulsed ultrasound (LIPUS) in fresh clavicle fractures: a multi-centre double blind randomised controlled trial," *Injury* **39**, 1444-1452 (2008).

[196] M. J. Lunt and F. A. Duck, "Ultrasonic power balances--effect of a coupling window on the power measured from physiotherapy ultrasound units," *Ultrasound Med Biol* **27**, 1127-1132 (2001).

[197] W. Lutz, M. F. Burritt, D. E. Nixon, P. C. Kao, and R. Kumar, "Zinc increases the activity of vitamin D-dependent promoters in osteoblasts," *Biochem Biophys Res Commun* **271**, 1-7 (2000).

[198] R. Lyon, X. C. Liu, and J. Meier, "The effects of therapeutic vs. high-intensity ultrasound on the rabbit growth plate," *J Orthop Res* **21**, 865-871 (2003).

[199] A. Maddi, H. Hai, S. T. Ong, L. Sharp, M. Harris, and S. Meghji, "Long wave ultrasound may enhance bone regeneration by altering OPG/RANKL ratio in human osteoblast-like cells," *Bone* **39**, 283-288 (2006).

[200] E. L. Madsen, H. J. Sathoff, and J. A. Zagzebski, "Ultrasonic shear wave properties of soft tissues and tissuelike materials," *J Acoust Soc Am* **74**, 1346-1355 (1983).

[201] G. Maintz, "Animal experiments in the study of the effect of ultrasonic waves on bone regeneration," *Strahlentherapie* **82**, 631-638 (1950).

[202] J. Man, R. M. Shelton, P. R. Cooper, G. Landini, and B. A. Scheven, "Low intensity ultrasound stimulates osteoblast migration at different frequencies," *J Bone Miner Metab* **30**, 602-607 (2012).

[203] J. Man, R. M. Shelton, P. R. Cooper, and B. A. Scheven, "Low-intensity low-frequency ultrasound promotes proliferation and differentiation of odontoblast-like cells," *J Endod* **38**, 608-613 (2012).

[204] R. Marsell and T. A. Einhorn, "Emerging bone healing therapies," *J Orthop Trauma* **24 Suppl 1**, S4-8 (2010).

[205] R. Marsell and T. A. Einhorn, "The biology of fracture healing," *Injury* **42**, 551-555 (2011).

[206] I. Martin, D. Wendt, and M. Heberer, "The role of bioreactors in tissue engineering," *Trends Biotechnol* **22**, 80-86 (2004).

[207] P. Martinez de Albornoz, A. Khanna, U. G. Longo, F. Forriol, and N. Maffulli, "The evidence of low-intensity pulsed ultrasound for in vitro, animal and human fracture healing," *Br Med Bull* **100**, 39-57 (2011).

[208] S. Marvel, S. Okrasinski, S. H. Bernacki, E. Loboa, and P. A. Dayton, "The development and validation of a LIPUS system with preliminary observations of ultrasonic effects on human adult stem cells," *IEEE Trans Ultrason Ferroelectr Freq Control* **57**, 1977-1984 (2010).

[209] C. Mason and P. Dunnill, "A brief definition of regenerative medicine," *Regen Med* **3**, 1-5 (2008).

[210] A. Matsiko, T. J. Levingstone, and F. J. O'Brien, "Advanced strategies for articular cartilage defect repair," *Materials* **6**, 637-668 (2013).

[211] E. Mayr, V. Frankel, and A. Ruter, "Ultrasound--an alternative healing method for nonunions?" *Arch Orthop Trauma Surg* **120**, 1-8 (2000).

[212] K. A. McBride and S. D. Pye, "The effect of back reflections on the acoustic power delivered by physiotherapy ultrasound machines," *Ultrasound Med Biol* **35**, 1672-1678 (2009).

[213] S. R. McClure, K. Miles, D. Vansickle, and T. South, "The effect of variable waveform low-intensity pulsed ultrasound in a fourth metacarpal osteotomy gap model in horses," *Ultrasound Med Biol* **36**, 1298-1305 (2010).

[214] S. M. McCormick, V. Saini, Y. Yazicioglu, Z. N. Demou, and T. J. Royston, "Interdependence of pulsed ultrasound and shear stress effects on cell morphology and gene expression," *Ann Biomed Eng* **34**, 436-445 (2006).

[215] R. T. Mihran, F. S. Barnes, and H. Wachtel, "Temporally-specific modification of myelinated axon excitability in vitro following a single ultrasound pulse," *Ultrasound Med Biol* **16**, 297-309 (1990).

[216] D. L. Miller, R. M. Thomas, and R. L. Buschbom, "Comet assay reveals DNA strand breaks induced by ultrasonic cavitation in vitro," *Ultrasound Med Biol* **21**, 841-848 (1995).

[217] M. W. Miller, D. L. Miller, and A. A. Brayman, "A review of in vitro bioeffects of inertial ultrasonic cavitation from a mechanistic perspective," *Ultrasound Med Biol* **22**, 1131-1154 (1996).

[218] M. W. Miller, L. F. Battaglia, and S. Mazza, "Biological and environmental factors affecting ultrasound-induced hemolysis in vitro: Medium tonicity," *Ultrasound Med Biol* **29**, 713-724 (2003).

[219] M. W. Miller, E. C. Everbach, W. M. Miller, and L. F. Battaglia, "Biological and environmental factors affecting ultrasound-induced hemolysis in vitro: 2. medium dissolved gas (pO2) content," *Ultrasound Med Biol* **29**, 93-102 (2003).

[220] B. H. Min, J. I. Woo, H. S. Cho, B. H. Choi, S. J. Park, M. J. Choi, et al., "Effects of low-intensity ultrasound (LIUS) stimulation on human cartilage explants," *Scand J Rheumatol* **35**, 305-311 (2006).

[221] K. Miyamoto, H. S. An, R. L. Sah, K. Akeda, M. Okuma, L. Otten, et al., "Exposure to pulsed low intensity ultrasound stimulates extracellular matrix metabolism of bovine intervertebral disc cells cultured in alginate beads," *Spine* **30**, 2398-2405 (2005).

[222] A. J. Mortimer and M. Dyson, "The effect of therapeutic ultrasound on calcium uptake in fibroblasts," *Ultrasound Med Biol* **14**, 499-506 (1988).

[223] V. G. Mozhaev and M. Weihnacht, "Subsonic leaky Rayleigh waves at liquid-solid interfaces," *Ultrasonics* **40**, 927-933 (2002).

[224] S. Mukai, H. Ito, Y. Nakagawa, H. Akiyama, M. Miyamoto, and T. Nakamura, "Transforming growth factor-beta1 mediates the effects of low-intensity pulsed ultrasound in chondrocytes," *Ultrasound Med Biol* **31**, 1713-1721 (2005).

[225] C. Murolo and F. Claudio, "Effect of ultrasonics on repair of fractures," *G Ital Chir* **8**, 897-903 (1952).

[226] G. F. Muschler, C. Nakamoto, and L. G. Griffith, "Engineering principles of clinical cell-based tissue engineering," *J Bone Joint Surg Am* **86-A**, 1541-1558 (2004).

[227] K. Naito, T. Watari, T. Muta, A. Furuhata, H. Iwase, M. Igarashi, et al., "Low-intensity pulsed ultrasound (LIPUS) increases the articular cartilage type II collagen in a rat osteoarthritis model," *J Orthop Res* **28**, 361-369 (2010).

[228] K. Naruse, Y. Mikuni-Takagaki, Y. Azuma, M. Ito, T. Oota, K. Kameyama, et al., "Anabolic response of mouse bone-marrow-derived stromal cell clone ST2 cells to low-intensity pulsed ultrasound," *Biochem Biophys Res Commun* **268**, 216-220 (2000).

[229] K. Naruse, A. Miyauchi, M. Itoman, and Y. Mikuni-Takagaki, "Distinct anabolic response of osteoblast to low-intensity pulsed ultrasound," *J Bone Miner Res* **18**, 360-369 (2003).

[230] K. Naruse, Y. Mikuni-Takagaki, K. Urabe, K. Uchida, and M. Itoman, "Therapeutic ultrasound induces periosteal ossification without apparent changes in cartilage," *Connect Tissue Res* **50**, 55-63 (2009).

[231] K. Naruse, H. Sekiya, Y. Harada, S. Iwabuchi, Y. Kozai, R. Kawamata, et al., "Prolonged endochondral bone healing in senescence is shortened by low-intensity pulsed ultrasound in a manner dependent on COX-2," *Ultrasound Med Biol* **36**, 1098-1108 (2010).

[232] I. Z. Nenadic, M. W. Urban, S. Aristizabal, S. A. Mitchell, T. C. Humphrey, and J. F. Greenleaf, "On Lamb and Rayleigh wave convergence in viscoelastic tissues," *Phys Med Biol* **56**, 6723-6738 (2011).

[233] I. Z. Nenadic, M. W. Urban, S. A. Mitchell, and J. F. Greenleaf, "Lamb wave dispersion ultrasound vibrometry (LDUV) method for quantifying mechanical properties of viscoelastic solids," *Phys Med Biol* **56**, 2245-2264 (2011).

[234] E. A. Neppiras, "Subharmonic and other low-frequency emission from bubbles in sound-irradiated liquids," *J Acoust Soc Am* **46**, 587-601 (1969).

[235] P. H. Nicholson, P. Moilanen, T. Kärkkäinen, J. Timonen, and S. Cheng, "Guided ultrasonic waves in long bones: modelling, experiment and in vivo application," *Physiol Meas* **23**, 755-768 (2002).

[236] E. A. Nicoll, "Fractures of the tibial shaft. A survey of 705 cases," *J Bone Joint Surg Br* **46**, 373-387 (1964).

[237] K. R. Nightingale, M. L. Palmeri, R. W. Nightingale, and G. E. Trahey, "On the feasibility of remote palpation using acoustic radiation force," *J Acoust Soc Am* **110**, 625-634 (2001).

[238] T. Nishikori, M. Ochi, Y. Uchio, S. Maniwa, H. Kataoka, K. Kawasaki, et al., "Effects of low-intensity pulsed ultrasound on proliferation and chondroitin sulfate synthesis of cultured chondrocytes embedded in Atelocollagen gel," *J Biomed Mater Res* **59**, 201-206 (2002).

[239] P. A. Nolte, J. Klein-Nulend, G. H. Albers, R. K. Marti, C. M. Semeins, S. W. Goei, et al., "Low-intensity ultrasound stimulates endochondral ossification in vitro," *J Orthop Res* **19**, 301-307 (2001).

[240] P. A. Nolte, A. van der Krans, P. Patka, I. M. Janssen, J. P. Ryaby, and G. H. Albers, "Low-intensity pulsed ultrasound in the treatment of nonunions," *J Trauma* **51**, 693-702; discussion 702-3 (2001).

[241] R. Norgaard, M. Kassem, and S. I. Rattan, "Heat shock-induced enhancement of osteoblastic differentiation of hTERT-immortalized mesenchymal stem cells," *Ann N Y Acad Sci* **1067**, 443-447 (2006).

[242] S. Noriega, T. Mamedov, J. A. Turner, and A. Subramanian, "Intermittent applications of continuous ultrasound on the viability, proliferation, morphology, and matrix production of chondrocytes in 3D matrices," *Tissue Eng* **13**, 611-618 (2007).

[243] W. D. O'Brien Jr, C. X. Deng, G. R. Harris, B. A. Herman, C. R. Merritt, N. Sanghvi, et al., "The risk of exposure to diagnostic ultrasound in postnatal subjects: thermal effects," *J Ultrasound Med* **27**, 517-35; quiz 537-40 (2008).

[244] K. B. Ocheltree, "Sound field calculation for rectangular sources," **36**, 242-248 (1989).

[245] M. Ohno, Y. Kiyama, H. Yamada, K. Takashima, and K. Ikushima, "Measurements of acoustically stimulated electromagnetic response from piezoelectric materials," *Proceedings of 32nd Symposium on Ultrasonic Electronics* **32**, 211-212 (2011).

[246] K. Okada, N. Miyakoshi, S. Takahashi, S. Ishigaki, J. Nishida, and E. Itoi, "Congenital pseudoarthrosis of the tibia treated with low-intensity pulsed ultrasound stimulation (LIPUS)," *Ultrasound Med Biol* **29**, 1061-1064 (2003).

[247] Optotherm Inc. Emissivity in the infrared - emissivity table . Available at: http://www.optotherm.com/emiss-table.htm. Accessed December 21, 2012.

[248] L. Ozgonenel, E. Aytekin, and G. Durmusoglu, "A double-blind trial of clinical effects of therapeutic ultrasound in knee osteoarthritis," *Ultrasound Med Biol* **35**, 44-49 (2009).

[249] H. G. Park, S. I. Han, S. Y. Oh, and H. S. Kang, "Cellular responses to mild heat stress," *Cell Mol Life Sci* **62**, 10-23 (2005).

[250] K. Park, B. Hoffmeister, D. K. Han, and K. Hasty, "Therapeutic ultrasound effects on interleukin-1beta stimulated cartilage construct in vitro," *Ultrasound Med Biol* **33**, 286-295 (2007).

[251] S. R. Park, S. H. Park, K. W. Jang, H. S. Cho, J. H. Cui, H. J. An, et al., "The effect of sonication on simulated osteoarthritis. Part II: alleviation of osteoarthritis pathogenesis by 1 MHz ultrasound with simultaneous hyaluronate injection," *Ultrasound Med Biol* **31**, 1559-1566 (2005).

[252] J. Parvizi, C. C. Wu, D. G. Lewallen, J. F. Greenleaf, and M. E. Bolander, "Low-intensity ultrasound stimulates proteoglycan synthesis in rat chondrocytes by increasing aggrecan gene expression," *J Orthop Res* **17**, 488-494 (1999).

[253] J. Parvizi, V. Parpura, J. F. Greenleaf, and M. E. Bolander, "Calcium signaling is required for ultrasound-stimulated aggrecan synthesis by rat chondrocytes," *J Orthop Res* **20**, 51-57 (2002).

[254] M. J. Perry, L. K. Parry, V. J. Burton, S. Gheduzzi, J. N. Beresford, V. F. Humphrey, et al., "Ultrasound mimics the effect of mechanical loading on bone formation in vivo on rat ulnae," *Med Eng Phys* **31**, 42-47 (2009).

[255] L. S. Phieffer and J. A. Goulet, "Delayed unions of the tibia," *J Bone Joint Surg Am* **88**, 206-216 (2006).

[256] M. J. Pickworth, P. P. Dendy, P. R. Twentyman, and T. G. Leighton, "Studies of the cavitational effects of clinical ultrasound by sonoluminescence: 4. The effect of therapeutic ultrasound on cells in monolayer culture in a standing wave field," *Phys Med Biol* **34**, 1553-1560 (1989).

[257] A. A. Pilla, M. Figueiredo, S. Lattuga, P. Nasser, J. M. Alves, J. J. Kaufman, et al., "Pulsed sine wave ultrasound accelerates bone fracture repair," *Proc IEEE Ultrason Symp* **2**, 1003-1005 (1989).

[258] A. A. Pilla, M. Figueiredo, P. Nasser, S. Lattuga, T. Kristiansen, J. Heckman, et al., "Non-invasive low intensity ultrasound accelerates bone repair: rabbit fibula model and human colles' and tibial fractures," *Engineering in Medicine and Biology Society, 1990 , Proceedings of the Twelfth Annual International Conference of the IEEE* , 1573-1574 (1990).

[259] A. A. Pilla, M. A. Mont, P. R. Nasser, S. A. Khan, M. Figueiredo, J. J. Kaufman, et al., "Non-invasive low-intensity pulsed ultrasound accelerates bone healing in the rabbit," *J Orthop Trauma* **4**, 246-253 (1990).

[260] A. A. Pilla, "Low-intensity electromagnetic and mechanical modulation of bone growth and repair: are they equivalent?" *J Orthop Sci* **7**, 420-428 (2002).

[261] M. F. Pittenger, A. M. Mackay, S. C. Beck, R. K. Jaiswal, R. Douglas, J. D. Mosca, et al., "Multilineage potential of adult human mesenchymal stem cells," *Science* **284**, 143-147 (1999).

[262] L. Poltawski and T. Watson, "Relative transmissivity of ultrasound coupling agents commonly used by therapists in the UK," *Ultrasound Med Biol* **33**, 120-128 (2007).

[263] V. C. Protopappas, D. I. Fotiadis, and K. N. Malizos, "Guided ultrasound wave propagation in intact and healing long bones," *Ultrasound Med Biol* **32**, 693-708 (2006).

[264] N. M. Rawool, B. B. Goldberg, F. Forsberg, A. A. Winder, and E. Hume, "Power Doppler assessment of vascular changes during fracture treatment with low-intensity ultrasound," *J Ultrasound Med* **22**, 145-153 (2003).

[265] P. Reher, e. I. Elbeshir, W. Harvey, S. Meghji, and M. Harris, "The stimulation of bone formation in vitro by therapeutic ultrasound," *Ultrasound Med Biol* **23**, 1251-1258 (1997).

[266] P. Reher, N. Doan, B. Bradnock, S. Meghji, and M. Harris, "Therapeutic ultrasound for osteoradionecrosis: an in vitro comparison between 1 MHz and 45 kHz machines," *Eur J Cancer* **34**, 1962-1968 (1998).

[267] P. Reher, N. Doan, B. Bradnock, S. Meghji, and M. Harris, "Effect of ultrasound on the production of IL-8, basic FGF and VEGF," *Cytokine* **11**, 416-423 (1999).

[268] P. Reher, M. Harris, M. Whiteman, H. K. Hai, and S. Meghji, "Ultrasound stimulates nitric oxide and prostaglandin E2 production by human osteoblasts," *Bone* **31**, 236-241 (2002).

[269] J. A. Robinson, M. Chatterjee-Kishore, P. J. Yaworsky, D. M. Cullen, W. Zhao, C. Li, et al., "Wnt/beta-catenin signaling is a normal physiological response to mechanical loading in bone," *J Biol Chem* **281**, 31720-31728 (2006).

[270] S. I. Rokhlin, D. E. Chimenti, and A. H. Nayfeh, "On the topology of the complex wave spectrum in a fluyd-coupled elastic layer," *J Acoust Soc Am* **85**, 1074-1080 (1989).

[271] J. L. Rose, *Ultrasonic waves in solid media* (Cambridge University Press, UK, 2004).

[272] X. Roussignol, C. Currey, F. Duparc, and F. Dujardin, "Indications and results for the Exogen ultrasound system in the management of non-union: a 59-case pilot study," *Orthop Traumatol Surg Res* **98**, 206-213 (2012).

[273] J. P. Rue, D. W. Armstrong 3rd, F. J. Frassica, M. Deafenbaugh, and J. H. Wilckens, "The effect of pulsed ultrasound in the treatment of tibial stress fractures," *Orthopedics* **27**, 1192-1195 (2004).

[274] A. W. Rutjes, E. Nuesch, R. Sterchi, and P. Juni, "Therapeutic ultrasound for osteoarthritis of the knee or hip," *Cochrane Database Syst Rev* **doi: 10.1002/14651858.CD003132.pub2.** (2010).

[275] S. Rutten, P. A. Nolte, G. L. Guit, D. E. Bouman, and G. H. Albers, "Use of low-intensity pulsed ultrasound for posttraumatic nonunions of the tibia: a review of patients treated in the Netherlands," *J Trauma* **62**, 902-908 (2007).

[276] P. G. Sacks, M. W. Miller, and R. M. Sutherland, "Influences of growth conditions and cell-cell contact on responses of tumor cells to ultrasound," *Radiat Res* **87**, 175-186 (1981).

[277] M. Saito, K. Fujii, T. Tanaka, and S. Soshi, "Effect of low- and high-intensity pulsed ultrasound on collagen post-translational modifications in MC3T3-E1 osteoblasts," *Calcif Tissue Int* **75**, 384-395 (2004).

[278] M. Saito, S. Soshi, T. Tanaka, and K. Fujii, "Intensity-related differences in collagen post-translational modification in MC3T3-E1 osteoblasts after exposure to low- and high-intensity pulsed ultrasound," *Bone* **35**, 644-655 (2004).

[279] S. Sakaguchi, Y. Nakatani, N. Takamatsu, H. Hori, A. Kawakami, K. Inohaya, et al., "Medaka unextended-fin mutants suggest a role for Hoxb8a in cell migration and osteoblast differentiation during appendage formation," *Dev Biol* **293**, 426-438 (2006).

[280] K. Sakurakichi, H. Tsuchiya, K. Uehara, T. Yamashiro, K. Tomita, and Y. Azuma, "Effects of timing of low-intensity pulsed ultrasound on distraction osteogenesis," *J Orthop Res* **22**, 395-403 (2004).

[281] L. J. Sandell and T. Aigner, "Articular cartilage and changes in arthritis. An introduction: cell biology of osteoarthritis," *Arthritis Res* **3**, 107-113 (2001).

[282] E. F. Sant'Anna, R. M. Leven, A. S. Virdi, and D. R. Sumner, "Effect of low intensity pulsed ultrasound and BMP-2 on rat bone marrow stromal cell gene expression," *J Orthop Res* **23**, 646-652 (2005).

[283] S. A. Sapareto and Dewey. W.C., "Thermal dose determination in cancer therapy," *Int J Radiation Oncol Biol Phys* **10**, 787-800 (1984).

[284] W. Sato, T. Matsushita, and K. Nakamura, "Acceleration of increase in bone mineral content by low-intensity ultrasound energy in leg lengthening," *J Ultrasound Med* **18**, 699-702 (1999).

[285] M. D. Schofer, J. E. Block, J. Aigner, and A. Schmelz, "Improved healing response in delayed unions of the tibia with low-intensity pulsed ultrasound: results of a randomized sham-controlled trial," *BMC Musculoskelet Disord* **11**, 229 (2010).

[286] J. Schortinghuis, B. Stegenga, G. M. Raghoebar, and L. G. de Bont, "Ultrasound stimulation of maxillofacial bone healing," *Crit Rev Oral Biol Med* **14**, 63-74 (2003).

[287] J. Schortinghuis, A. L. Bronckers, B. Stegenga, G. M. Raghoebar, and L. G. de Bont, "Ultrasound to stimulate early bone formation in a distraction gap: a double blind randomised clinical pilot trial in the edentulous mandible," *Arch Oral Biol* **50**, 411-420 (2005).

[288] J. Schortinghuis, A. L. Bronckers, J. Gravendeel, B. Stegenga, and G. M. Raghoebar, "The effect of ultrasound on osteogenesis in the vertically distracted edentulous mandible: a double-blind trial," *Int J Oral Maxillofac Surg* **37**, 1014-1021 (2008).

[289] D. Schumann, R. Kujat, J. Zellner, M. K. Angele, M. Nerlich, E. Mayr, et al., "Treatment of human mesenchymal stem cells with pulsed low intensity ultrasound enhances the chondrogenic phenotype in vitro," *Biorheology* **43**, 431-443 (2006).

[290] F. J. Secreto, L. H. Hoeppner, and J. J. Westendorf, "Wnt signaling during fracture repair," *Curr Osteoporos Rep* **7**, 64-69 (2009).

[291] A. R. Selfridge, "Approximate material properties in isotropic materials," *IEEE Trans Sonics Ultrason* **SU-32**, 381-394 (1985).

[292] K. Sena, R. M. Leven, K. Mazhar, D. R. Sumner, and A. S. Virdi, "Early gene response to low-intensity pulsed ultrasound in rat osteoblastic cells," *Ultrasound Med Biol* **31**, 703-708 (2005).

[293] K. Sena, S. R. Angle, A. Kanaji, C. Aher, D. G. Karwo, D. R. Sumner, et al., "Low-intensity pulsed ultrasound (LIPUS) and cell-to-cell communication in bone marrow stromal cells," *Ultrasonics* **51**, 639-644 (2011).

[294] K. Shakouri, B. Eftekharsadat, M. R. Oskuie, J. Soleimanpour, M. K. Tarzamni, Y. Salekzamani, et al., "Effect of low-intensity pulsed ultrasound on fracture callus mineral density and flexural strength in rabbit tibial fresh fracture," *J Orthop Sci* **15**, 240-244 (2010).

[295] D. Sheyn, N. Kimelman-Bleich, G. Pelled, Y. Zilberman, D. Gazit, and Z. Gazit, "Ultrasound-based nonviral gene delivery induces bone formation in vivo," *Gene Ther* **15**, 257-266 (2008).

[296] B. Shi, J. Liang, X. Yang, Y. Wang, Y. Zhao, H. Wu, et al., "Integration of estrogen and Wnt signaling circuits by the polycomb group protein EZH2 in breast cancer cells," *Mol Cell Biol* **27**, 5105-5119 (2007).

[297] A. Shimazaki, K. Inui, Y. Azuma, N. Nishimura, and Y. Yamano, "Low-intensity pulsed ultrasound accelerates bone maturation in distraction osteogenesis in rabbits," *J Bone Joint Surg Br* **82**, 1077-1082 (2000).

[298] C. Shui and A. Scutt, "Mild heat shock induces proliferation, alkaline phosphatase activity, and mineralization in human bone marrow stromal cells and Mg-63 cells in vitro," *J Bone Miner Res* **16**, 731-741 (2001).

[299] D. Silkstone, H. Hong, and B. A. Alman, "Beta-catenin in the race to fracture repair: in it to Wnt," *Nat Clin Pract Rheumatol* **4**, 413-419 (2008).

[300] Smith & Nephew Inc. Exogen 4000+, Patient's instructions for use & package insert. 2011.

[301] C. Soti, E. Nagy, Z. Giricz, L. Vigh, P. Csermely, and P. Ferdinandy, "Heat shock proteins as emerging therapeutic targets," *Br J Pharmacol* **146**, 769-780 (2005).

[302] J. A. Spadaro and S. A. Albanese, "Application of low-intensity ultrasound to growing bone in rats," *Ultrasound Med Biol* **24**, 567-573 (1998).

[303] J. Spengler and M. Jekel, "Ultrasound conditioning of suspensions--studies of streaming influence on particle aggregation on a lab- and pilot-plant scale," *Ultrasonics* **38**, 624-628 (2000).

[304] H. C. Starritt, F. A. Duck, and V. F. Humphrey, "An experimental investigation of streaming in pulsed diagnostic ultrasound beams," *Ultrasound Med Biol* **15**, 363-373 (1989).

[305] H. C. Starritt, F. A. Duck, and V. F. Humphrey, "Forces acting in the direction of propagation in pulsed ultrasound fields," *Phys Med Biol* **36**, 1465-1474 (1991).

[306] R. Staruch, R. Chopra, and K. Hynynen, "Hyperthermia in bone generated with MR imaging-controlled focused ultrasound: control strategies and drug delivery," *Radiology* **263**, 117-127 (2012).

[307] H. F. Stewart, "Ultrasonic measurement techniques and equipment output levels," in *Essentials of medical ultrasound. A practical introduction to the principles, techniques and biomedical applications*, M. H. Repacholi and D. A. Benwell, eds. (Humana Press, Clifton, NJ, USA, 1982), pp. 81-92.

[308] A. Subramanian, J. A. Turner, G. Budhiraja, S. Guha Thakurta, N. P. Whitney, and S. S. Nudurupati, "Ultrasonic bioreactor as a platform for studying cellular response," *Tissue Eng Part C Methods* **19**, 244-255 (2013).

[309] J. S. Sun, Y. H. Tsuang, F. H. Lin, H. C. Liu, C. Z. Tsai, and W. H. Chang, "Bone defect healing enhanced by ultrasound stimulation: an in vitro tissue culture model," *J Biomed Mater Res* **46**, 253-261 (1999).

[310] J. S. Sun, R. C. Hong, W. H. Chang, L. T. Chen, F. H. Lin, and H. C. Liu, "In vitro effects of low-intensity ultrasound stimulation on the bone cells," *J Biomed Mater Res* **57**, 449-456 (2001).

[311] R. Takeuchi, A. Ryo, N. Komitsu, Y. Mikuni-Takagaki, A. Fukui, Y. Takagi, et al., "Low-intensity pulsed ultrasound activates the phosphatidylinositol 3 kinase/Akt pathway and stimulates the growth of chondrocytes in three-dimensional cultures: a basic science study," *Arthritis Res Ther* **10**, R77 (2008).

[312] S. Takikawa, N. Matsui, T. Kokubu, M. Tsunoda, H. Fujioka, K. Mizuno, et al., "Low-intensity pulsed ultrasound initiates bone healing in rat nonunion fracture model," *J Ultrasound Med* **20**, 197-205 (2001).

[313] K. F. Tam, W. H. Cheung, K. M. Lee, L. Qin, and K. S. Leung, "Osteogenic effects of low-intensity pulsed ultrasound, extracorporeal shockwaves and their combination - an in vitro comparative study on human periosteal cells," *Ultrasound Med Biol* **34**, 1957-1965 (2008).

[314] A. M. Tang, D. F. Kacher, E. Y. Lam, K. K. Wong, F. A. Jolesz, and E. S. Yang, "Simultaneous ultrasound and MRI system for breast biopsy: compatibility assessment and demonstration in a dual modality phantom," *IEEE Trans Med Imaging* **27**, 247-254 (2008).

[315] C. H. Tang, R. S. Yang, T. H. Huang, D. Y. Lu, W. J. Chuang, T. F. Huang, et al., "Ultrasound stimulates cyclooxygenase-2 expression and increases bone formation through integrin, focal adhesion kinase, phosphatidylinositol 3-kinase, and Akt pathway in osteoblasts," *Mol Pharmacol* **69**, 2047-2057 (2006).

[316] C. H. Tang, D. Y. Lu, T. W. Tan, W. M. Fu, and R. S. Yang, "Ultrasound induces hypoxia-inducible factor-1 activation and inducible nitric-oxide synthase expression through the integrin/integrin-linked kinase/Akt/mammalian target of rapamycin pathway in osteoblasts," *J Biol Chem* **282**, 25406-25415 (2007).

[317] M. Tanzer, E. Harvey, A. Kay, P. Morton, and J. D. Bobyn, "Effect of noninvasive low intensity ultrasound on bone growth into porous-coated implants," *J Orthop Res* **14**, 901-906 (1996).

[318] M. Tanzer, S. Kantor, and J. D. Bobyn, "Enhancement of bone growth into porous intramedullary implants using non-invasive low intensity ultrasound," *J Orthop Res* **19**, 195-199 (2001).

[319] F. Tascioglu, S. Kuzgun, O. Armagan, and G. Ogutler, "Short-term effectiveness of ultrasound therapy in knee osteoarthritis," *J Int Med Res* **38**, 1233-1242 (2010).

[320] J. M. Temkin, N. B. Smith, and F. Shapiro K, "Thermal effects of focused ultrasound energy on bone tissue," *Proc IEEE Ultrason Symp* **2**, 1427-1430 (1998).

[321] G. ter Haar, I. J. Stratford, and C. R. Hill, "Ultrasonic irradiation of mammalian cells in vitro at hyperthermic temperatures," *Br J Radiol* **53**, 784-789 (1980).

[322] M. Terakawa, S. Sato, H. Ashida, K. Aizawa, M. Uenoyama, Y. Masaki, et al., "In vitro gene transfer to mammalian cells by the use of laser-induced stress waves: effects of stress wave parameters, ambient temperature, and cell type," *J Biomed Opt* **11**, 014026 (2006).

[323] B. W. Ti, W. D. O'Brien JR, and J. G. Harris, "Measurements of coupled Rayleigh wave propagation in an elastic plate," *J Acoust Soc Am* **102**, 1528-1531 (1997).

[324] Y. C. Tien, S. D. Lin, C. H. Chen, C. C. Lu, S. J. Su, and T. T. Chih, "Effects of pulsed low-intensity ultrasound on human child chondrocytes," *Ultrasound Med Biol* **34**, 1174-1181 (2008).

[325] J. E. Tis, C. R. Meffert, N. Inoue, E. F. McCarthy, M. S. Machen, K. A. McHale, et al., "The effect of low intensity pulsed ultrasound applied to rabbit tibiae during the consolidation phase of distraction osteogenesis," *J Orthop Res* **20**, 793-800 (2002).

[326] G. R. Torr, "The acoustic radiation force," *Am J Phys* **52**, 402-408 (1984).

[327] C. L. Tsai, W. H. Chang, and T. K. Liu, "Preliminary studies of duration and intensity of ultrasonic treatments on fracture repair," *Chin J Physiol* **35**, 21-26 (1992).

[328] N. Tsumaki, M. Kakiuchi, J. Sasaki, T. Ochi, and H. Yoshikawa, "Low-intensity pulsed ultrasound accelerates maturation of callus in patients treated with opening-wedge high tibial osteotomy by hemicallotasis," *J Bone Joint Surg Am* **86-A**, 2399-2405 (2004).

[329] K. Uenaka, S. Imai, K. Ando, and Y. Matsusue, "Relation of low-intensity pulsed ultrasound to the cell density of scaffold-free cartilage in a high-density static semi-open culture system," *J Orthop Sci* **15**, 816-824 (2010).

[330] Y. Ulus, B. Tander, Y. Akyol, D. Durmus, O. Buyukakincak, U. Gul, et al., "Therapeutic ultrasound versus sham ultrasound for the management of patients with knee osteoarthritis: a randomized double-blind controlled clinical study," *Int J Rheum Dis* **15**, 197-206 (2012).

[331] E. C. Unger, T. Porter, W. Culp, R. Labell, T. Matsunaga, and R. Zutshi, "Therapeutic applications of lipid-coated microbubbles," *Adv Drug Deliv Rev* **56**, 1291-1314 (2004).

[332] J. Unsworth, S. Kaneez, S. Harris, J. Ridgway, S. Fenwick, D. Chenery, et al., "Pulsed low intensity ultrasound enhances mineralisation in preosteoblast cells," *Ultrasound Med Biol* **33**, 1468-1474 (2007).

[333] M. W. Urban, C. Pislaru, I. Z. Nenadic, R. R. Kinnick, and J. F. Greenleaf, "Measurement of viscoelastic properties of in vivo swine myocardium using Lamb wave dispersion ultrasound vibrometry (LDUV)," *IEEE Trans Med Imaging* **32**, 247-261 (2013).

[334] H. Vanharanta, I. Eronen, and T. Videman, "Effect of ultrasound on glycosaminoglycan metabolism in the rabbit knee," *Am J Phys Med* **61**, 221-228 (1982).

[335] N. M. Vaughan, J. Grainger, D. L. Bader, and M. M. Knight, "The potential of pulsed low intensity ultrasound to stimulate chondrocytes matrix synthesis in agarose and monolayer cultures," *Med Biol Eng Comput* **48**, 1215-1222 (2010).

[336] C. J. Wang, "Extracorporeal shockwave therapy in musculoskeletal disorders," *J Orthop Surg Res* **7**, 11 (2012).

[337] F. S. Wang, Y. R. Kuo, C. J. Wang, K. D. Yang, P. R. Chang, Y. T. Huang, et al., "Nitric oxide mediates ultrasound-induced hypoxia-inducible factor-1alpha activation and vascular endothelial growth factor-A expression in human osteoblasts," *Bone* **35**, 114-123 (2004).

[338] S. J. Wang, D. G. Lewallen, M. E. Bolander, E. Y. Chao, D. M. Ilstrup, and J. F. Greenleaf, "Low intensity ultrasound treatment increases strength in a rat femoral fracture model," *J Orthop Res* **12**, 40-47 (1994).

[339] Y. X. Wang, K. C. Leung, W. H. Cheung, H. H. Wang, L. Shi, D. F. Wang, et al., "Low-intensity pulsed ultrasound increases cellular uptake of superparamagnetic iron oxide nanomaterial: results from human osteosarcoma cell line U2OS," *J Magn Reson Imaging* **31**, 1508-1513 (2010).

[340] S. J. Warden, K. L. Bennell, M. R. Forwood, J. M. McMeeken, and J. D. Wark, "Skeletal effects of low-intensity pulsed ultrasound on the ovariectomized rodent," *Ultrasound Med Biol* **27**, 989-998 (2001).

[341] S. J. Warden, K. L. Bennell, B. Matthews, D. J. Brown, J. M. McMeeken, and J. D. Wark, "Efficacy of low-intensity pulsed ultrasound in the prevention of osteoporosis following spinal cord injury," *Bone* **29**, 431-436 (2001).

[342] S. J. Warden, J. M. Favaloro, K. L. Bennell, J. M. McMeeken, K. W. Ng, J. D. Zajac, et al., "Low-intensity pulsed ultrasound stimulates a bone-forming response in UMR-106 cells," *Biochem Biophys Res Commun* **286**, 443-450 (2001).

[343] S. J. Warden, R. K. Fuchs, C. K. Kessler, K. G. Avin, R. E. Cardinal, and R. L. Stewart, "Ultrasound produced by a conventional therapeutic ultrasound unit accelerates fracture repair," *Phys Ther* **86**, 1118-1127 (2006).

[344] S. J. Warden, D. E. Komatsu, J. Rydberg, J. L. Bond, and S. M. Hassett, "Recombinant human parathyroid hormone (PTH 1-34) and low-intensity pulsed ultrasound have contrasting additive effects during fracture healing," *Bone* **44**, 485-494 (2009).

[345] K. R. Waters, M. S. Hughes, J. Mobley, and J. G. Miller, "Differential forms of the Kramers-Krönig dispersion relation," *IEEE Trans Ultrason Ferroelectr Freq Control* **50**, 68-76 (2003).

[346] K. A. Wear, "Ultrasonic attenuation in human calcaneus from 0.2 to 1.7 MHz," *IEEE Trans Ultrason Ferroelectr Freq Control* **48**, 602-608 (2001).

[347] D. F. Webster, J. B. Pond, M. Dyson, and W. Harvey, "The role of cavitation in the in vitro stimulation of protein synthesis in human fibroblasts by ultrasound," *Ultrasound Med Biol* **4**, 343-351 (1978).

[348] D. F. Webster, W. Harvey, M. Dyson, and J. B. Pond, "The role of ultrasound-induced cavitation in the 'in vitro' stimulation of collagen synthesis in human fibroblasts," *Ultrasonics* **18**, 33-37 (1980).

[349] H. G. Welgus, J. J. Jeffrey, and A. Z. Eisen, "Human skin fibroblast collagenase. Assessment of activation energy and deuterium isotope effect with collagenous substrates," *J Biol Chem* **256**, 9516-9521 (1981).

[350] P. J. Westervelt, "The theory of steady forces caused by sound waves," *J Acoust Soc Am* **23**, 312-315 (1951).

[351] D. White, J. A. Evans, J. G. Truscott, and R. A. Chivers, "Can ultrasound propagate in the joint space of a human knee?" *Ultrasound Med Biol* **33**, 1104-1111 (2007).

[352] A. Wiltink, P. J. Nijweide, W. A. Oosterbaan, R. T. Hekkenberg, and P. J. Helders, "Effect of therapeutic ultrasound on endochondral ossification," *Ultrasound Med Biol* **21**, 121-127 (1995).

[353] D. G. Woo, C. Y. Ko, H. S. Kim, J. B. Seo, and D. Lim, "Evaluation of the potential clinical application of low-intensity ultrasound stimulation for preventing osteoporotic bone fracture," *Ann Biomed Eng* **38**, 2438-2446 (2010).

[354] J. Wu, F. Cubberley, G. Gormley, and T. L. Szabo, "Temperature rise generated by diagnostic ultrasound in a transcranial phantom," *Ultrasound Med Biol* **21**, 561-568 (1995).

[355] J. Wu and F. Cubberley, "Measurement of velocity and attenuation of shear waves in bovine compact bone using ultrasonic spectroscopy," *Ultrasound Med Biol* **23**, 129-134 (1997).

[356] J. Wu, "Determination of velocity and attenuation of shear waves using ultrasonic spectroscopy," *J Acoust Soc Am* **99**, 2871-2875 (1996).

[357] K. H. Yang, J. Parvizi, S. J. Wang, D. G. Lewallen, R. R. Kinnick, J. F. Greenleaf, et al., "Exposure to low-intensity ultrasound increases aggrecan gene expression in a rat femur fracture model," *J Orthop Res* **14**, 802-809 (1996).

[358] K. H. Yang and S. J. Park, "Stimulation of fracture healing in a canine ulna full-defect model by low-intensity pulsed ultrasound," *Yonsei Med J* **42**, 503-508 (2001).

[359] R. S. Yang, Y. Z. Chen, T. H. Huang, C. H. Tang, W. M. Fu, B. Y. Lu, et al., "The effects of low-intensity ultrasound on growing bone after sciatic neurectomy," *Ultrasound Med Biol* **31**, 431-437 (2005).

[360] R. S. Yang, W. L. Lin, Y. Z. Chen, C. H. Tang, T. H. Huang, B. Y. Lu, et al., "Regulation by ultrasound treatment on the integrin expression and differentiation of osteoblasts," *Bone* **36**, 276-283 (2005).

[361] C. P. Ye, B. C. Heng, H. Liu, W. S. Toh, and T. Cao, "Culture media conditioned by heat-shocked osteoblasts enhances the osteogenesis of bone marrow-derived mesenchymal stromal cells," *Cell Biochem Funct* **25**, 267-276 (2007).

[362] J. Ye, H. Haro, M. Takahashi, H. Kuroda, and K. Shinomiya, "Induction of apoptosis of articular chondrocytes and suppression of articular cartilage proteoglycan synthesis by heat shock," *J Orthop Sci* **8**, 387-395 (2003).

[363] J. H. Yoon, E. Y. Roh, S. Shin, N. H. Jung, E. Y. Song, D. S. Lee, et al., "Introducing pulsed low-intensity ultrasound to culturing human umbilical cord-derived mesenchymal stem cells," *Biotechnol Lett* **31**, 329-335 (2009).

[364] V. G. Zarnitsyn and M. R. Prausnitz, "Physical parameters influencing optimization of ultrasound-mediated DNA transfection," *Ultrasound Med Biol* **30**, 527-538 (2004).

[365] J. Zemanek, "Beam behavior within the nearfield of a vibrating piston," *J Acoust Soc Am* **49**, 181-191 (1971).

[366] D. Zeng, Q. Luo, H. Lin, J. Zhang, and C. He, "The effect of therapeutic ultrasound to apoptosis of chondrocyte and caspase-3 and caspase-8 expression in rabbit surgery-induced model of knee osteoarthritis," *Rheumatol Int* **32**, 3771-3777 (2012).

[367] S. Zhang, J. Cheng, and Y. X. Qin, "Mechanobiological modulation of cytoskeleton and calcium influx in osteoblastic cells by short-term focused acoustic radiation force," *PLoS One* **7**, e38343 (2012).

[368] Z. J. Zhang, J. Huckle, C. A. Francomano, and R. G. Spencer, "The influence of pulsed low-intensity ultrasound on matrix production of chondrocytes at different stages of differentiation: an explant study," *Ultrasound Med Biol* **28**, 1547-1553 (2002).

[369] Z. J. Zhang, J. Huckle, C. A. Francomano, and R. G. Spencer, "The effects of pulsed low-intensity ultrasound on chondrocyte viability, proliferation, gene expression and matrix production," *Ultrasound Med Biol* **29**, 1645-1651 (2003).

[370] S. M. Zia Uddin, J. Cheng, W. Lin, and Y. X. Qin, "Low-intensity amplitude modulated ultrasound increases osteoblastic mineralization," *Cell Mol Bioeng* **4**, 81-90 (2011).

Jarkko Leskinen

Ultrasound Stimulation of Bone and Cartilage — Interactions in Common In Vitro and Tissue Engineering Configurations

Therapeutic ultrasound is a stimulating technique in regenerative medicine and tissue engineering of bone and cartilage. The ultrasound mechanism causing these effects is unclear. Ultrasound in vitro studies form the bases for the method. In this thesis, bone and cartilage cells sonications and detailed measurements of the exposure circumstances were done. The results and the reviewed literature highlight the variability and complexity of these exposures which hinder its optimal use.

UNIVERSITY OF EASTERN FINLAND

Publications of the University of Eastern Finland
Dissertations in Forestry and Natural Sciences

ISBN 978-952-61-1682-2